DE GRUYTER

GLASS FIBRE-REINFORCED POLYMER COMPOSITES

MATERIALS, MANUFACTURING AND ENGINEERING

Edited by Jalumedi Babu, J. Paulo Davim

ADVANCED COMPOSITES

Glass Fibre-Reinforced Polymer Composites
Advanced Composites

Also of interest

Series: Advanced Composites
J. Paulo Davim (Ed.)
ISSN 2192-8983
Published titles in this series:
Vol. 11: Polymers and Composites Manufacturing (2020) Ed. by K. Kumar, J. P. Davim
Vol. 10: Biodegradable Composites (2019) Ed. by K. Kumar, J. P. Davim
Vol. 9: Wear of Composite Materials (2018) Ed. by J. P. Davim
Vol. 8: Hierarchical Composite Materials (2018) Ed. by K. Kumar, J. P. Davim
Vol. 7: Green Composites (2017) Ed. by J. P. Davim
Vol. 6: Wood Composites (2017) Ed. by A. Alfredo, J. P. Davim
Vol. 5: Ceramic Matrix Composites (2016) Ed. by J. P. Davim
Vol. 4: Machinability of Fibre-Reinforced Plastics (2015) Ed. by J. P. Davim
Vol. 3: Metal Matrix Composites (2014) Ed. by J. P. Davim
Vol. 2: Biomedical Composites (2013) Ed. by J. P. Davim
Vol. 1: Nanocomposites (2013) Ed. by J. P. Davim, C. A. Charitidis

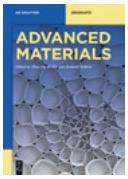

Advanced Materials
Ed. by T. van de Ven, A. Soldera, 2020
ISBN 978-3-11-053765-9, e-ISBN 978-3-11-057017-5

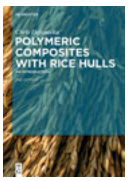

Polymeric Composites with Rice Hulls
Ch. Defonseka, 2019
ISBN 978-3-11-063968-1, e-ISBN 978-3-11-046974-5

Glass Fibre-Reinforced Polymer Composites

Materials, Manufacturing and Engineering

Edited by
Jalumedi Babu and J. Paulo Davim

DE GRUYTER

Editors
Dr. Jalumedi Babu
St. Joseph's College of Engineering & Technology
Department of Mechanical Engineering
Choondacherry 686579
Kottayam, Kerala
India
jalumedi.babu@gmail.com

Prof. Dr. J. Paulo Davim
University of Aveiro
Dept. of Mechanical Engineering
Campus Santiago
3810-193 Aveiro
Portugal
pdavim@ua.pl

ISBN 978-3-11-060828-1
e-ISBN (PDF) 978-3-11-061014-7
e-ISBN (EPUB) 978-3-11-060858-8
ISSN 2192-8983

Library of Congress Control Number: 2019956285

Bibliographic information published by the Deutsche Nationalbibliothek
The Deutsche Nationalbibliothek lists this publication in the Deutsche Nationalbibliografie; detailed bibliographic data are available on the Internet at http://dnb.dnb.de.

Cover image: gettyimages/thinkstockphotos, Abalone Shell
Typesetting: Integra Software Services Pvt. Ltd.
Printing and binding: CPI books GmbH, Leck

www.degruyter.com

Preface

Glass fibre-reinforced composites (GFRC) are now widely used in sport equipment, construction, transportation and power generation industries. Therefore, machining of these materials with appropriate strategies is important for defect-free products.

The current volume provides the recent information on advances in GFRC in five chapters. Chapter 1 provides the information on mechanical performance of glass and bio-fibre reinforced hybrid composites. Chapter 2 describes the influence of fibre arrangement on mechanical properties of glass fibre-reinforced aluminium sandwich laminates. Chapter 3 focuses on GFRC and their drilling-induced delamination. Chapter 4 describes drilling of GFRC. Last chapter describes the influence of milling process parameters on surface quality of glass fibre-reinforced plastic composites.

The current volume can be used as a research book for final undergraduate engineering course or a topic on GFRC at the postgraduate level. In addition to this, the book can serve as a useful reference for academics, researchers and professionals in composites and related fields. The scientific importance of the book is obvious for many important centres of research, laboratories and universities as well as industries. Consequently, it is expected this book will inspire and stimulate others to launch research in the field of GFRC.

Editors acknowledge De Gruyter for this opportunity and professional support. Finally, editors thank all the chapter authors for their availability for this editorial project.

J. Babu
St. Joseph's College of Engineering & Technology, India

J. Paulo Davim
University of Aveiro, Portugal
March 2020

https://doi.org/10.1515/9783110610147-202

Contents

About the editors

Jalumedi Babu received his Ph.D. in mechanical engineering in 2010, M.Tech. in production engineering in 2002 and B.Tech. in mechanical engineering in 1996 from Osmania University, Hyderabad, India. Currently, he is professor and dean of research at the Department of Mechanical Engineering, St. Joseph's College of Engineering and Technology, Pala, Kottayam, Kerala, India. He has more than 20 years of experience in teaching and research in manufacturing, engineering materials, composites and superplastic forming. He has guided a large number of undergraduate and postgraduate students in their research projects. He is the editorial member for several international technical journals. He is a reviewer for more than 10 international journals. In addition, he has published three research book chapters and more than 50 articles in journals and conferences.

J. Paulo Davim received his Ph.D. degree in Mechanical Engineering in 1997, M.Sc. degree in Mechanical Engineering (materials and manufacturing processes) in 1991, Mechanical Engineering degree (5 years) in 1986, from the University of Porto (FEUP), the Aggregate title (Full Habilitation) from the University of Coimbra in 2005 and the D.Sc. (Higher Doctorate) from London Metropolitan University in 2013. He is Senior Chartered Engineer by the Portuguese Institution of Engineers with an MBA and Specialist titles in Engineering and Industrial Management as well as in Metrology. He is also Eur Ing by FEANI-Brussels and Fellow (FIET) by IET-London. Currently, he is Professor at the Department of Mechanical Engineering of the University of Aveiro, Portugal. He has more than 30 years of teaching and research experience in Manufacturing, Materials, Mechanical and Industrial Engineering, with special emphasis in Machining & Tribology. He has also interest in Management, Engineering Education and Higher Education for Sustainability. He has guided large numbers of postdoc, Ph.D. and master's students as well as has coordinated and participated in several financed research projects. He has received several scientific awards and honors. He has worked as evaluator of projects for ERC-European Research Council and other international research agencies as well as examiner of Ph.D. thesis for many universities in different countries. He is the Editor in Chief of several international journals, Guest Editor of journals, books Editor, book Series Editor and Scientific Advisory for many international journals and conferences. Presently, he is an Editorial Board member of 30 international journals and acts as reviewer for more than 100 prestigious Web of Science journals. In addition, he has also published as editor (and co-editor) more than 125 books and as author (and co-author) more than 10 books, 80 book chapters and 400 articles in journals and conferences (more than 250 articles in journals indexed in Web of Science core collection/h-index 54+/9500+ citations, SCOPUS/h-index 59+/11500+ citations, Google Scholar/h-index 76+/19000+).

https://doi.org/10.1515/9783110610147-204

List of contributors

Gehan Anthonys
Department of Electrical and Computer Engineering, Faculty of Engineering Technology
The Open University of Sri Lanka
Nugegoda 10250, Sri Lanka

Jalumedi Babu
Department of Mechanical Engineering
St. Joseph College of Engineering
Palai, Kottayam
Kerala 686 579, India

Chandra Mouli Badiganti
Department of Mechanical Engineering
RISE Krishna Sai Prakasam Group of Institutions
Ongole, India

Nagaraju Bejgam
Department of Mechanical Engineering
RISE Krishna Sai Prakasam Group of Institutions
Ongole, India

G. Ramya Devi
Sathyabama University
Chennai 600119, India
Department of Mechanical Engineering,
St. Peter's College of Engineering and Technology
Chennai 600054, India

M. Manzoor Hussain
Department of Mechanical Engineering
Jawaharlal Nehru Technological University (JNTUH)
Kukatpally
Hyderabad, India

K. Jessy
Department of Mechanical Engineering
Amal Jyothi College of Engineering
Kanjirappally, Kottayam
Kerala 686 518, India

Vishal John Mathai
Department of Mechanical Engineering
Amal Jyothi College of Engineering
Kanjirappally, Kottayam
Kerala 686 518, India

K. Palanikumar
Department of Mechanical Engineering
Sri Sai Ram Institute of Technology
Chennai 600044, India

Sunil Pathak
Faculty of Engineering Technology
University Malaysia Pahang
Malaysia

I. S. N. V. R. Prasanth
Department of Mechanical Engineering
Guru Nanak Institute of Engineering and Technology
Hyderabad, India

D. V. Ravishankar
Department of Mechanical Engineering
T.K.R. College of Engineering and Technology
Meerpet, Hyderabad, India

Mostafa Seifan
School of Engineering, Faculty of Science and Engineering
The University of Waikato
Hamilton 3216, New Zealand

https://doi.org/10.1515/9783110610147-205

Vinod Kumar Sharma
School of Mechanical Engineering
VIT University
Vellore, India

Tom Sunny
Department of Mechanical Engineering
Amal Jyothi College of Engineering
Kerala 686518, India

R. Vinayagamoorthy
Department of Mechanical Engineering
Sri Chandrasekharendra Saraswathi Viswa Maha Vidyalaya University
Kancheepuram 631561
Tamil Nadu, India

R. Vinayagamoorthy

1 Mechanical performance of glass- and biofibre-reinforced hybrid composites

Abstract: Polymer-based materials are mainly intended for structural applications in industries. Due to their competitive properties, they are used as a replacement for wood and other conventional materials. During their manufacture, fibres are reinforced into the polymer resin in different shapes as required. Among several available reinforcements, glass fibre in many researches showed the best in mechanical characters, ability to get reinforced in the matrix and handling ability. In contrast, bio-reinforcements from various natural sources are also used as an alternative and they provide an equal performance like the man-made reinforcements. When both the artificial fibre and natural fibre are used in a composite material, the composite attains the iconic characters of each reinforcement; thus, the material as a whole shows excellent characteristics. This chapter provides a clear picture on characterization of composites with glass reinforcement in sandwich form, and also shows various trends like the elevation or decline in their strengths, their possible reasons and the potential ways for elevating the characters of the composite.

Keywords: glass fibre, biofibre, hybrid composites, properties, strengths

1.1 Introduction

Composites are identified based on the matrix material used and when a polymeric matrix is used, it is said to be a fibre-reinforced plastic (FRP) or simply polymer matrix composite. Polymer composites are mostly suitable for designing exterior parts like boat housing, wings in aircrafts, partitioning, seating and making dashboard in automobiles. Polymer composites are determined by the characteristics of the reinforcement present, whereas the matrix provides a regular shape to the component [1]. At the inception, reinforcements are man-made by various physical techniques as well as by chemical synthesis. Due to the wide usage of reinforcements, they are produced in mass and supplied to different industries for composite fabrication. Among the different classes of artificial fibres, glass is used in different forms like long fibres, short fibres and woven mats during the synthesis. Carbon, on the other hand, is majorly used as nanoparticles and kevlar is meagerly used in sports industries. Several investigations have recently been made to synthesize and characterize synthetic glass [2, 3],

R. Vinayagamoorthy, Department of Mechanical Engineering, Sri Chandrasekharendra Saraswathi Viswa Mahavidyalaya, Tamil Nadu, India

https://doi.org/10.1515/9783110610147-001

carbon [4, 5] and kevlar [6, 7] fibre-reinforced composites. All these man-made fibres are proven to be good in most of the mechanical properties and, among these, glass is found to be superior for its properties, usability, cost and availability. Glass fibres are of different types based on a specific application. They are classified and nominated with symbols such as A-glass or alkali glass, C-glass which offers high resistance to chemicals, E-glass for electrical applications and S-glass for structural applications. Among these types of glasses, E-glass has been used by many researchers as it is electrically and mechanically strong [8–10].

Although glass shows best characteristics, it fails in reusability and bio-degradability. Due to this reason, researchers looked on an alternative, which supports both reusability and bio-degradability [11–13]. This created the evolution of natural fibre-based composites, and many bio-reinforcements have been arrived from several plants, animal wastes and earth minerals such as rocks and sediments. Plant reinforcements are obtained from different parts of a tree such as barks and branches [14, 15], leaves [16], fruits [17] and radix [18], which have been focused mainly by the researchers. Investigations on the mechanical properties of such natural fibre-based composites many times revealed a dominant than conventional polymer-based materials. As each reinforcement has its iconic property, investigations have evolved to analyze the behavior of composite materials with multiple layers of fibres. All such studies revealed that the behavior of multiple fibre-reinforced materials or sandwich materials is better than the single fibre layered materials [19, 20]. In addition, it has been shown that by including a natural fibre along with an artificial fibre enhances the ease of machining the material [21–24]. Hybrid formulation could be made in two ways: one way is by adding two artificial fibres [25] and other way is by adding an artificial fibre and a natural fibre or any other fibre [26–28]. During the preparation of sandwich polymeric materials, many parameters need to be taken care for enhancing the behavior of the material. Some of them are preprocessing methods of reinforcements, orientation of the fibres molding method adopted, operating conditions such as pressure and temperature [29]. This research presents a detailed picture on processing, molding, characterization and machining ability of glass-reinforced sandwich composites (GSC).

1.2 GSC under tension

Many biofibres are processed and are utilized as one of the reinforcements in sandwich materials. Few works used a biofibre with glass and some used two fibres along with glass, and different results have been produced. In an investigation, an artificial reinforcement namely glass and two natural reinforcements such as banana fibre and particulate rice husk are utilized to develop sandwich composites [30]. The reinforcements are added in different proportions to select a best composite. Among the different

composites fabricated, the performance of 20% glass + 5% banana-reinforced composite (G20B5), 20% glass +10% banana-reinforced composite (G20B10), 20% glass + 15% banana-reinforced composite (G20B15), 20% glass + 5% rice husk-reinforced composite (G20R5), 20% glass + 10% rice husk-reinforced composite (G20R10) and 20% glass + 15% rice husk-reinforced composite (G20R15) are shown in Figure 1.1(a). A highest tensile strength of 45 MPa is produced by G20B15, which is followed by two composites such as G20B10 and G20R10. It is well understood that the inclusion of banana fibre is preferred than the inclusion of rice husk but the inclusion of 10% banana and 10% rice husk produces a better mechanical performance. As the least strength is produced by sample G20R15, it is understood that banana is the more suitable reinforcement to take up the loads in combination with glass.

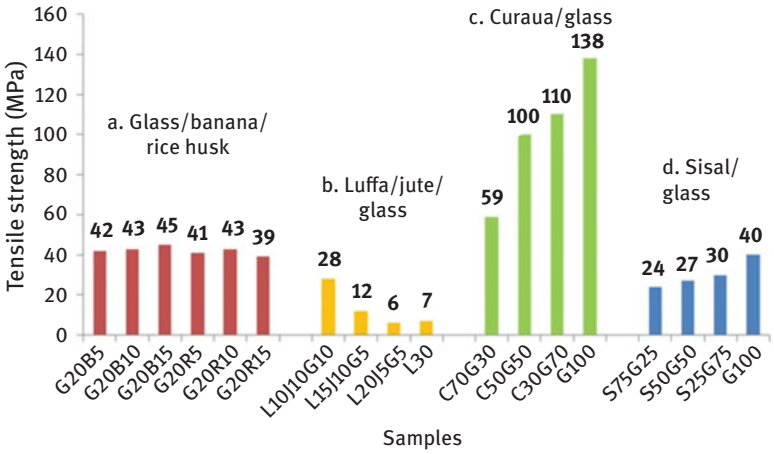

Figure 1.1: Tensile behavior of GSC.

A research utilized processed luffa and woven jute mat as the natural reinforcements in combination with the artificial glass [31]. Among the composites, the performance of 10% luffa + 10% jute + 10% glass composite (L10J10G10), 15% luffa + 10% jute + 5% glass composite (L15J10G5), 20% luffa + 5% jute + 5% glass composite (L20J5G5) and 30% luffa composite are shown in Figure 1.1(b). A highest tensile retention of 28 MPa is presented by laminate L10J10G10, which is followed by L15J10G5. The performance of other two composites seems to be poor as compared to that of the former composites. Here it is clear that glass fibre inclusion is vital for enhancing the tensile resistance of the materials, and a nominal glass composition of 10% is to be utilized for attaining a highest tensile resistance. It is also suggested that in order to produce a maximum tensile resistance a uniform composition of all reinforcements is to be used during fabrication.

Investigations on curaua and glass-reinforced hybrid laminates fabricated composites with 30% of fibre and 70% of resin [32]. The 30% of fibre shared by curaua and glass in different ways is shown in Figure 1.1(c). The performance of 70% curaua +30% glass composite (C70G30), 50% curaua + 50% glass composite (C50G50), 30% curaua +70% glass composite (C30G70) and 100% glass composite (G100) is evaluated. A highest tensile resistance of 138 MPa is produced by composite G100. Composites C30G70 and C50G50, respectively, follow G100. This shows that an elevation in the glass content hikes the tensile strength gradually. Also, the inclusion of curaua fibre does not help to elevate the tensile resistance, and the sample with glass alone would be appropriate for resisting high tensile loads. Hence, it is witnessed that the hybridization of curaua fibre with glass does not work well for achieving a highest tensile strength.

A research has been made to investigate the usability of sisal fibre along with glass in hybrid form. The proportions of fibres are kept at 8% by volume, and composite samples have been manufactured by altering the compositions of both sisal and glass [33]. The behavior of 75% sisal + 25% glass composite (S75G25), 50% sisal + 50% glass composite (S50G50), 25% sisal + 75% glass composite (S25G75) and 100% glass composites is shown in Figure 1.1(d). The results revealed that tensile strength elevates with a hike in the glass composition, and a maximum strength is obtained in 100% glass composite. This behavior is quite similar to the previously presented study on curaua-reinforced composite. Hence, the behavior of each natural fibre with glass is different and an utmost care must be taken on the proportions of fibres while fabricating the composites. The tensile behavior of glass and some other FRP is given in Table 1.1.

Table 1.1: Tensile behavior of glass-reinforced hybrid composites.

S. no.	Fibres/matrix used	Optimum fibre compositions/fibre length	Max. tensile strength (MPa)	Ref.
1.	Vetiver + jute + glass/vinyl ester	Vetiver 13%, jute 13%, glass 8%	74.14	[1]
2.	Luffa, steel, glass/polyester	Luffa 10%, steel10%, glass 10%	52	[17]
3.	Jute, glass, bronze, steel/ polyester	Jute 20%, glass 10%	26	[34]
4.	Sisal, jute, glass/epoxy	Sisal 15%, glass 15%	53.55	[35]
5.	Banana + glass/polyester	Banana 10%, glass 20%	22.1	[36]
6.	Glass + kenaf/polyester	Glass 70%, kenaf 30%	160	[37]
7.	Jute + glass/polyester	Jute 10%, glass 30%	96	[38]
8.	Ridge gourd + glass/phenol formaldehyde	Ridge gourd and glass 40%	42	[39]

Table 1.1 (continued)

S. no.	Fibres/matrix used	Optimum fibre compositions/fibre length	Max. tensile strength (MPa)	Ref.
9.	Kapok + glass/polyester	Kapok 0%, glass 100%	112.87	[40]
10.	Bamboo + glass/epoxy	Bamboo 20%, glass 30%	243	[41]
11.	Coconut sheath + glass/phenol formaldehyde	Coconut sheath 20%, glass 20%	29.67	[42]
12.	Silk + glass/epoxy	Silk 12.5%, glass 12.5%	84.04	[43]
13.	Jute + glass/polyester	Jute 17.1%, glass 25.2%	130	[44]
14.	Cotton + glass/polyethylene	Cotton 12.5%, glass 10%	13.5	[45]
15.	Flax + glass/polypropylene	Flax 0%, glass 27.4%	26	[46]

1.3 GSC under flexure

Like tensile characteristics, resistance to flexure is also an important character, which determines the resistance of composite against bending. Hence, several studies have been done to evaluate the flexural behavior of sandwich composites. The flexural behavior of banana, rice husk, luffa, jute and curaua fibre-reinforced composites is shown in Figure 1.2. Among the banana and rice husk-reinforced hybrid composites, a highest flexural resistance of 89 MPa is given by G20B15. Composites G20R10 and G20B10, respectively, follow G20B15. A least flexural resistance of 78 MPa is given by G20R15. An elevation in the banana content enhances the strength, whereas elevation in the rice rusk content does not show any trend on the flexural behavior [30]. It is observed that banana is amicable with glass, whereas rice husk is incompatible with glass in hybrid form. Studies on the processed luffa

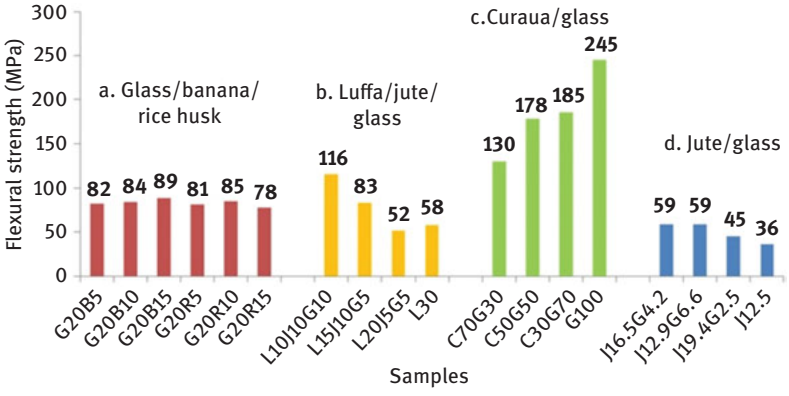

Figure 1.2: Flexural behavior of GSC.

fibre, woven jute fibre and synthetic glass-filled materials almost show a trend similar to the tensile strength [31]. Pure luffa composite is not on par with the other composites, and it is shown that by taking same proportions of luffa, glass and jute, a maximum flexural resistance could be achieved.

The flexural behavior of curaua-reinforced composite is also similar in nature with its tensile behavior, that is, a hike in the glass proportion improves the flexural resistance and the composite with only glass fibres gives a highest flexural resistance of 245 MPa. This shows that curaua does not show a positive influence and is found to be not compatible with glass in enhancing the flexural strength [32]. A study on the characteristics of sandwich composites has been done by taking 16.5% jute + 4.1% glass composite (J16.5G4.2), 12.9% jute + 6.6% glass composite (J12.9G6.6), 19.4% jute + 2.5% glass composite (J19.4G2.5) and 12.5% jute composite (J12.5). A highest flexural resistance of 59 MPa is given by two composites such as J16.5G4.2 and J12.9G6.6. This is followed by composites J19.4G2.5 and J12.5. This shows that as the glass content is decreased beyond 4.2%, the flexural strength drops severely [47]. Also, pure jute composite does not show a positive sign on the flexural strength. Hence, the glass fibre is important for elevating the flexural resistance of the material and a nominal glass of 4.2% would be suitable to achieve a highest flexural resistance. The flexural behavior is also estimated under a combination of glass and other fibres, which are presented in Table 1.2.

Table 1.2: Flexural behavior of glass-reinforced hybrid composites.

S. no.	Fibres/matrix used	Optimum fibre compositions/fibre length	Max. flexural strength (MPa)	Ref.
1.	Vetiver + jute + glass/vinyl ester	Vetiver 10%, jute 10%, glass 14%	137.6	[1]
2.	Luffa, steel, glass/polyester	Luffa 10%, steel 10%, glass 10%	223	[17]
3.	Jute, glass, bronze, steel/ polyester	Jute 20%, glass 10%	210	[34]
4.	Glass + kenaf/polyester	Glass 70%, kenaf 30%	272	[37]
5.	Jute + glass/polyester	Jute 10%, glass 30%	102.83	[38]
6.	Coconut sheath + glass/phenol formaldehyde	Coconut sheath 20%, glass 20%	59.7	[42]
7.	Silk + glass/epoxy	Silk 12.5%, glass 12.5%	114.5	[43]
8.	Cotton + glass/polyethylene	Cotton 12.5%, glass 10%	17.5	[45]
9.	Bamboo + glass/epoxy	Bamboo 10%, glass 30%	213	[48]
10.	Jute + glass/epoxy	Jute 0%, glass 16.6%	115	[49]
11.	Banana + glass/polystyrene	Banana 14%, glass 6%	44	[50]
12.	Coir + glass/polyester	Coir 0%, glass 20%	140.9	[51]
13.	Oil palm + glass/polyester	Oil palm 3.5%, glass 31.5%	132	[52]

1.4 GSC under impact

Impact behavior of three different types of composites is shown in Figure 1.3. Among the banana, glass and rice husk composites, a highest impact strength of 9 J is produced by two composites, namely G20B15 and G20R10, which is followed by G20B10. A least impact strength of 8.1 J is produced by G20R15. It is noticed that an elevation in the banana content elevates the impact energy of the composite, whereas a hike in the rice husk content does not show a clear trend [30]. Although there is no clear trend, maximum impact energy is also shown by adding 10% of rice husk fibres; hence, rice husk is also a possible alternate to elevate the impact strength of materials. It is clear that by adding either 15% of banana or 10% of rice husk along with 20% of glass, maximum impact strength could be achieved, and this point is not witnessed in tensile and flexural analysis.

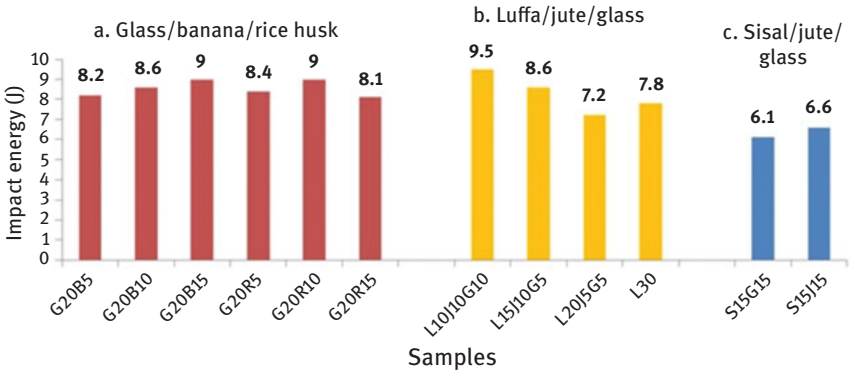

Figure 1.3: Impact behavior of GSC.

Behavior of luffa-, jute- and glass-reinforced composites shows a trend similar to the tensile and flexural behaviors. Addition of 5% of jute and 5% of glass with 20% of luffa gives minimum impact energy of 7.2 J. As the luffa content is decreased by elevating the jute and glass compositions, the impact energy goes up and a highest impact strength of 9.5 J is produced by L10J10G10. Here it is clear that by taking an equal composition of all the three fibres, maximum impact energy could be attained [31]. This trend clearly makes to know that the compositions of fibres significantly decide the mechanical characters of the material. In a study, 15% sisal + 15% glass composite (S15G15) and 15% sisal + 15% jute composite (S15J15) have been synthesized. The impact resistance of these two composites is shown in Figure 1.3(c). A highest impact resistance of 6.6 J is exhibited by composite laminates with both sisal and jute as reinforcements. It is evidenced that glass is not amicable with sisal to elevate the impact energy of the fabricated materials. Also, it is clear that the

natural reinforcement subjugates the glass reinforcement in terms of taking the loads amicably with the sisal fibres. Impact strength of composites under different combinations with glass fibres is shown in Table 1.3.

Table 1.3: Impact behavior of glass-reinforced hybrid composites.

S. no.	Fibres/matrix used	Optimum fibre compositions/ fibre length	Max. impact energy	Ref.
1.	Vetiver + jute + glass/vinyl ester	Vetiver 10%, jute 10%, glass 14%	18.33 J	[1]
2.	Luffa, steel, glass/polyester	Luffa 10%, steel 10%, glass 10%	28 J	[17]
3.	Jute, glass, bronze, steel/polyester	Jute 20%, steel 10%	34 J	[34]
4.	Banana + glass/polyester	Banana 10%, glass 20%	5 J	[36]
5.	Jute + glass/polyester	Jute 10%, glass 30%	235.46 J/m^2	[38]
6.	Coconut sheath + glass/phenol formaldehyde	Coconut sheath 20%, glass 20%	0.228 J/mm^2	[42]
7.	Cotton + glass/polyethylene	Cotton 12.5%, glass 0%	190.1 KJ/m^2	[45]
8.	Coir + glass/polyester	Coir 0%, glass 20%	202.6 KJ/m^2	[51]
9.	Oil palm + glass/polyester	Oil palm 3.5%, glass 31.5%	16.5 KJ/m^2	[52]
10.	Sisal + glass/epoxy	Sisal and glass 9%, fibre length = 2 cm	12.9 J	[53]
11.	Jute + glass/polyester	Jute 17.1%, glass 25.2%	17.05 J	[54]
12.	Sisal + glass/polyester	Sisal 0%, glass 8%	6.3 J/m	[55]

1.5 GSC under compression

Compressive behavior of four different composite groups is presented in Figure 1.4. The first group of specimens is made from vetiver, jute and glass fibres with 24% vetiver + 10% glass composite (V24G10), 19% vetiver + 15% glass composite (V19G15), 10% vetiver + 24% glass composite (V10G24), 13% vetiver + 13% jute + 8% glass composite (V13J13G8), 10% vetiver + 10% jute + 14% glass composite (V10J10G14) and 17% vetiver + 17% glass composite (V17G17) as shown in Figure 1.4(a). A comparative analysis presented a maximum compressive resistance of 128 MPa with composite V10J10G14, which is followed by two samples, namely V13J13G8 and V17G17. A lowest strength is exhibited by composite V24G10. This analysis clearly makes to know that an elevation in the glass content enhances the compressive strength considerably in both bi-fibre and tri-fibre composites [1]. Another interesting point witnessed is the behavior of composite V17J17, which is on par with the composite V13J13G8. This shows that glass fibre could be completely neglected by introducing the natural fibres

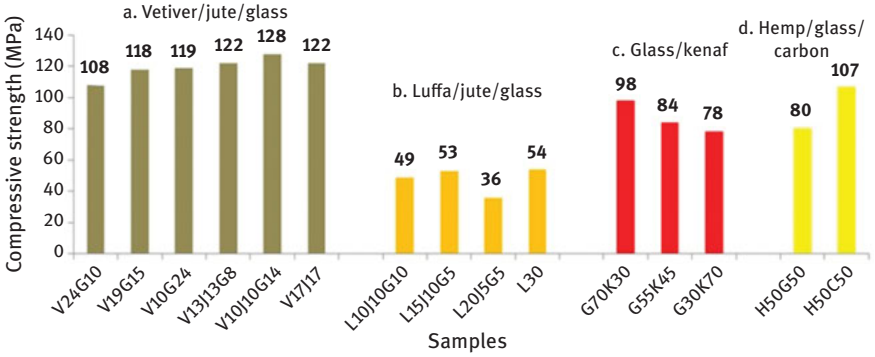

Figure 1.4: Compressive behavior of GSC.

in equal proportions. In contrast, to attain a highest strength in bi-fibre and tri-fibre laminates, a minimum glass content of 24% in bi-fibre composites and 14% in tri-fibre composites are to be maintained.

Studies on the processed luffa, woven jute and synthetic glass-reinforced materials showed a highest compressive resistance of 54 MPa in L30. L15J10G5 and L10J10G10, respectively, go behind L30. This behavior is quite different from the tensile, flexural and compressive behaviors. In this analysis, the compressive strength of pure luffa seems to be predominant than the hybrid composites [31]. Hence, the hybridization of luffa with glass does not show a positive sign on the compressive behavior. Studies on the glass- and kenaf-reinforced composites made 70% glass + 30% kenaf composite (G70K30), 55% glass + 45% kenaf composite (G55K45) and 30% glass + 70% kenaf composite (G30K70). A comparison among the fabricated specimens presented a highest compressive resistance of 98 MPa in composite G70K30 and a minimum strength of 78 MPa in composite G30K70. Here, the elevation of glass content from 30% to 70% enhances the compressive strength from 78 to 98 MPa. Hence, the use of glass is important to attain a highest compressive resistance [37]. This behavior is totally different from the luffa–jute–glass composites; hence, it is concluded that the performance of glass is not similar with all-natural fibres. Therefore, to acquire a highest compressive resistance, properly choosing the natural fibre is a primary work during composite development. Investigations on the synthetic glass-, carbon- and natural hemp-reinforced composite made two different samples by taking equal composition of hemp and glass in the first and hemp and carbon in the second as shown in Figure 1.4(d) [56]. The results showed that the hemp–carbon composite is superior to the hemp–glass composite; hence, the usage of glass along with hemp must be eliminated to attain a highest compressive resistance. The behavior of glass and other fibre-reinforced sandwich materials under compression is given in Table 1.4.

Table 1.4: Compressive behavior of glass-reinforced hybrid composites.

S. no.	Fibres/matrix used	Optimum fibre compositions/fibre length	Max. compressive strength (MPa)	Ref.
1.	Luffa, steel, glass/polyester	Luffa 10%, steel 10%, glass 10%	82	[17]
2.	Jute, glass, bronze, steel/ polyester	Jute 20%, steel 10%	110	[34]
3.	Bamboo + glass/epoxy	Bamboo 20%, glass 20%	218	[48]
4.	Sisal + glass/polyester	Sisal 0%, glass 5%	12.7	[55]
5.	Jute + glass/epoxy	Jute 0%, glass 64%	325	[57]
6.	Kenaf + glass/polyester	Kenaf 12.5%, glass 24.3%	89	[58]
7.	Cow dung + glass/polyester	Cow dung 5%, glass 10%	152.5	[59]
8.	Bagasse + glass/epoxy	Bagasse 10%, glass 0%	49.85	[60]
9.	Jute + glass/polyester	Jute 11.8%, glass 8.2%	75	[61]

1.6 Water absorption of chemical resistance of GSC

The intake of water by a composite is measured on a timely basis and calculated through the increase in the weight of the material. The resistance offered by the composite against water absorption is very important when the composite is subjected to moisture. The ability to absorb water is different for each fibre and this capacity also varies when two or more fibres are used in combination [62, 63]. A characteristic study of polyester material with woven jute and glass as reinforcements concluded that jute has more capacity of absorbing water than the glass fibre [38]. The elevation in the jute content enhances the water absorption, and this behavior is observed under 20%, 30% and 40% of total fibre content. Water absorption studies on the coconut sheath, glass and jute composite plates concluded that the composite with jute as the extreme layers is more hydrophilic in nature, whereas the composite containing glass as the extreme layers is more hydrophobic. It is suggested that in order to arrest the water absorption, a proper chemical treatment must be given to the jute fibres before using it in the composite [42]. Hence, the stacking sequence of fibres has a major impact on the water absorption of the composite [64, 65]. Water intake character of silk and glass epoxy hybrid laminates showed a positive sign on the resistance to water absorption. Silk fibre seems to be more hydrophilic in nature than the glass fibre and when silk fibre is used along with glass, glass acts as a barrier to arrest the water entering into the composite. Thus, the hybridization has a major impact over the water absorption [43]. An almost same result is presented in another study on vetiver + glass + jute sandwich composites [66]. The resistance to chemical is another vital property for a composite as many times the structural composites are made up of glass-reinforced hybrid composites like boilers and containers. A research

on the chemical opposition property of sisal + glass composites produced a high resistance to chemicals such as HCl, HNO_3, CH_3COOH, NaOH, NH_4OH, H_2O, C_6H_6 and CCl_4. Hence, it is suggested that sisal–glass composites suit well for chemical storage tanks [53]. Chemical opposition property of bamboo + glass composites is investigated with several chemicals. It is found that bamboo- and glass-reinforced composite is highly resistive to HCl, HNO_3, CH_3COOH and NaOH but the composite is more reactive with NH_4OH, C_6H_6, C_7H_8, CCl_4 and H_2O [41].

1.7 Hardness and machining characteristics of GSC

The ability of a material to resist load on its surface is called as hardness. Hardness is also majorly influenced by both the matrix and reinforcements. Investigations on the hardness behavior of sisal + glass composites studied the effect of length of the fibre on the material property. It is observed that among the three fibre lengths, namely 1, 2 and 3 cm, a highest hardness is recorded by the composite containing 2 cm length of fibres [53]. Investigation of the hardness behavior of kapok + glass composites revealed that an elevation in glass and a decline in the kapok contents enhance the hardness of the material to a maximum extent. A highest hardness is seen in composite containing only glass fibres. This shows that kapok is not a compatible fibre with glass for promoting the hardness of the composites [40]. In another research, hardness property of hybrid composites made up of coconut sheath, jute and glass reinforcements is analyzed. The influence of sequence of reinforcements in the material is studied and concluded that the material containing only coconut sheath and jute fibres produced a maximum hardness. It is suggested that in order to get a maximum hardness, a minimum of two jute layers must be used at extremities in the material. Glass does not have a positive sign on the hardness of the composite [42]. Hardness of flax- and glass-reinforced composites has been evaluated before and after ultraviolet ageing. It is reported that the hardness of composites before ultraviolet ageing is higher than the composites after ultraviolet ageing. Also, a maximum hardness is recorded for material with 30% of glass + 10% of flax [46].

Machining of materials is an important work after molding the composites. In order to make the material to suit for assembly, the sharp corners and edges are to be smoothened and many times holes are to be made in the materials [67–69]. Machining investigations on materials reinforced with green fibres are carried out to some extent, whereas machining of glass-reinforced hybrid composites is meagre. A research work on the drilling ability of vetiver + glass composites suggested that the glass elevates the delamination and damage of walls while hole making. These failures may be avoided by using green reinforcements. In addition, the green fibres also reduce the drilling forces developed during hole making [18]. In one of the research studies, vetiver + jute + glass in vinyl ester is used for developing composites. Holes are

made on the fabricated material and it is observed that both the green reinforcements decline the failures such as delamination and inner wall roughness [8]. More or less same results are presented in other researches on hole making of glass + green fibre plastics [10, 15].

1.8 Summary

An extensive survey has been done on the characterization of polymeric materials with glass as reinforcements in hybrid form. The major points identified are as follows:

- Glass in a composite is important along with any fibre in order to attain highest mechanical characters.
- Glass is amicable with green fibres in elevating all mechanical properties. For some fibres, pretreatments must be given to elevate the compatibility.
- In certain cases, glass is better than green fibres and, in other cases, green fibres are better than glass. Therefore, the characteristics of each reinforcements must be suitably selected before developing a composite material.
- The composition of glass and other reinforcements plays a dominant role in determining the characters of the material. In general, a fibre composition between 10% and 50% would be optimum to attain highest strengths.
- Apart from mechanical strengths, the water resistivity of GSC is unique and found to be the best when glass is placed at the extremities in the composite. Glass at the extremity serves as a potential barrier to the water and other chemicals entering into the composite and thus enhances the resistance to water and chemical absorption.
- During machining, glass elevates the failure such as delamination; therefore, usage of a green fibre is essential to alleviate the forces and associated failures, thereby attaining a maximum machinability.

References

[1] Vinayagamoorthy, R., and Rajeswari, N. Mechanical performance studies on Vetiveria zizanioides/jute/glass fibre-reinforced hybrid polymeric composites, Journal of Reinforced Plastics Composites 2014, 33, 81–92.

[2] Ou, Yunfu., Zhu, Deju., Zhang, Huaian., Huang, Liang., Yao, Yiming., Li, Gaosheng., and Mobasher, Barzin. Mechanical characterization of the tensile properties of glass fibre and its reinforced polymer (GFRP) composite under varying strain rates and temperatures, Polymer 2016, 8, 1–16.

[3] Asi, Osman. Mechanical properties of glass-fibre reinforced epoxy composites filled with Al_2O_3 particles, Journal of Reinforced Plastics Composites 2008, 28, 286–2867.

[4] Akihama, Shigeyuki., Suenaga, Tatsuo., and Banno, Tadashi. Mechanical properties of carbon fibre reinforced cement composites, International Journal of Cement Composites Lightweight Concrete 1986, 8, 21–38.
[5] Dong, Liang., and Haydn, Wadley. Mechanical properties of carbon fibre composite octet-truss lattice structures, Composites Science Technology 2015, 119, 26–33.
[6] Singh, Thingujam Jackson., and Samanta, Sutanu. Characterization of kevlar fibre and its composites: A review, Materials Today Proceedings 2015, 2, 1381–1387.
[7] Warbhe, NO., Shrivastava, Ramakant., and Adwani, PS. Mechanical properties of kevlar/jute reinforced epoxy composite, International Journal of Innovative Research Science Engineering Technology 2016, 5, 16407–16418.
[8] Vinayagamoorthy, R., Rajeswari, N., Vijayshankar, S., and Balasubramanian, K. Drilling performance investigations on hybrid composites by using d-optimal design, International Review Mechanical Engineering 2014, 8, 952–960.
[9] Devendra, K., and Rangaswamy, T. Strength characterization of E-glass fibre reinforced epoxy composites with filler materials, Journal of Minerals and Materials Characterization and Engineering 2013, 1, 353–357.
[10] Vinayagamoorthy, R., Rajeswari, N., and Karthikeyan, S. Investigations of damages during drilling of natural sandwich composites, Applied Mechanics and Materials 2015, 766–767, 812–817.
[11] Vinayagamoorthy, R., and Rajeswari, N. Analysis of cutting forces during milling of natural fibred composites using fuzzy logic, International Journal of Composite Material and Manufacturing 2012, 2, 15–21.
[12] Singha, AS., and Thakur, VK. Synthesis, characterization and study of pine needles reinforced polymer matrix-based composites, Journal of Reinforced Plastics and Composites 2010, 29, 700–709.
[13] Vinayagamoorthy, R. Influence of fibre surface modifications on the mechanical behavior of Vetiveria zizanioides reinforced polymer composites, Journal of Natural Fibres 2017, 16, 163–174.
[14] Alcock, Mercedes., Ahmed, Shabbir., Charme, Shawna Du., and Chad Ulven, A. Influence of stem diameter on fibre diameter and the mechanical properties of technical flax fibres from linseed flax, Fibres 2018, 6, 1–16.
[15] Vinayagamoorthy, R., Rajeswari, N., Sivanarasimha, S., and Balasubramanian, K. Fuzzy based optimization of thrust force and torque during drilling of natural hybrid composites, Applied Mechanics and Materials 2015, 787, 265–269.
[16] Ashish, Hulle., Kadole, Pradyumkumar., and Katkar, Pooja. Agave Americana leaf fibres, Fibres 2015, 3, 64–75.
[17] Vinayagamoorthy, R., Saswath Kaundinya, SL., Mani Teja, GLSN., and Adithya, Kovuru. A study on the properties of natural sandwich laminates, Indian Journal of Science and Technology 2016, 9, 1–6.
[18] Vinayagamoorthy, R., Rajeswari, N., Vijayshankar, S., and Vivekanandan, M. Surface and sub-surface analysis of hybrid polymer composites during machining operations, Procedia Materials Science 2014, 5, 2075–2083.
[19] Idicula, M., Joseph, K., and Thomas, S. Mechanical performance of short banana/sisal hybrid fibre reinforced polyester composites, Journal of Reinforced Plastics and Composites 2010, 2, 12–29.
[20] Vinayagamoorthy, R., Subramanyam, Kanakadandi Guru., Kumar, Tuduru Nikhil., and Reddy, Yerasi Harshavardhan. Modeling and analysis of drilling induced damages on hybrid composites, Indian Journal of Science and Technology 2016, 9, 1–10.

[21] Sridharan, V., Raja, T., and Muthukrishnan, N. Study of the effect of matrix, fibre treatment and graphene on delamination by drilling jute/epoxy nanohybrid composite, Arabian Journal for Science and Engineering 2016, 41, 1883–1894.
[22] Vinayagamoorthy, R., and Rajmohan, T. Machining and its challenges on bio-fibre reinforced plastics: A critical review, Journal of Reinforced Plastics and Composites 2018, 37, 1037–1050.
[23] Ramesh, M., Palanikumar, K., and Hemachandra Reddy, K. Influence of tool materials on thrust force and delamination in drilling sisal-glass fibre reinforced polymer (S-GFRP) composites, Procedia Materials Science 2014, 5, 1915–1921.
[24] Vinayagamoorthy, R., Manoj, IV., Narendra Kumar, G., Sai Chand, I., Sai Charan Kumar, GV., and Suneel, Kumar K. A central composite design based fuzzy logic for optimization of drilling parameters on natural fibre reinforced composite, Journal of Mechanical Science and Technology 2018, 32, 2011–2020.
[25] Irina, MMW., Azmi, AI., Tan, CL., Lee, CC., and Khalil, ANM. Evaluation of mechanical properties of hybrid fibre reinforced polymer composites and their architecture, Procedia Manufacturing 2015, 2, 236–240.
[26] Vinayagamoorthy, R., Rajeswari, N., and Balasubramanian, K. Optimization studies on thrust force and torque during drilling of natural fibre reinforced sandwich composites, Jordan Journal of Mechanical & Industrial Engineering 2014, 8, 385–392.
[27] Yusri Muhammad, H., Ahmad, Sahrim., Mimi Abu Bakar, A., Abdullah Mamun, A., and Hans Heim, P. Mechanical properties of hybrid glass/kenaf fibre-reinforced epoxy composite with matrix modification using liquid epoxidised natural rubber, Journal of Reinforced Plastics and Composites 2015, 34, 896–906.
[28] Vinayagamoorthy, R. A review on the machining of fibre-reinforced polymeric laminates, Journal of Reinforced Plastics and Composites 2018, 37, 49–59.
[29] Vinayagamoorthy, R. A review on the polymeric laminates reinforced with natural fibres, Journal of Reinforced Plastics and Composites 2017, 36, 1577–1589.
[30] Gupta, G., Gupta, A., Dhanola, D., and Raturi, A. Mechanical behavior of glass fibre polyester hybrid composite filled with natural fillers, IOP Conference Series: Materials Science and Engineering 2016, 149, 1–9.
[31] Vinayagamoorthy, R., Sivanarasimha, S., Vinay Kumar, KR., and Padmanabhan, Vijay. Characteristic investigations on loofah, jute and glass fibre reinforced sandwich polymeric composites, Applied Mechanics and Materials 2015, 813–814, 14–18.
[32] José Humberto Santos, Almeida Júnior., Amico, Sandro Campos., Botelho, Edson Cocchieri., and Amado, Franco Dani Rico. Hybridization effect on the mechanical properties of curaua/glass fibre composites, Composites: Part B 2013, 55, 492–497.
[33] John, K., and Venkata Naidu, S. Tensile properties of unsaturated polyester-based sisal fibre–glass fibre hybrid composites, Journal of Reinforced Plastics and Composites 2004, 23, 1815–1819.
[34] Vinayagamoorthy, R., Karthikeyan, S., Prem Bhargav, RS., and Rajivalochan, TV. Properties investigations on metallic fibre reinforced sandwich composites, Applied Mechanics and Materials 2015, 813–814, 101–105.
[35] Sathish, S., Kumaresan, M., Karthi, N., and Dhilip Kumar, T. Tensile and impact properties of natural fibre hybrid composite materials, International Journal of Modern Engineering and Research 2014, 4, 9–12.
[36] Sanjay, MR., Arpitha, GR., Laxmana Naik, L., Gopalakrishna, K., and Yogesha, B. Studies on mechanical properties of banana/e-glass fabrics reinforced polyester hybrid composites, Journal of Material and Environmental Science 2016, 7, 3179–3192.
[37] Mohaiman Sharba, J., Leman, Zulkifle., Mohamed Sultan, TH., Mohamad Ishak, R., and Mohammad Azmah Hanim, A. Partial replacement of glass fibre by woven kenaf in hybrid

composites and its effect on monotonic and fatigue properties, Bio-Resources 2016, 11, 2665–2683.
[38] Amit, Kumar., and Satnam, Singh. Analysis of mechanical properties and cost of glass/ jute fibre-reinforced hybrid polyester composites, Proceedings of the Institution of Mechanical Engineers, Part L: Journal of Materials: Design and Applications 2015, 229, 202–208.
[39] Varada Rajulu, A., and Rama Devi, R. Tensile properties of ridge gourd/phenolic composites and glass/ridge gourd/phenolic hybrid composites, Journal of Reinforced Plastics and Composites 2007, 26, 629–638.
[40] Venkata Reddy, G., Venkata Naidu, S., and Shobha Rani, T. Kapok/glass polyester hybrid composites: tensile and hardness properties, Journal of Reinforced Plastics and Composites 2008, 27, 1775–1787.
[41] Venkata Subba Reddy, E., Varada Rajulu, A., Hemachandra Reddy, K., and Ramachandra Reddy, G. Chemical resistance and tensile properties of glass and bamboo fibres reinforced polyester hybrid composites, Journal of Reinforced Plastics and Composites 2010, 29, 2119–2123.
[42] Bharath, KN., Sanjay, MR., Jawaid, Mohammad., Harisha, Basavarajappa B., and Siengchin, Suchart. Effect of stacking sequence on properties of coconut leaf sheath/jute/ E-glass reinforced phenol formaldehyde hybrid composites, Journal of Industrial Textiles 2018. doi: 10.1177/1528083718769926.
[43] Padma Priya, S., and Rai, SK. Mechanical performance of biofibre/glass-reinforced epoxy hybrid composites, Journal of Industrial Textiles 2006, 35, 217–226.
[44] Sabeel Ahmed, K., Vijayarangan, S., and Chhaya, Rajput. Mechanical behavior of isophthalic polyester-based untreated woven jute and glass fabric hybrid composites, Journal of Reinforced Plastics and Composites 2006, 25, 1549–1569.
[45] Mehmet Bodur, S., Bakkal, Mustafa., and Englund, Karl. Experimental study on the glass fibre/waste cotton fabric-reinforced hybrid composites: Mechanical and rheological investigations, Journal of Composite Materials 2016, 51, 3257–3268.
[46] Ghasemzadeh-Barvarz, Massoud., Duchesne, Carl., and Rodrigue, Denis. Mechanical, water absorption, and aging properties of polypropylene/flax/glass fibre hybrid composites, Journal of Composite Materials 2015, 49, 3781–3798.
[47] Zhaoa, Defang., Maoa, Kai., Yangb, Yuqiu., and Hamada, Hiroyuki. Flexural behavior evaluation of needle-punched glass/jute hybrid mat reinforced polymer composites, Procedia Engineering 2017, 200, 10–17.
[48] Ragavendra Rao, H., Varada Rajulu, A., Ramachandra Reddy, G., and Hemachandra Reddy, K. Flexural and compressive properties of bamboo and glass fibre-reinforced epoxy hybrid composites, Journal of Reinforced Plastics and Composites 2010, 29, 1446–1450.
[49] Gujjala, Raghavendra., Ojha, Shakuntala., Acharya, SK., and Pal, SK. Mechanical properties of woven jute–glass hybrid-reinforced epoxy composite, Journal of Composite Materials 2013, 48, 3445–3455.
[50] Haneefa, Anshida., Bindu, Panampilly., Aravind, Indose., and Thomas, Sabu. Studies on tensile and flexural properties of short banana/glass hybrid fibre reinforced polystyrene composites, Journal of Composite Materials 2008, 42, 1471–1489.
[51] Jayabal, S., Natarajan, U., and Murugan, M. Mechanical property evaluation of woven coir and woven coir–glass fibre-reinforced polyester composites, Journal of Composite Materials 2011, 45, 2279–2285.
[52] Abdul Khalil, HPS., Hanida, S., Kang, CW., and Nik Fuaad, NA. Agro-hybrid composite: the effects on mechanical and physical properties of oil palm fibre (EFB)/Glass hybrid reinforced polyester composites, Journal of Reinforced Plastics and Composites 2007, 26, 203–218.

[53] Ashok Kumar, M., Ramachandra Reddy, G., Siva Bharathi, Y., Venkata Naidu, S., and Naga Prasad Naidu, V. Frictional coefficient, hardness, impact strength, and chemical resistance of reinforced sisal-glass fibre epoxy hybrid composites, Journal of Composite Materials 2010, 44, 3195–3202.
[54] Sabeel Ahmed, K., Vijayarangan, S., and Anish, Kumar. Low velocity impact damage characterization of woven jute–glass fabric reinforced isophthalic polyester hybrid composites, Journal of Reinforced Plastics and Composites 2007, 26, 959–976.
[55] John, K., and Venkata Naidu, S. Sisal fibre/glass fibre hybrid composites: the impact and compressive properties, Journal of Reinforced Plastics and Composites 2004, 23, 1253–1258.
[56] Suresha, KV., Sumana, BG., Shivanand, HK., and Mahesha, Tensile, compression and flexural behavior of hybrid fibre (hemp, glass, carbon) reinforced composites, International Journal of Engineering and Development Research 2017, 5, 688–694.
[57] Mohan, R., Kishore, Shridhar MK., and Rao, RMVGK. Compressive strength of jute-glass hybrid fibre composites, Journal of Materials Science Letters 1983, 2, 99–102.
[58] Mohaiman Sharba, J., Leman, Z., Sultan, MTH., Ishak, MR., and Azmah Hanim, MA. Tensile and compressive properties of woven kenaf/glass sandwich hybrid composites, International Journal of Polymer Science 2016, 2016, 1–6.
[59] Ranjeth Kumar Reddy, AT., Subba Rao, BT., and Padma Suvarna, CR. Effect on compressive and flexural properties of cow dung/glass fibre reinforced polyester hybrid composites, Indian Journal of Advances in Chemical Science 2014, 2, 162–166.
[60] Tewari, Maneesh., Singh, VK., Gope, PC., and Arun Chaudhary, K. Evaluation of mechanical properties of bagasse-glass fibre reinforced composite, Journal of Material and Environmental Science 2012, 3, 171–184.
[61] Md.Nadeem, Ahmad., Madhava Reddy, D., and Baba Saheb, K. Experimental investigation on hybrid composites for characterization and prediction of properties, International Journal of Current Engineering and Technology 2016, 6, 1–9.
[62] Rajmohan, T., Vinayagamoorthy, R., and Mohan, K. Review on effect machining parameters on performance of natural fibre–reinforced composites (NFRCs), Journal of Thermoplastic Composite Materials 2018. doi: 10.1177/0892705718796541.
[63] Vinayagamoorthy, R., and Venkatakoteswararao, G. Synthesis and property analysis of green resin-based composites, Journal of Thermoplastic Composite Materials 2018. doi: 10.1177/0892705719828783.
[64] Vinayagamoorthy, R., Ankur, Sharma., Vignesh, Iyer., and Navneeth, G. Investigation of Surface Damages in Hole Making on Luffa/Jute/Glass Reinforced Plastics, Advanced Manufacturing Processes, Lecture Notes of Mechanical Engineering 2019, 521–532.
[65] Vinayagamoorthy, R. Friction and wear characteristics of fibre reinforced plastic composites, Journal of Thermoplastic Composite Materials 2018. doi: 10.1177/0892705718815529.
[66] Vinayagamoorthy, R., Sivanarasimha, S., Padmanabhan, Vijay., Ganesh, Vedula., and Karthikeyan, S. Experimental studies on water absorption and thermal degradation of natural composites, International Journal of Applied Engineering Research 2015, 10, 663–668.
[67] Vinayagamoorthy, R. Parametric optimization studies on drilling of sandwich composites using the Box–Behnken design, Materials and Manufacturing Processes 2017, 32, 645–653.
[68] Vinayagamoorthy, R., Manoj, I.V., Narendra Kumar, G., Sai Chand, I., Sai Charan Kumar, G.V., and Suneel Kumar, K. Challenges on the synthesis, characterization and machining of green fibre plastics: A review, IOP Conference Series: Materials Science and Engineering 2018, 390, 012029.
[69] Vinayagamoorthy, R. Trends and challenges on the development of hybridized natural fibre composites, Journal of Natural Fibres 2019. Doi: 10.1080/15440478.2019.1598916.

K. Palanikumar and G. Ramya Devi

2 Influence of fibre arrangement on mechanical properties of glass fibre-reinforced aluminium sandwich laminates

Abstract: The requirement for structures with sustainable weight is in well progress nowadays. Filaments (fibres) with good capability and less weight are preferred. Sandwich consisting of fibre metal laminates replaces substantial solid metals in helicopters, air vehicles and so on. In this chapter, sandwich utilizing aluminium and glass fibre sheets with various fibre frameworks, for example, unidirectional, woven roving and chopped strand matrix, is manufactured. The composites are tested for tensile, flexural and impact. The outcomes revealed that the unidirectional glass fibre-reinforced polymer-Al stack performs better obstruction in contrast to cleaved strand and woven network under shifting stacking conditions. The cross-segment of the broken examples is seen under examined electron microscopy to dissect the holding quality among metal and fibre layers.

Keywords: mechanical properties, sandwich laminates, aluminium, glass fibre

2.1 Introduction

The sandwich layer of fibre and metal overlays is favored in airplane and vehicle ventures for its lightweight, phenomenal exhaustion opposition, high quality, better consumption obstruction, sway obstruction, high harm resilience, high fire obstruction contrasted with solid aluminium laminates [1] combining the metal/fibre innovation intermixing the benefits of both the frameworks. Hence, the sandwich of metal/fibre has a commendable attribute of exhaustion and erosion obstruction, and also has high quality effect and better stiffness [2]. In aviation and vehicle applications, this half and half overlay substitutes the solid metal, where little decrease in weight results in extensive decrease of fuel cost [3, 4]. Fibre metal covers discover the application in aviation businesses for their outstanding mechanical properties and safe capabilities [5–7]. The verifiable fragile nature of glass fibre epoxy covers can be diminished by changing the fibre–framework interface [8]. Application of fibre metal covers in flying machine structures grants for

K. Palanikumar, Department of Mechanical Engineering, Sri Sai Ram Institute of Technology, Chennai, India
G. Ramya Devi, Department of Mechanical Engineering, St. Peter's College of Engineering and Technology, Research Scholar, Sathyabama Institute of Science and Technology, Chennai, India

https://doi.org/10.1515/9783110610147-002

simple fix procedures like bolted patches. The metal and filaments are reinforced either precisely or adhesively. Precisely reinforced covers are flimsier than the adhesively fortified structures [9]. The researchers demonstrated the tension fatigue test on the arrangement of fibre metal covers and furthermore demonstrated that the rate of inception of split in fibre metal overlays is incredibly low compared to plain aluminium sheet [10, 11]. Alderliesten [12] has demonstrated that the moisture content influences the cyclic stress produced in fibre metal laminates (FMLs) especially at low frequencies. Corte's and Cantwell [13] suggested to include a greater number of layers for protection from effect stacking over the plain solid materials. Additionally, he demonstrated that the glass fibre/polypropylene FML shows preferable life over the plain magnesium composites. Alderliesten [14] conferred the material property and security necessities of glass fibre strengthened aluminium cover in the fuselage skin structures, for example, exhaustion and harm resilience in contrast with solid aluminium composites. Elanchezhian et al. [15] contemplated the mechanical execution for fortified covers at various temperatures and strains, and found that carbon fibre reinforced polymer outperforms the glass fibre. Thermoplastic fibre metal covers are providing better mechanical capability, and can be utilized in the production of boards for air ships and/or cars [16]. Cantwell et al. examined the mechanical properties of a combination of self-reinforced polypropylene composite and an aluminium alloy, a new type of thermoplastic FML [17, 18]. The mechanical properties of different composite materials have been analyzed and compared with the theoretical results [19–22]. The fibre metal composites consolidate firmness and simple machinability with remarkable strength and quality.

In this chapter, the sandwich made of different layers of glass fibre-strengthened polymer and aluminium sheets is tried for assessment of mechanical qualities. The reason for this investigation is to think about the tensile, flexural and impact qualities. The composite laminate consists of five layers, in which the aluminium forms the second and fourth layers and the remaining is glass fibres.

2.2 Materials and methods

2.2.1 Materials used

Fibre glass stands out amongst the most famously utilized composite materials in household and industries. The glass fibre composite is fabricated with a mix of fibre and epoxy. The epoxy used is utilized to resist the shear and the strands that take up the loads, which are lightweight and amazingly solid, and more affordable. Likewise, it is more preferable than metal overlays because of its less weight and mass quality. Epoxy (LY 556) and hardener (HY 951) are used for the fabrication and are blended with 10:1 proportion. Aluminium is the most generally

utilized because of its quality, better erosion obstruction. The aluminium sheet used is AA1050 and is normally used in industries having proportionate strength and other properties, and it also possesses good electrical and thermal properties. Additionally, it is simple to reuse.

2.2.2 Fabrication of specimen

Hand lay-up process is the most popular method used for the fabrication of composite laminates. This method is adopted here to build the layers of sandwich laminate of glass fibre and aluminium laminate. The grade of aluminium sheet used is AA 1050 H14 of thickness 1.2 mm and size 300 mm × 300 mm. The mats of glass fibres are selected with different fibre orientation viz., unidirectional (UD), chopped strand (CSM) and woven roving mat (WRM). The alternate layers of fibre and metal are laid between the epoxy resins to build a laminate of five layers of thickness of 5 mm approximately. For strong bonding between the layers, the surface of aluminium sheet is roughened and cleaned before laying. Acetone is used for cleaning to ensure the removal of oxide layers. The mold as per the specimen size is taken. A wax coating is made on the cavity and then the resin mixture is applied over it. Now UD mats of glass fibre cut to the specimen shape is laid on it. The roller is used to apply uniform pressure. Presently the filaments are soaked with epoxy hardener blend; the aluminium sheet is put over it. Again, a gum blend is covered over the aluminium surface. Now the third layer of UD glass fibre is placed to make 90° orientations with the first layer of UD. The same procedure is repeated for 0° orientation, and then the mold is covered with a sheet of wax-coated acrylic. Pressure is maintained uniform by keeping weights and the excess resin is removed. This arrangement is left undisturbed for 6 hours for curing. Later, the laminate is removed out of the mold and its surfaces are cleaned. The same fabrication process is carried out to make the laminates of combination of aluminium with WRM and chopped strand mats (CSM).

2.3 Mechanical testing

The tensile test is performed on three different combinations of sandwich laminates made of aluminium and uni-directional glass fibres, aluminium and woven roving glass fibres and aluminium and chopped strand glass fibres. The sandwich laminates are cut into required dimensions for the tensile test as per ASTM D3039 standard [23]. The specimen edges are filed for good finishing. The speed of the cross-head and gauge length are also chosen as per the standard and carried out using universal testing machine (UTM), model: WDW 100. The structure of the specimen used before and after the testing is presented in Figure 2.1.

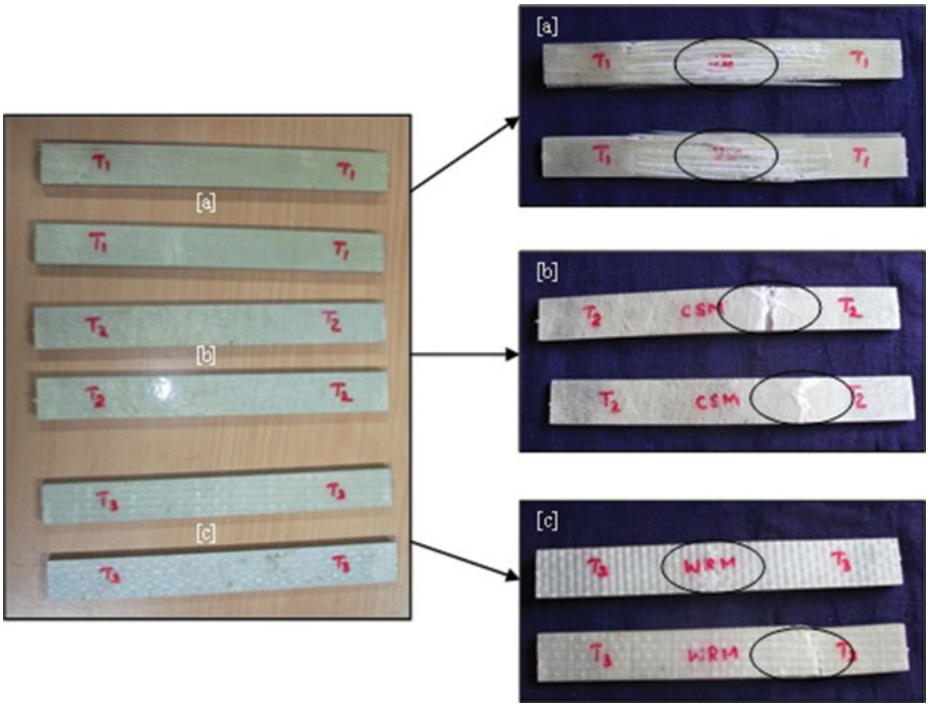

Figure 2.1: Specimens before and after the tensile test: (a) Al-UD (GFRP) laminate, (b) Al-CSM (GFRP) laminate and (c) Al-WRM (GFRP) laminate.

Flexural specimens are fabricated as per the ASTM D790 [24]. Specimens before and after the flexural testing are shown in Figure 2.2. The three-point flexural testing fixture is used for conducting the experiment. The fixture consists of two supporting part set a distance apart and the third point is the loading pin which is lowered at a constant rate till the specimen fails. During the application of load, the specimen initially starts bending till the crack appears on the stressed region and breaks at the ultimate load. This ultimate flexural load is the maximum compression load that the specimen can withstand without failure.

The Izod test is conducted on the specimens to determine their maximum impact strength [25]. It is found by measuring the energy absorbed when it is stricken with a suddenly released high velocity swinging pendulum. A single blow of this pendulum will make the specimen to break into pieces. The absorbed energy in joules is recorded which is the maximum impact strength. Toughness and ductility also can be analyzed by using this test. The specimens before and after the test are presented in Figure 2.3.

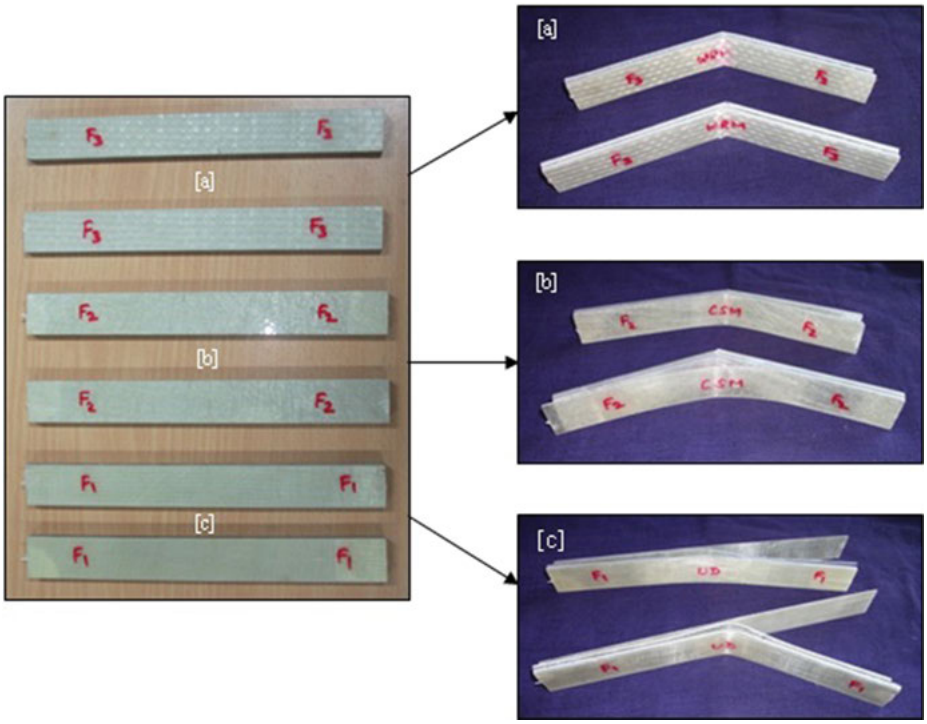

Figure 2.2: Flexural test specimens before and after the test: (a) Al-UD (GFRP) laminate, (b) Al-CSM (GFRP) laminate and (c) Al-WRM (GFRP) laminate.

2.4 Results and discussion

Tensile, flexural and impact strength of the sandwich laminates is the main objective of investigation in this chapter. Although the impact behavior of aluminium is significantly more than the glass fibre, the impact strength of sandwich of glass fibre and aluminium is comparatively better than aluminium.

Effect of fibre matrix

It is noticed that the uni-directional network of glass fibre-reinforced polymer (GFRP)-aluminium cover has more flexible modulus:

- The results show that uni-directional matrix laminate is prone to more elastic modulus when compared with other two matrix types.
- FRP (fibre-reinforced polymer) layer is first to fail in all the tests followed by the rupture of aluminium as it takes the entire load after the FRP fails.

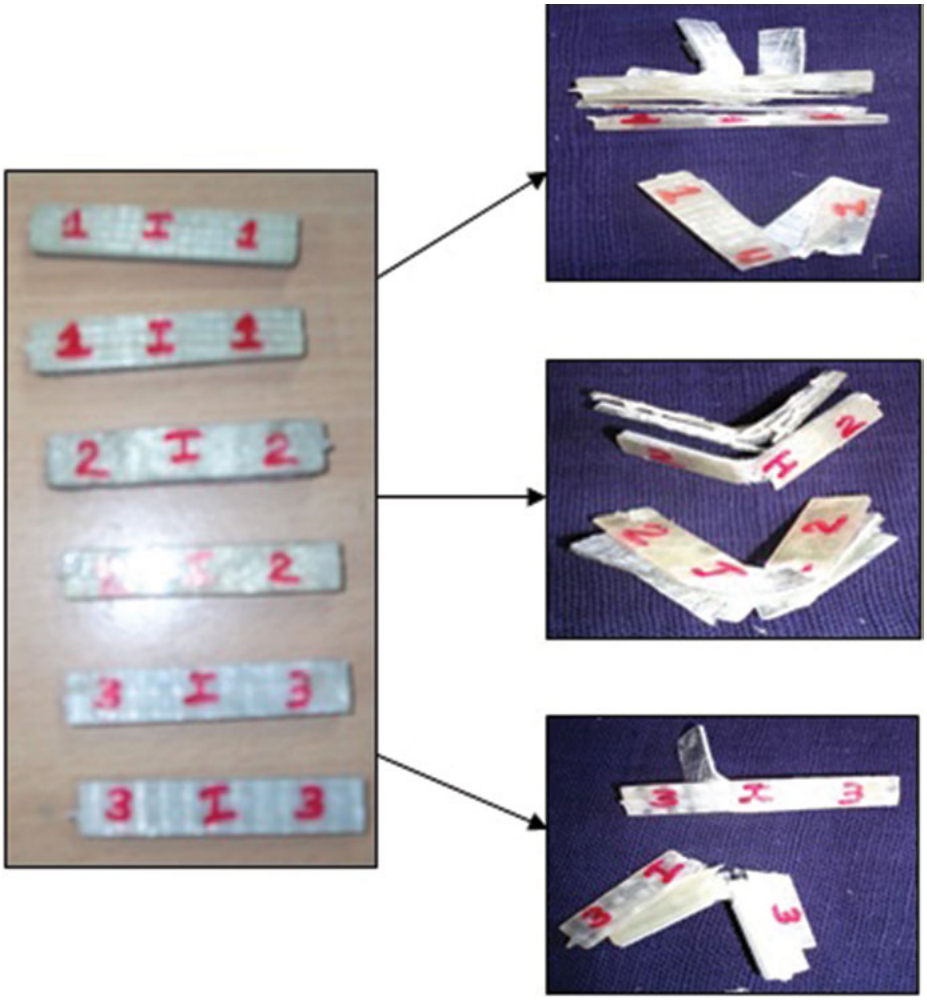

Figure 2.3: Impact test specimens before and after the test: (a) Al-UD (GFRP) laminate, (b) Al-CSM (GFRP) laminate and (c) Al-WRM (GFRP) laminate.

2.4.1 Tensile properties

Specimens made with the combinations of different matrices of glass fibre stacked with aluminium are loaded in the UTM, and tensile testing is carried out. The specimen starts elongating until its yield point is achieved and then fractures after the ultimate tensile strength is reached. Load versus displacement graphs for the matrices considered are provided in Figure 2.4. Comparison of tensile load for different combinations of hybrid composites is shown in figures. The outcome shows that the Al-UD

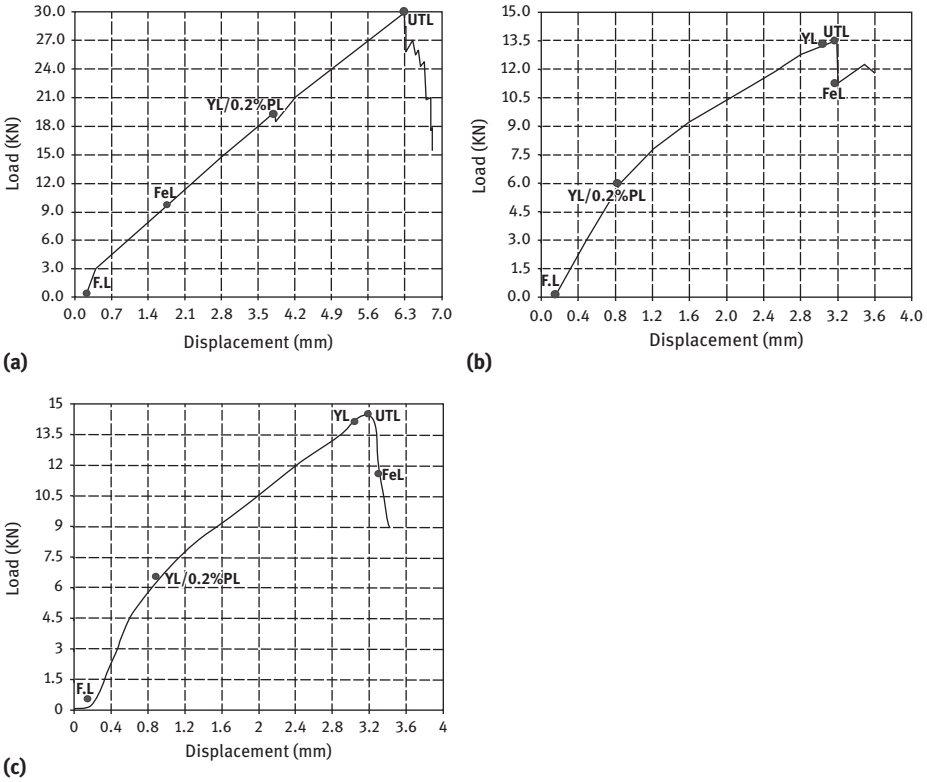

Figure 2.4: Load versus displacement graph of tensile test: (a) Al-UD (GFRP) laminate, (b) Al-CSM (GFRP) laminate and (c) Al-WRM (GFRP) laminate.

GFRP stretches better than other specimens considered. The ultimate tensile strength of the aluminium-UD, aluminium-CSM and aluminium-WRM are in the range of 179.85, 89.67 and 99.77 MPa, respectively.

Load–displacement curve in Figure 2.4 is linear until the ultimate tensile load is reached. As load increases; the displacement goes on increasing and the maximum displacement of 6.3 mm occurs at ultimate load of 30 kN, after which the specimen breaks. Figure 2.4 shows load versus displacement graph of three sandwich laminates. Figure 2.5 shows the results of the break load, displacement and elongation % of different composites.

Stress–strain relationship established shows near-linear relation till the maximum stress after which fracture occurred due to brittle property and is shown in the graphs in Figure 2.6(a–c). The application of continuous loads lead to the damage of the sandwich plate considered due to the high strain rate. It is clear that the hybrid composite made of aluminium-UD (GFRP) laminate make a ductile behavior consisting of plastic deformation till the top load of 179.85 MPa than other laminates.

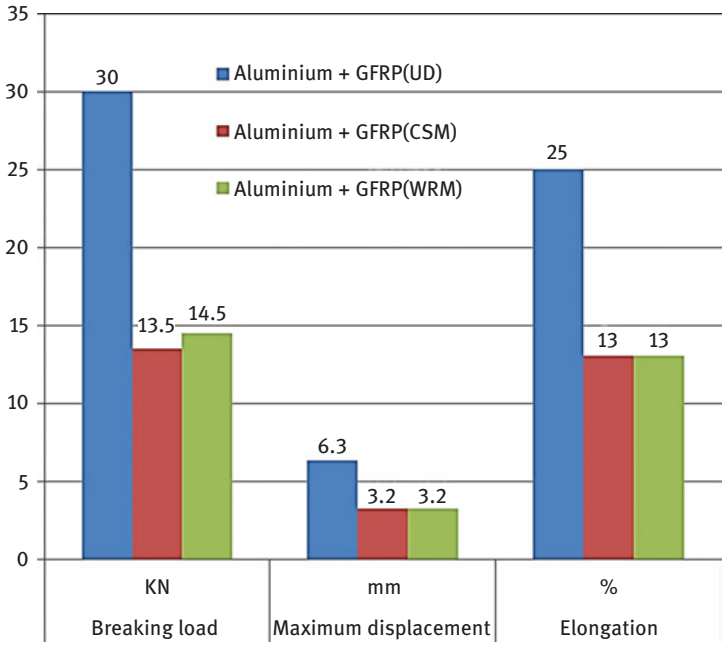

Figure 2.5: Comparison of break load, displacement and elongation % after tensile test.

The graphs in Figure 2.6 clearly show that the yield point and ultimate tensile strength of aluminium-UD combination are high when compared with the other two curves. The comparison of tensile strength of the three sandwich laminates is shown in Figure 2.7.

2.4.2 Flexural properties

When the flexural load is applied, the specimen tends to bend till the cross-sectional area where the displacement occurs reaches the yield point and then fractures begin. The specimen of UD/aluminium sandwich exhibited maximum displacement during flexural loading and its maximum flexural strength is 12 MPa. The breaking load attained is 12 kN. Load–displacement curve generated during the flexural loading condition for three different combinations of sandwich laminates is shown in Figure 2.8(a–c).

Figure 2.9 indicates the relation between the breaking load and displacement for different composites.

Figures 2.10(a–c) show the stress–strain curves of different combinations of sandwich composite laminates.

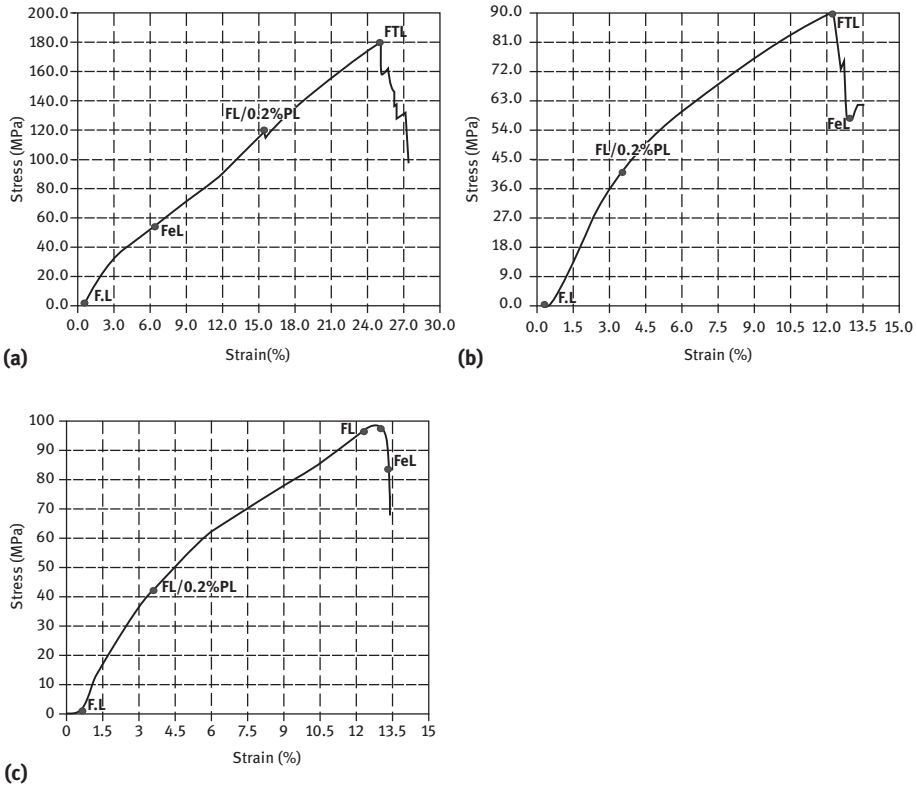

Figure 2.6: Stress–strain graph of tensile test: (a) Al-UD (GFRP) laminate, (b) Al-CSM (GFRP) laminate and (c) Al-WRM (GFRP) laminate.

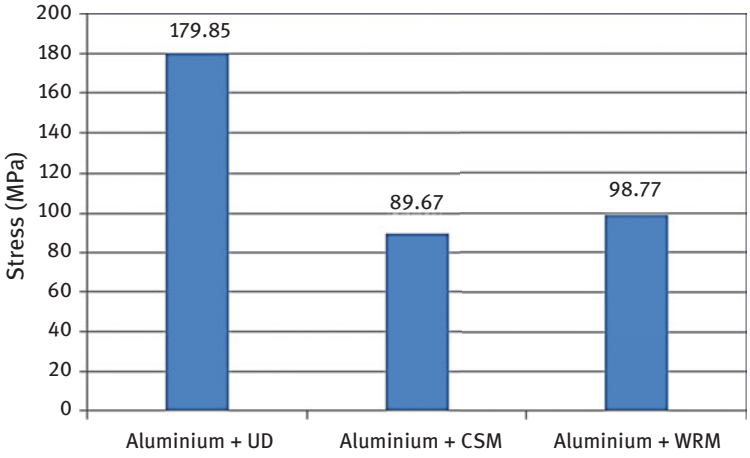

Figure 2.7: Comparison of tensile strength of the three sandwich laminates.

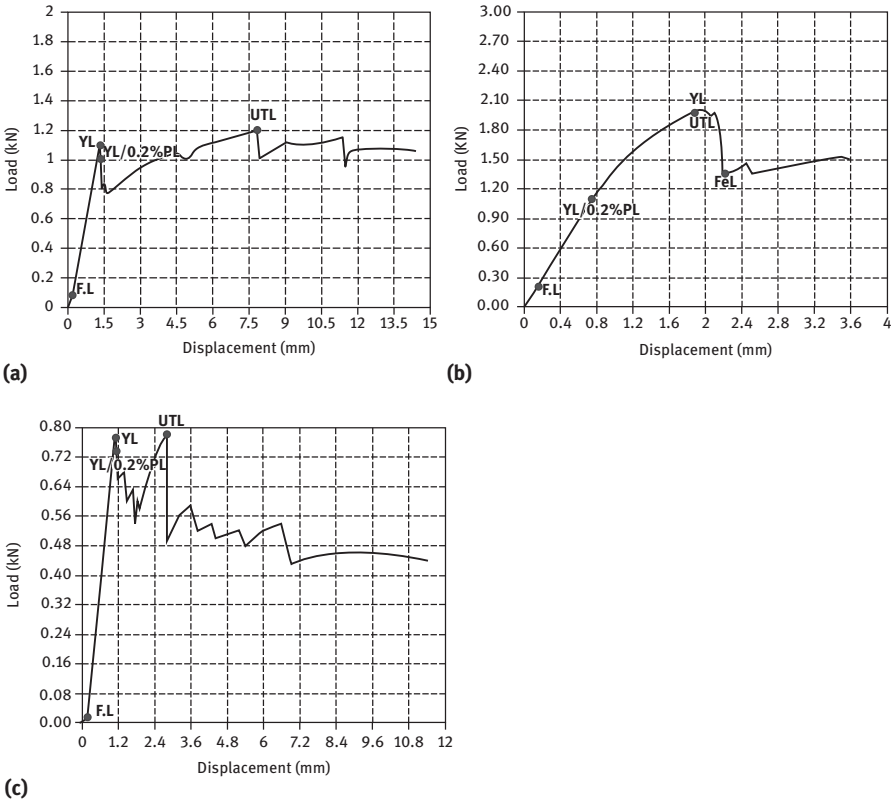

Figure 2.8: Load versus displacement graph of flexural test: (a) Al-UD (GFRP) laminate, (b) Al-CSM (GFRP) laminate and (c) Al-WRM (GFRP) laminate.

The ultimate flexural strengths of the aluminium-UD, aluminium-CSM and aluminium-WRM in the range of 12, 12.45 and 11.1 MPa, respectively, are shown in Figure 2.11.

2.4.3 Impact properties

The impact load for the aluminium-UD is higher compared with the other two mixes of composites. Comparison of the results of different composites is shown in Figure 2.12. The UD/aluminium sandwich laminate withstands maximum impact energy, which improves the impact strength of the whole composite material.

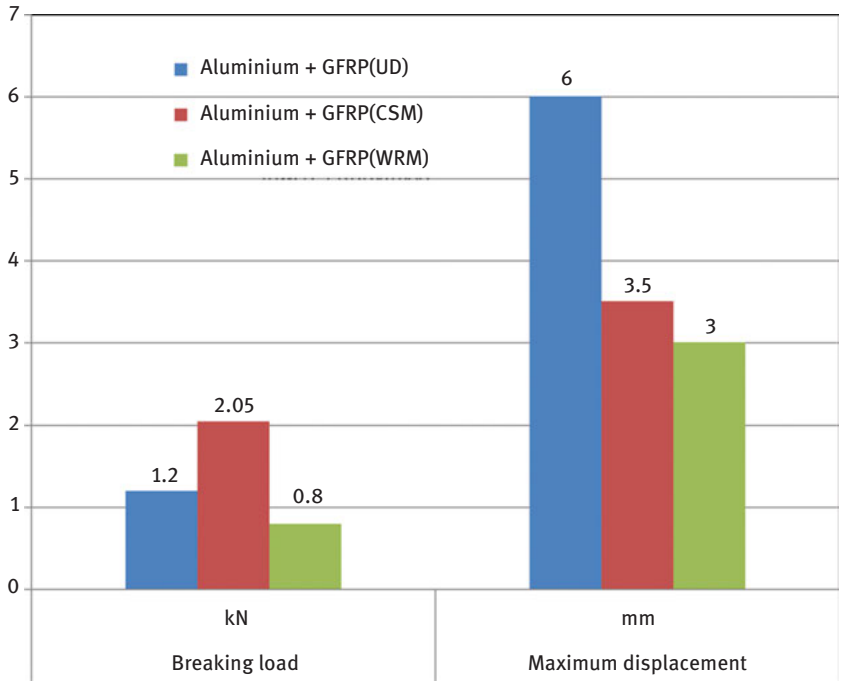

Figure 2.9: Comparison of break load and displacement after flexural test.

2.5 Scanning electron microscopy analysis

The fractured topography is analyzed through scanning electron microscopy (SEM). The images revealed the fact that the fibre failure is due to its pullout, breakage and matrix debonding. The microscopic image of the aluminium UD (GFRP) specimen failed under tensile loading is shown in Figure 2.13(a). The necking of aluminium layer during tensile loading occurs in specimen that dislocates the alignment of the sandwich laminates but still the UD fibres withstand the high tensile strength compared to the WRM and CSM of the glass fibre. The fibres are being pulled out and broken due to the high tensile force that is applied, which is clearly visible in the microstructure.

The voids formed and delamination in the specimen prior to aluminium layer fracture is also visibly seen in Figure 2.13(b). In chopped strand matrix the randomly distributed fibres will take up the load from any direction compared to UD and WRM of glass fibres. Though it withstands all types of loads, the maximum limit is comparably less due to the discontinuity in the length. Discontinuity is also one of the reasons for the delamination of the aluminium layer from the fibre layer.

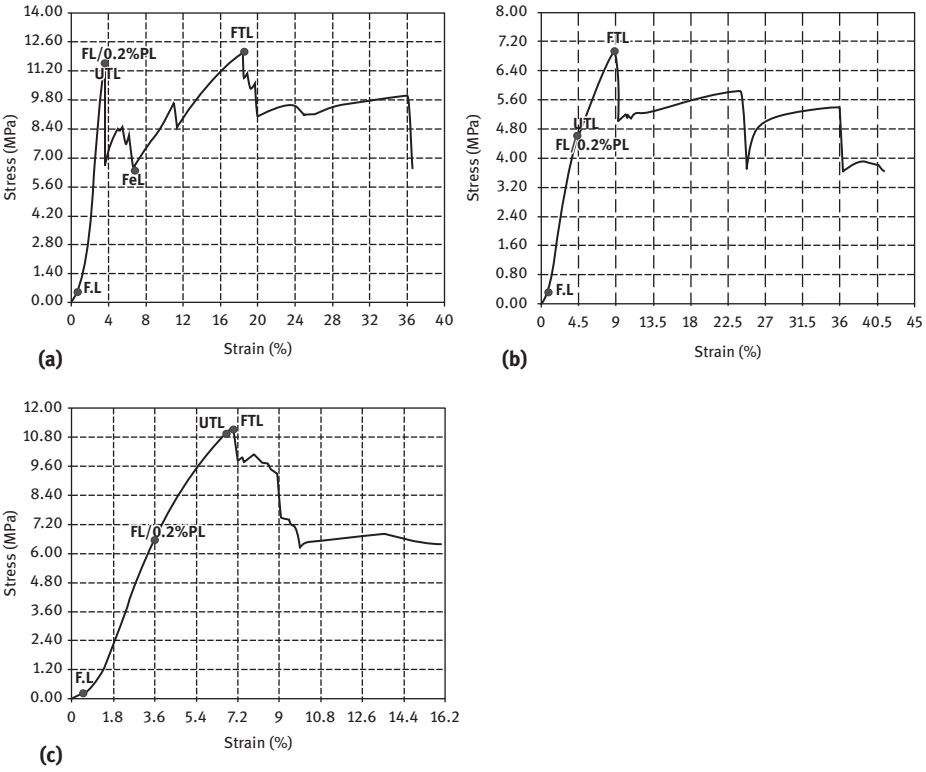

Figure 2.10: Stress–strain graph of flexural test (a) Al-UD (GFRP) laminate, (b) Al-CSM (GFRP) laminate and (c) Al-WRM (GFRP) laminate.

Figure 2.13(c) shows the cracking and delamination of aluminium and FRP layer of the third composite of aluminium with WRM stacking. The woven roving specimen is the most damaged specimen under tensile loading. The image shows clearly how the fibres had been pulled out enormously, which leads to initiation of cracking in the fibre–resin matrix and due to this cracking, the delamination occurs in between the FRP layer and aluminium layer. Finally, it is clearly evidenced from the microstructure of the fractured specimen that the UD mat GFRP and aluminium stack exhibits better surface texture with less voids, minimum fibre pullouts and less damage, while the other two combinations of sandwich laminates possess many damages, cavity formations, cleavages and others. Therefore, it is concluded that the UD fibre matrix with aluminium sandwich performs better under tensile loading.

After the three-point flexural testing, the specimens had undergone severe fracture in FRP layers. The images of failed specimens under SEM display the formation

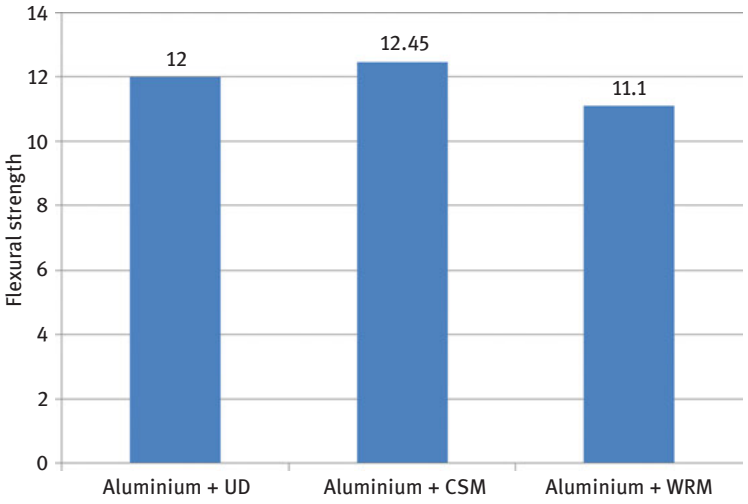

Figure 2.11: Comparison of flexural strength of three sandwich laminates.

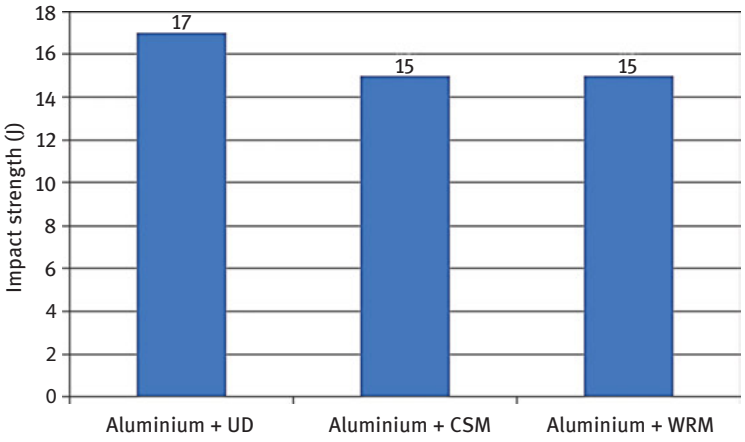

Figure 2.12: Impact energy comparison of different composite materials.

of big cavity in the FRP layer and also the delamination of aluminium and fibre layers. Due to heavy compressive load, the fibre had been pulled out in a mass from a particular area where the stress induced is more. The fractured flexural-loaded specimen of UD/aluminium sandwich laminate is shown in Figure 2.14(a), which displays cracking to occur in the matrix bonding between aluminium and GFRP

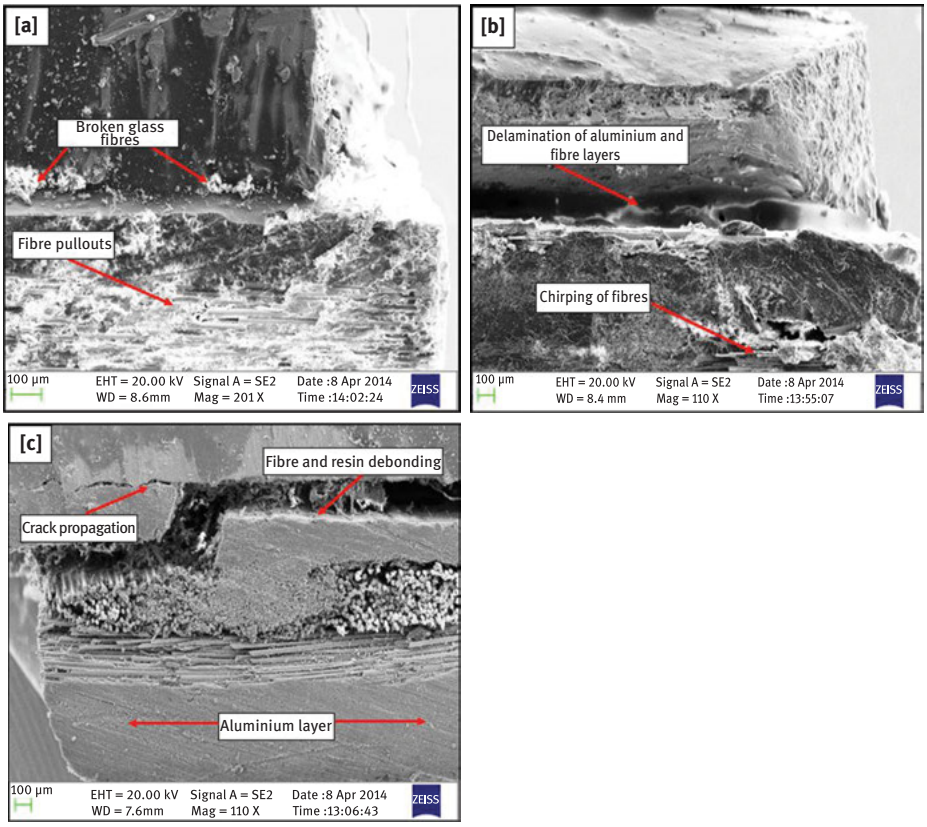

Figure 2.13: SEM images of the fractured tensile loaded specimen: (a) Al-UD (GFRP) laminate, (b) Al-CSM (GFRP) laminate and (c) Al-WRM (GFRP) laminate.

layers. This debonding leads to failure of the specimen in compression load. The clusters of fibres have been pulled out from the portion of FRP layer.

The microstructure of the fractured aluminium-CSM sandwich laminate is shown in Figure 2.14(b), which clearly shows how the sandwich layers are being dislocated after flexural loading. The dislocation leads to the delamination of the laminates and the composite fails. Figure 2.14(c) also indicates that the most damaged specimen is the aluminium-CSM sandwich comparable with the other two combinations. During bending, the resin in between the fibres also gets damaged, which lead to resin fissures. The other common damages include fibre pullouts, parting of aluminium and GFRP layers.

The image shown in Figure 2.14(c) is the fractured surface of the aluminium WRM sandwich laminates under flexural loading. The main injuries are fibre chipping, delamination and fibre damages. The failure of this specimen may be due to the parting of the layers.

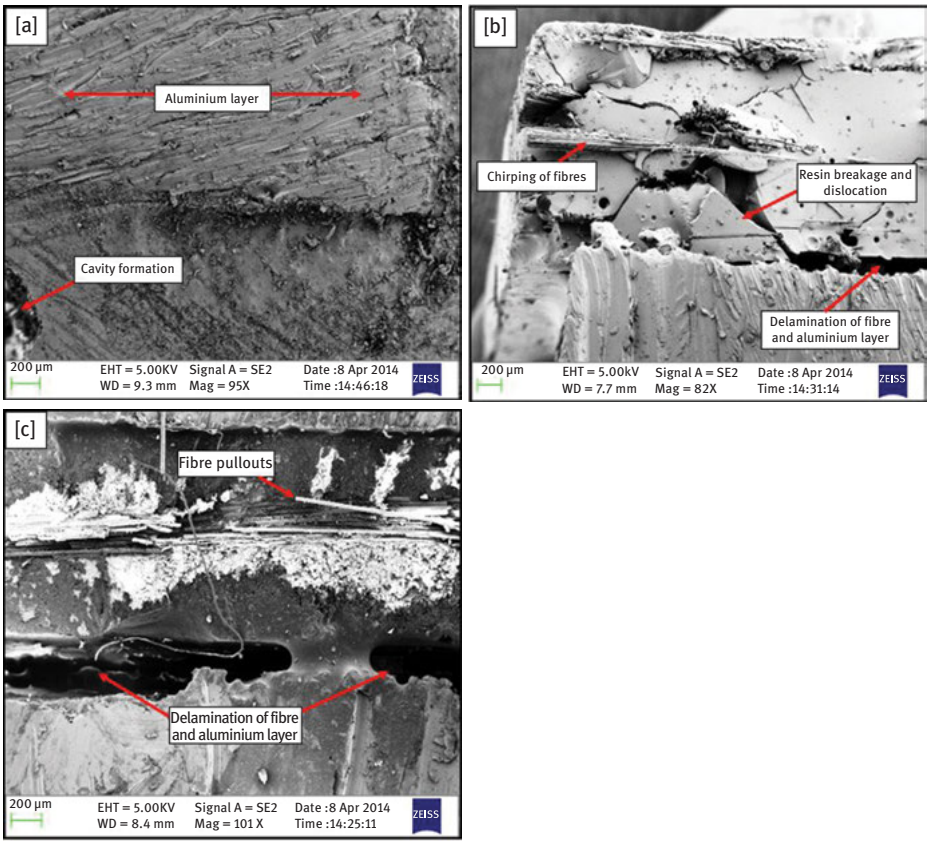

Figure 2.14: SEM images of fractured flexural-loaded specimen: (a) Al-UD (GFRP) laminate, (b) Al-CSM (GFRP) laminate and (c) Al-WRM (GFRP) laminate.

Finally, it is concluded that the structure of all specimens undergoes severe damages during flexural damage and that is the reason that the flexural strength of the specimens is low compared with their tensile strength. So this sandwich laminates can be applied in the components that have to withstand more tensile loads.

2.6 Conclusions

1. The ultimate tensile strength of UD glass fibre sandwich is 179.85 MPa and is relatively more comparable with the other two combinations.
2. The percentage elongation of Al/UD glass fibre is more than the other laminates considered under tensile loading. Therefore, the aluminium-UD combination of composite behaves more elastically before failure.

3. The ultimate flexural strength of the sandwich laminates are less than their tensile strength and aluminium–CSM combination has the highest flexural strength of 12.45 MPa than the other two combination.
4. The impact energy of aluminium-UD sandwich laminate is 17 J, while for CSM and WRM sandwich composite is 15 J.

The outcome of the various tests shows that the UD/aluminium sandwich laminate is found to possess good tensile and impact strength. Using SEM, the topographical structure of the failed specimens is also analyzed for the reason of failures. Finally, it is concluded that the fibre orientation and pattern of fibre mat influences the mechanical behavior of the sandwich laminate considered in this work.

References

[1] Vogelesang, L.B., and Vlot, A. Development of Fibre metal laminates for advanced aerospace structures, Journal of Materials Processing Technology 2000, 103, 1–5.
[2] Chang, PY., Yeh, PC., and Yang, JM. Fatigue crack initiation in hybrid boron/glass/aluminium fibre metal laminates, Materials Science Engineering 2008, A 496, 273–280.
[3] Mathivanan, P., Balakrishnan, M., and Krishnan, H. Metal thickness, fibre volume fraction effect on the tensile properties, debonding of hybrid laminates, Journal of Reinforced Plastics and Composites 2010, 29.
[4] Asundi, A., and Choi, Y. N. Fibre metal laminates: an advanced material for future aircraft, Journal of Material Processing Technology 1997, 63, 384394.
[5] Vlot, A., and Gunnink., JW. Chapter 1, Fibre Metal Laminates – An Introduction, Dordrecht, 2001, The Netherlands, Kluwer Academic Publishers.
[6] Hancox, N.L. Fibre composite hybrid materials, Applied Science, 1981, London.
[7] Hibbs, M.F., Tse, M.K., and Bradley, W.L. Interlaminar fracture toughness and real-time fracture mechanics of some toughened graphite/epoxy composites, N.J. Johnston, Ed., Toughened Composites ASTM STP, Vol. 937, American Society for Testing and Materials, 115–130.
[8] Kim, J.K., and Mai, Y.-W. Effects of interfacial coating and temperature on the fracture behaviour of unidirectional Kevlar and carbon fibre reinforced epoxy composites, Journal of Material. Science 1991, 26, 4702–4720.
[9] Sinmazçelik, Tamer., Avcu, Egemen., Bora, Mustafa Özgür., and Çoban, Onur. A review: fibre metal laminates, background, bonding types and applied test methods. Materials and Design 2011, 32, 3671–3685.
[10] Alderliesten, R. On the development of hybrid material concepts for aircraft structures, Recent Patents Engineering 2009, 3, 25–38.
[11] Vogelsang, LB., Schijve, J., and Fredell, R. In: Demaid A, de Wit JHW editors. Case studies in manufacturing with advanced materials, 1995, Vol. 2, Amsterdam, Elsevier.
[12] Alderliesten, RC. Chapter 11 in Fibre metal laminates; an introduction, 2001, Dordrecht, Kluwer Academic Publishers.
[13] Corte´s, P., and Cantwell, W.J. The fracture properties of a fibre–metal laminate based on magnesium alloy, Composites: Part B 2006, 37, 163–170.
[14] Alderliesten, R.C., and Homan, J.J. Fatigue and damage tolerance issues of Glare in aircraft structures, International Journal of Fatigue 2006, 28, 1116–1123.

[15] Elanchezhian, C., Ramnath, B. Vijaya., and Hemalatha, J. Mechanical behaviour of glass and carbon fibre reinforced composites at varying strain rates and temperatures, Procedia Materials Science 2014, 6, 1405–1418.
[16] Reyes, G., and Kang, H. Mechanical behavior of lightweight thermoplastic fibre–metal laminates, Journal of Materials Processing Technology 2007, 186, 284–290.
[17] Wu, H.F., and Wu, L.L. A study of tension test specimens of laminated hybrid composites. Part II. Size and alignment effect, Journal of Materials Science 1994, 29, 5847–5851.
[18] Carrillo, J.G., and Cantwell, W.J. Mechanical properties of a novel fibre–metal laminate based on a polypropylene composite, Mechanics of Materials 2009, 41, 828–838.
[19] Ramya Devi, G., and Palanikumar, K. Tensile property evaluation of woven glass fibre reinforced plastic and aluminium stack, Applied Mechanics and Materials 2015, 766–767, 44–49.
[20] Anand, P., and Anbumalar, V. Mechanical properties of cellulose-filled epoxy hybrid composites reinforced with alkali-treated hemp fibre, Polymer (Korea), 39(1), 46–55.
[21] Athijayamani, A., Ganesamoorthy, R., Loganathan, K. T., and Sidhardhan, S. Physical and mechanical properties of unidirectional aligned agave Sisalana variegata fibre-reinforced vinyl ester composite, Polymer (Korea) 2016, 40(1), 1–8.
[22] Ramya Devi, G., and Palanikumar, K. Mechanical properties evaluation of unidirectional glass fibre reinforced aluminium sadwich laminate, Silicon 2018, 10, 2329–2340.
[23] ASTM standards: D 3039, Annual Book of ASTM Standards volume information, 15.03, 1 (2008).
[24] ASTM standards: D 790 Annual Book of ASTM Standard, Vol. 08.01 (2002).
[25] ASTM standards: D 256 Annual Book of ASTM Standard, Vol. 08.01 (2002).

Mostafa Seifan, Tom Sunny, and Gehan Anthonys

3 Glass fibre-reinforced composites and their drilling-induced delamination

Abstract: Due to the unique characteristics, polymer matrix composites have been widely produced and used in various applications. In this chapter, the effects of synthetic fibres and polymers on the final characteristics of polymer composites, particularly glass fibre-reinforced polymer (GFRP), are discussed. Additionally, the influence of machining processes on the generation of delamination and development of defects in GFRP are elaborated. Finally, the delamination assessment as a major defect caused by machining processes is modelled by an algorithm. The proposed approach shows promising and can effectively interpret a large amount of data in a short period of time.

Keywords: GFRP, delamination, delamination pixel ratio, image processing, machining process

3.1 Introduction

Over the last decades, lightweight design has become an important factor for many industrial sectors such as marine, aeronautical and construction industry. Among all fabricated materials, fibre-reinforced composites have drawn much attention over conventional monolithic materials because of their excellent stiffness and strength as well as low density and lightweight. In these materials, fibres are placed into a matrix to form a composite. Fibres are categorized into two main classes, namely natural and synthetic. Natural fibres are classified according to their origin where they are extracted. This type of fibre is generally obtained from plant, animal or mineral sources. High specific strength and stiffness, cheap price and low density are the most advantages of natural fibres. Moreover, natural fibres are sustainable and less hazardous to the environment. However, low durability and impact resistance, high moisture absorption and sensitivity to high temperature are the main shortcomings associated with natural fibres [1].

On the other hand, synthetic fibres are obtained from a chemical synthesis. This type of fibres is known for their high mechanical properties, excellent resistance to

Mostafa Seifan, School of Engineering, Faculty of Science and Engineering, The University of Waikato, Hamilton, New Zealand
Tom Sunny, Department of Mechanical Engineering, Amal Jyothi College of Engineering, Kerala, India
Gehan Anthonys, Department of Electrical and Computer Engineering, Faculty of Engineering Technology, The Open University of Sri Lanka, Nugegoda, Sri Lanka

https://doi.org/10.1515/9783110610147-003

corrosion and relatively good impact characteristics. Due to being inexpensive and possessing a relatively high mechanical properties, one of the mostly used reinforcements in composite materials is glass fibres. It has reported that glass fibre alone has more than US$7 billion global market as it is durable under different environmental conditions [2]. However, when glass fibre-reinforced polymers (GFRPs) reach the end of their lifespan, they become a source of unsustainability as they are not biodegradable and recyclable. Moreover, the majority of synthetic fibre-reinforced composites including GFRPs are susceptible to machining process, which may significantly decrease their functionality and performance. It has been reported that in aerospace industry, delamination caused by drilling is responsible for more than half (60%) of part rejections [3]. There are two main types of mode of failures: peel-up and push-out delamination, which results in a decrease in the mechanical and toughness of the composite.

In this chapter, we describe the mostly used synthetic fibres as reinforcement in thermoplastic and thermoset polymeric matrices. Furthermore, the general applications of glass fibre-reinforced composites and the negative effect machining on the properties of GFRPs are discussed. Finally, the delamination evaluation as the major defects caused by machining processes is modelled by an algorithm.

3.2 Fibre-reinforced polymer composites

Composites are described as the materials that compose two (or more) physically or chemically distinct phases, namely reinforcement and matrix. The main purpose of incorporating reinforcement in a matrix is increasing the load-resistant capacity in specific directions, while the matrix transfers the load by providing the effective bonding of reinforcements. Particle, flake, fibre and laminar are the mostly used reinforcements in fabrication of composite products. Particulate composites are made of particles (in form of flakes or powder) distributed or incorporated in a matrix. It has been noted that particulate fillers like micro/nano-SiO_2, $Mg(OH)_2$, Al_2O_3, $CaCO_3$ and glass modify the mechanical and physical properties of polymers [4]. The presence of particulate fillers can improve the stiffness of a composite as the rigid inorganic particles possess reasonably higher stiffness rather than polymeric matrices [5–7], whereas their effectiveness on strength relies on the rate of stress transferring between the embedded particles and matrix [8]. Liang et al. [9] conducted a research on the effects of glass bead fillers on the mechanical properties of polyethylene (PE) composites. Their results showed that the tensile strain of composites declines with the increase in bead weight fraction. As compared to untreated beads, a higher tensile strength of composites was noticed when the surface of glass beads was pre-treated with the coupling agent. Likewise, another research group in France [10] studied the influence of nano-SiO_2 fillers on the properties, especially mechanical properties of reinforced PA6, and the authors concluded that

both compressive and tensile strength are sensitive to the filler contents and their dispersion. This indicates how efficient bonding of particles and matrix contributes to increasing the mechanical properties of composites.

Flakes are another type of reinforcements that are thin and flat. They usually reinforce in two dimensions and have even properties (mechanical) in the plane of flakes along with a low production costs. Similar to particulate composites, the behavior of flake-reinforced polymer composites depends on the properties of interfacial strength of the polymer and the embedded flake. The coupling agents offer a potential solution to address the poor bonding between reinforcement and matrix by promoting interfacial adhesion as well as protecting against environmental degradation. In 2010, Broughton et al. [11] explored the effect of various coupling agents, specifically aminosilane and titanate, on both thermal and mechanical properties of glass flake-reinforced polypropylene (PP) composite. Their findings revealed that the stiffness and strength of glass flake-reinforced polymer rely on the type and also on the amount of the coupling agent. It was found that treated glass flakes with aminosilane had a higher flexural property than both PP (as a matrix) and untreated glass flake PP composite. Overall, the addition of glass flake coated with aminosilane showed higher mechanical properties than those flakes treated with titanate. This phenomenon is due to an efficient adhesion between glass flakes and matrix, which can effectively transfer the stress in the composite. In another study, the thermal behavior of graphite flake-reinforced polymers was investigated [12]. It was shown that the incorporation of graphite flake (40% v) in acrylonitrile butadiene styrene (ABS) resulted in a 35% improvement in the thermal decomposition temperature.

Fibrous composites are the most commonly used form of composite in which reinforcements are embedded into a matrix in the form of individual fibres or laminae [13]. Laminae are an arrangement of unidirectional or woven fibres and a laminate is formed by stacking of lamina in at least two different directions. Over the past few decades, researchers' attention has been drawn to FRP materials as the potential alternative to monolithic materials. Due to the unique characteristics of FRP composites, including ease of handling, high strength-to-weight ratio, non-magnetic properties and chemical and corrosion resistance, they are extensively used in many industries such as aerospace, automotive, construction and sporting industry [14]. However, FRP composites have a brittle failure and are fairly weak in transverse or shear stresses, poor fire resistant and sensitive to stress-rupture effects [15].

3.2.1 Synthetic fibres used as reinforcements

The main role of fibres is the provision of strength and stiffness to the composite, and they are classified into two main groups, namely (i) advanced fibres such as carbon and aramid and (ii) glass fibres. Carbon fibre is one of the inorganic fibrous

materials used as a reinforcement in different matrices. It is estimated that more than 90% of carbon fibres are made up on the carbonization of a carbon-containing polymer precursor fibre "polyacrylonitrile" at high temperature through control stretching phases [16]. The remaining 10% is fabricated when rayon or petroleum pitch is carbonized. Carbon fibres can be categorized according to the different factors, including the properties of carbon fibres, precursor fibre materials and the temperature used for a heat treatment process. For instance, based on the properties of carbon fibres, they are categorized into (i) ultra-high modulus with modulus of elasticity (E) greater than 450 GPa, (ii) high modulus with an E ranging from 350 to 450 GPa, (iii) intermediate modulus with an E ranging from 200 to 350 GPa, (iv) low modulus of elasticity/high tensile with an E less than 100 GPa and tensile strength greater than 3 GPa and lastly (v) super high tensile with a tensile strength greater than 4.5 GPa [15]. Carbon fibres have a high stiffness, and this feature varies based on their grades. For example, the stiffness and strength of carbon fibre polymer composites (CFRP) are five times higher than steel. However, factors like the types of matrix and carbon fibre, distribution and alignment of carbon, fibre content, fibre void content, the interfacial strength between fibre and matrix, as well as the method of manufacturing have been reported to be influential on the final characteristics of CFRP [17]. As compared to metallic materials, CFRPs are distinguished by their exceptional fatigue resistance when subjected to the cycling stresses [18]. The performance of CFRP under cyclic loads relies on many factors, including the type of stress (compression or tension), quality of bonding between fibre and matrix and stacking sequence [19–21]. However, the transverse flexural strength of CFRP is considerably decreased when it exposes to water or alkaline medium at a high temperature [22]. This reduction is mainly due to a decrease in the bonding quality between fibres and matrix.

Aramid fibres are another type of synthetic fibres that are known under their trade names Kevlar (para-aramid) and Nomex (meta-aramid). As depicted in Figure 3.1, aramid fibres are considered as the polymer belonging to the polyamide

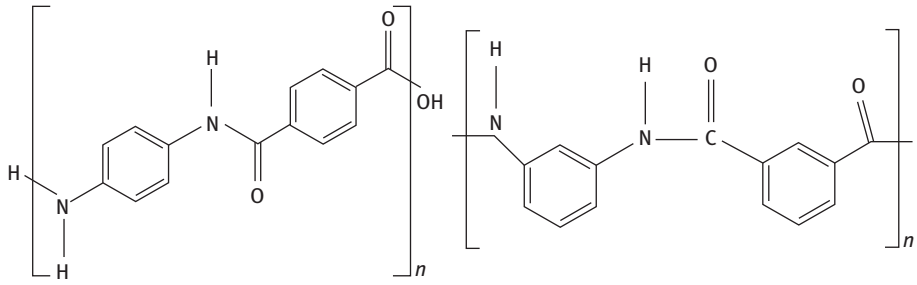

Figure 3.1: The structure of aramid fibres: (a) Kevlar and (b) Nomex.

family that at least 85% of the amide groups are joined to two aromatic rings [23]. Mechanical and physical properties of these organic fibres have been summarized in Table 3.1. Impact resistant applications and textile are the most uses of aramid fibres. It has been reported that these fibres have higher creep rates than carbon and glass fibres [24]. Pıhtılı and Tosun [25] conducted an investigation using a block-on-shaft set-up to define the behavior of wearing in aramid fibre-reinforced composite at various sliding speeds. The authors noticed that the weight loss in aramid fibre composites was lower than glass fibre composites, suggesting that the aramid fibres had a higher wear strength as compared to glass fibres. In another investigation, the influence of heat treatment on mechanical properties of Kevlar-29 fibres was explored [26]. The increase in the heat treatment temperature negatively influenced the tensile strength and tensile strain of the Kevlar fibres. However, no such effect was noticed when the fibres were treated at a constant temperature, which might be due to a relatively short heating duration.

Table 3.1: The mechanical and physical properties of aramid fibres [27, 28].

Fibre	Modulus (GPa)	Elongation (%)	Density (g/cm^3)
Kevlar-29	70	3.6	1.43
Kevlar-49	135	2.8	1.45
Kevlar-119	55	4.4	1.44
Kevlar-129	99	3.3	1.45
Kevlar-149	143	1.5	1.47
Nomex	17	22	1.38

Among the high performance fibres, glass fibres have drawn much attention and been used for many applications due to an array of characteristics like being corrosion resistant, lightweight, excellent in damping characteristics, electrical insulator, cheap and, most importantly, efficient bonding with polymeric matrix surrounding. The extraordinary fabrication adaptability and flexibility have resulted in a massive investigation for the development of GFRP. These features make this advanced composite as a material of choice for many prime applications such as renewable energy, transportation and infrastructure. It has been reported that every year more than 5 million metric tons of glass fibres are consumed worldwide [29]. Depending on the key properties for specific composite applications, glass fibres are classified into different groups as follows:

- E: General-purpose fibre
- E-CR: Electrical insulation and high acid corrosion resistance
- C: High acid corrosion resistance
- AR: High alkaline resistance (mostly used in Portland cement)
- D: Excellent electric performance

- R: High modulus
- S: High strength, high modulus of elasticity as well as extreme temperature resistance

In general, E and E-CR glass fibres are the mostly used commercial fibres as compared to other classes that exhibit unique properties to meet a special requirement. Li et al. [29, 30] extensively discussed the chemical composition of continuous glass fibres used as reinforcement. Compounds including Al_2O_3 and SiO_2 are the main constituents of glass fibres. The addition of other chemicals, such as MgO, CaO, BaO, R_2O, F_2, ZrO_2, Fe_2O_3, TiO_2 and Re_2O_3, can bring new characteristics to the glass fibre system. For instance, the addition of both MgO and CaO into S glass fibre results in designing new subclass of S glass fibre that has a lower liquidus temperature. The various combinations of the above-mentioned compounds in a basic form of glass fibres lead to fabrication of glass fibres with different mechanical and physical properties, including viscosity, liquidus temperature, thermal behavior, chemical resistance and density. As a result of these flexibilities, functional GFRP with different properties can be easily designed and produced.

3.2.2 Selection of polymers

Selection of polymeric matrices is one of the most significant factors in manufacturing of an FRP composite product. The polymeric matrix transfers the load to the incorporated fibres via shear stress at the interface [14]. As a result of this, the role of fibre matrix adhesion has become a significant parameter to provide an effective bonding between the embedded fibres and the polymeric matrix. It has been reported that the poor adhesion at the interface not only decreases the mechanical properties but also makes the composite susceptible to the chemical and environmental attacks, which substantially reduces its durability and service life [14]. Matrices are responsible for protecting the composite against the surrounding environment and mechanical abrasion. In addition, they have a key role in determining heat resistance and processability of composites, in-plane shear strength and interlaminar shear strength. They are also effective in improvement of impact and fracture resistance by decreasing crack growth propagation. For an efficient fabrication of functional composites, different criteria need to be considered to produce a high-quality FRP composite. Therefore, the matrix must be able to tolerate harsh environment such as temperature, humidity, abrasion, ultraviolet radiation and chemical attack, in addition to transferring the excreted stresses.

There are different matrix phases to be used in composite materials, including ceramics, metals and polymers. Polycondensation, polymineralization and polyaddition are the most common practices for the fabrication of synthetic polymers [15]. Due to their macromolecular properties, polymeric materials differ from other forms

of matrices such as metals and ceramics. In general, there are two common polymer classifications used as a matrix for the fabrication of FRP, namely thermoplastic and thermoset. The type of polymeric matrix is determined based on the application, type of reinforcement, required mechanical properties and operating conditions. The following lists are among the mostly used thermoplastic matrices:

- cellulose acetate;
- PP;
- polystyrene (PS);
- nylon, PE;
- polyvinyl chloride;
- polyethylene terephthalate;
- polyetherimide;
- polybutylene terephthalate;
- polyether ether ketone;
- polycarbonate;
- ABS.

The physical and mechanical properties of thermoplastic matrices are listed in Table 3.2 [31]. A high impact resistance, re-formability, stability, excellent chemical and thermal resistance are the most significant attributes of thermoplastic matrices.

Table 3.2: The physical and mechanical properties of thermoplastic and thermoset matrices.

Matrix	Name	Density (g/cm^3)	Tensile modulus (GPa)	Tensile strength (MPa)
Thermoplastic	Cellulose acetate	1.28–1.32	2.40–4.10	31.00–55.20
	Polyether ether ketone	1.32	3.60	90.00–100.00
	Polypropylene	0.90–0.91	1.10–1.60	20.00–40.00
	Polyetherimide	1.25–1.32	2.81–2.98	89.50–109.00
	Polyethylene	0.91–0.95	0.30–0.50	25.00–45.00
	Polyethylene terephthalate	1.38–1.46	2.80–3.10	55.00–75.00
	Polyvinyl chloride	1.38	3.00	53.00
	Polystyrene	1.04–1.05	2.50–3.50	35.00–60.00
	Acrylonitrile butadiene styrene	1.02–1.20	1.00–2.65	22.10–59.30
	Polycarbonate	1.20–1.22	2.00–2.40	55.00–75.00
Thermoset	Polyester	1.00–1.50	2.00–4.50	40.00–90.00
	Polyurethane	1.03–1.72	1.34–2.03	48.47–57.64
	Phenolic	1.29	2.80–4.80	35.00–62.00
	Epoxy	1.10–1.60	3.00–5.80	28.00–100.00
	Polyamide	1.09–1.14	2.60–3.30	78.00–82.00
	Vinyl ester	1.20–1.40	3.10–3.80	69.00–86.00

On the other hand, polyester, polyurethane, vinyl ester, epoxy, polyamide and phenolic are the mostly used thermoset polymers. Unlike thermoplastic matrices, these types of polymers are usually liquid at ambient temperature and this feature makes them favorable for impregnation of reinforcement fibres. Excellent resistance to heat and chemical corrosion, high fatigue strength, efficient adhesion with fibres and excellent finishing are the other beneficial characteristics of thermoset matrices. On the contrary, the recycling of thermoset composites is a matter of challenge as they cannot be remolded. Moreover, some of the thermoset matrices are sensitive to UV irradiation, which may limit their applications where UV radiates to the composite.

3.2.3 General applications

The advances in the design and fabrication of high-performance synthetic FRP composites have led to a broad array of applications. FRP composites have turned to structurally viable construction materials for various purposes such as load bearing elements in formworks, bridges, modular structures and buildings. GFRP composites are used as external or internal reinforcements for building elements. Among all FRPs, GFRP has been extensively used for construction purposes because of its specific strength properties and economical benefit. Currently, many research groups are actively exploring different aspects of GFRP as a reinforcement element in concrete to not only improve the durability but also extend the serviceability of structures under non-ideal conditions. In this context, Benmokrane and Masmoudi [32] performed a study to explore the impact of GFRP reinforcing bar on the flexural behavior of the concrete specimen. The characterization study showed an effective bonding between GFRP reinforcement bar and concrete environment. Surprisingly, a similar behavior in the crack pattern and spacing was observed for both GFRP and steel-reinforced concrete samples when they are subjected to a low load. Most strikingly, the GFRP-reinforced concrete beam showed a greater ultimate strength than steel-reinforced sample, whereas a higher deflection was noticed in GFRP-reinforced specimen. In another study, Ahmed et al. [33] incorporated sand-coated GFRP stirrups of 9.5 mm into a concrete beam. It was found that the reinforced beam with GFRP had a similar behavior to the steel-reinforced beam. GFRP also showed promising when used as reinforcement for column [34–36] and slab [37, 38]. Apart from these, in highways and transportation system, advances in FRP composites allow for a rapid deployment of bridge decks [39]. Despite the usefulness of GFRP composites in structural industry, the lack of plastic behavior and a low shear strength capacity may limit their large-scale applications. The combination of such shortcoming in reinforced concrete with shear cracking planes may result in a premature tendon rupture [15]. Therefore, further research on improvement of GFRP is required to address these issues for finding its way into the construction market in a near future.

Repairing the deteriorated or damaged pipelines is another application of GFRP. Currently, the transportation of oil and gas over a long distance is done using metal pipelines, which are mostly made of ferrous steel. The transportation pipes are susceptible to corrosion when exposed to a harsh environment such as underwater or underground. In conventional approaches, the damaged sections are replaced with a new steel pipe. However, this technique is costly and not a permanent solution. Moreover, the transportation is interrupted during the replacement and welding process. Over recent years, attempt has been made to repair the damaged or corroded steel pipes in an effective way using FRP [40–43]. FRPs have also been successfully tested in a harsh environment, including chemical storage and underground tanks. Apart from the structural and infrastructure applications, GFRPs are used in automotive, aerospace, marine, medical, sporting gear, pre-fabricated house, naval platform, furniture and appliance.

3.3 The effect of machining process on FRP

In the present scenario, composite materials possess tremendous potential over conventional metals as these have high specific stiffness and high specific strength. Despite these unique characteristics and the potential applications for many industries, GFRP is susceptible to delamination during machining processes. For instance, the drilling operation is carried out on the composite components for structural joining, which can result in drilling-induced delamination. Delamination damage is a prominent critical machining defect found in composite parts. This damage mainly affects the bearing strength of the joints. The proportion of the delaminated area is directly proportional to the push (thrust) force induced by drilling operation. Studies have been performed by many researchers with various processing parameters; spindle speed and feed rate for the optimization of process parameters. However, delamination free holes are difficult to obtain in drilling. Since delamination of composites occurs as inter-laminar damages, drilling damage prediction in composites is imperative for manufacturing quality.

Considerable research to study the effect of drilling on composite materials has been going on. As aforementioned, the proportion of the delaminated area is in relation to the drilling (thrust) force induced and is supposed that below the critical thrust force the chances for the occurrence of damage due to delamination are very low [44]. Literature reports for many unconventional drilling operations used for making holes in laminates, mainly using laser, water-jet and electrical discharge. However, drilling by employing conventional or specially designed drill bits is the main hole-making machining operation for composite laminates. Hocheng and Tsao used different drill bits such as twist drill, candlestick drill, saw drill, core drill and step drill to assess the influence of delamination induced via drilling of the laminates. They reported that the core dill offered the maximum critical feed rate,

whereas the conventional twist drill offered the minimum. The core drill followed by the candlestick drill offered intermediate feed rate between the core drill and the twist drill [45]. Literature also reported for some other drill bits such as core-saw and brad point, which has been developed to reduce drilling-induced delamination.

There are several methods developed over a period of time to reduce delamination in composites, which are:

a) Pilot holes: pilot holes are generally employed [46, 47] to avoid the interaction of chisel with the material. Generally, the dimensions of the pilot hole is fixed equivalent to the edge length of the chisel of a drill bit (twist drill). However, for drill bit such as core drill, the drill bit's internal diameter is chosen for the dimensions of the pilot hole.
b) Active backup force: drilling with active backup force [48, 49] for supporting the back side of a laminate to avoid exit delamination. The applied backup force aids suppression of drilling-induced composite exit delamination by 60–80%.
c) Drilling assisted with vibration: drilling assisted with vibrations (ultrasonic) has been reported [50] for the reduction of thrust forces generated during drilling, reduction of delamination up to 50%.
d) High-speed drilling: it has been reported that the high speed drilling [51] leads to higher productivity at the same time to minimize the delamination.
e) Drilling using backup plate: The use of backup plates during drillings [48] avoids deformations that could lead to exit delamination. Generally, the backup support prevents inflexions.

Literature study on delamination has revealed that there are several approaches in order to assess the delamination induced as a result of drilling. Commonly, measurements in relation to the size and shape of the damage occurred during drilling. Researchers [52–55] employed approaches such as X-ray [56], optical microscopy [57], ultrasonic C-scan [58], acoustic emission [59], laser-based imaging technique [60] and digital imaging [61] for the measurements. Similarly, there are different methods reported to quantify the delamination occurred during drilling a hole: delamination factor (F_d) [56], delamination size [62], 2D-delamination factor (F_a) [63], adjusted delamination factor (F_{da}) [64], effective delamination factor (F_{ed}) [58], minimum delamination factor (F_{dmin}) [65] and refined delamination factor (F_{DR}) [66]. Surprisingly, there is no common agreement on both measuring methods and assessments of delamination.

Many works have been reported in the literature on the prediction of delamination. FE (finite element) analysis methods by means of a suitable mathematical model could predict the damage during drilling, including influential parameters such as thrust force and torque. Numerical [67] and FE models [68] using linear elastic fracture mechanics theory have been reported for determining the critical thrust force at the onset of the delamination. Hocheng and Dharan [67] made available the first model, but these models only account for the inter-laminar fracture

during drilling. Numerical predictions of onset delamination during drilling in composite (carbon/epoxy) were presented by a mixed-mode damage propagation [69]. However, most of these models supposed the outline of the delamination as elliptical. It has also been reported that numerical models adopted with FE simulations could predict the delamination factor more precisely. Literature also reports the use of progressive failure model and progressive delamination model for the prediction of delamination damage in CFRP laminates [70]. It has been also reported elsewhere that the 3D FE model accounts for complex kinematics to simulate inter-ply delamination of drilling in composite laminates [24]. However, more research is still required for accurately measuring and predicting drilling-induced delamination. In this chapter, an attempt to assess delamination using image analysis is described. This method can assess many images files effectively on time. The algorithm was used in MATLAB. More details of the analysis are described in the next section.

3.4 Delamination assessment using MATLAB

In this study, we suggest a time-effective method to measure drilling-induced delamination. The proposed method could interpret a large amount of data effectively in less time.

Figure 3.2(a) shows a captured (original) image of a drilled hole using a twist drill in an E-glass composite. Figure 3.2(b–d) shows the three different cases we considered: minimum, medium and maximum delaminated surface area, respectively. The marking for the delaminated surface area on the images should be carefully carried out using an appropriate tool (e.g. MS Paint). Although for this study we used only peel-up delaminated surface, it is advised to perform the study in peel-down delamination as well.

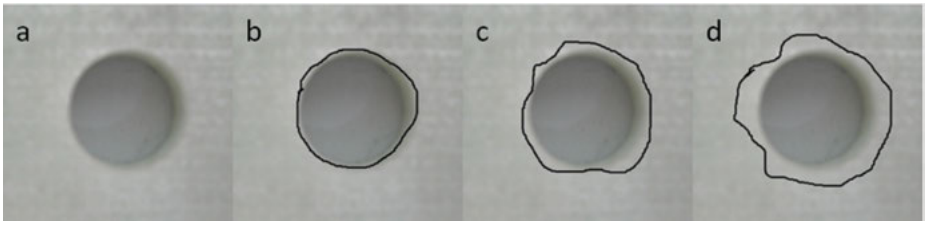

Figure 3.2: (a) Captured image with 10 mm drilled hole, marks displaying delaminated surface area (only peel-up) for the cases: (b) minimum, (c) medium and (d) maximum.

MATLAB was used to generate the delamination pixel ratio, D_{PR}. D_{PR} can be defined as the ratio pixels of the surface delaminated to the original drilled hole. When the

ratio is near to 0, the delamination is minimum. The proposed method is shown in Algorithm 3.1. The D_{PR} values obtained for the three cases are shown in Table 3.3.

Input: Original image and marked delaminated surface image

Output: Delamination pixel-ratio, D_{PR}

```
Start program
#1.  Load captured (original) image and transform it to binary image, 'imgO';
     Load marked image and transform it to binary image, 'imgEX';
#2.  Add the two binary images, 'newImg = imgO + imgX';
#3.
   (a) Read from left to write of each pixel of 'newImg'
       If pixel(newImg) == 2 then change that pixel value (e.g., say 20) as
          pixel(newImg) = 20;
       Else
          Break;
       End
   (b) Read from right to left of each pixel of 'newImg' then repeat the same as in #3(a);
#4. Count the number of pixels that have the value of 2 and 0 (i.e., black pixels) in 'newImg'.
    Say C2 and Cbk, respectively;

#5. Take the number of pixels ratio, C2/Cbk. This gives the ratio of the delaminated surface
to the original drilled hole, DPR.

Close program
```

Algorithm 3.1: Proposed method for the calculation of delamination using images.

Table 3.3: Calculated DPR values for each case.

Cases	Minimum, Figure 3.2(b)	Medium, Figure 3.2(c)	Maximum, Figure 3.2(d)
D_{PR}	0.0461	0.2792	0.6410

3.5 Concluding remarks

Drilling-induced delamination is a limiting factor for glass fibre composites for high-end applications. Proper drill bit geometries and manufacturing methods for composites should be developed to overcome this limiting factor. It was found from the literature that using different drill bit geometries as well as drill bit materials to drill holes in composite laminates could offer many advantages and benefits, but

delamination free holes are challenging to drill. Further studies in this field are necessary to produce delamination free holes. Moreover, an accurate delamination assessment method that can assess the delamination damage with high accuracy should be developed.

References

[1] Pickering, K.L., Efendy, M.G.A., and Le, T.M. A review of recent developments in natural fibre composites and their mechanical performance, Composites Part A: Applied Science and Manufacturing 2016, 83, 98–112.
[2] Singh, J. et al. Properties of glass-fibre hybrid composites: a review, Polymer-Plastics Technology and Engineering 2017, 56(5), 455–469.
[3] Palanikumar, K., Prakash, S., and Shanmugam, K. Evaluation of delamination in drilling GFRP composites, Materials and Manufacturing Processes 2008, 23(8), 858–864.
[4] Fu, S.-Y. et al. Effects of particle size, particle/matrix interface adhesion and particle loading on mechanical properties of particulate–Polymer composites, Composites Part B: Engineering 2008, 39(6), 933–961.
[5] Dekkers, M., and Heikens, D. The effect of interfacial adhesion on the tensile behavior of polystyrene–Glass-bead composites, Journal of Applied Polymer Science 1983, 28(12), 3809–3815.
[6] Fu, S.-Y., and Lauke, B. Characterization of tensile behaviour of hybrid short glass fibre/calcite particle/ABS composites, Composites Part A: Applied Science and Manufacturing 1998, 29(5–6), 575–583.
[7] Spanoudakis, J., and Young, R. Crack propagation in a glass particle-filled epoxy resin, Journal of Materials Science 1984, 19(2), 473–486.
[8] Pukanszky, B., and VÖRÖS, G. Mechanism of interfacial interactions in particulate filled composites, Composite Interfaces 1993, 1(5), 411–427.
[9] Liang, J., Li, R.K., and Tjong, S. Tensile fracture behaviour and morphological analysis of glass bead filled low density polyethylene composites, Plastics, Rubber and Composites Processing and Applications 1997, 26(6), 278–282.
[10] Reynaud, E. et al. Nanofillers in polymeric matrix: a study on silica reinforced PA6, Polymer 2001, 42(21), 8759–8768.
[11] Broughton, W.R., Lodeiro, M.J., and Pilkington, G.D. Influence of coupling agents on material behaviour of glass flake reinforced polypropylene, Composites Part A: Applied Science and Manufacturing 2010, 41(4), 506–514.
[12] Pandey, A.K. et al. Mechanical and thermal behaviours of graphite flake-reinforced acrylonitrile–Butadiene–Styrene composites and their correlation with entanglement density, adhesion, reinforcement and C factor, RSC Advances 2016, 6(56), 50559–50571.
[13] Miskolczi, N. 3 – Polyester resins as a matrix material in advanced fibre-reinforced polymer (FRP) composites, in Advanced Fibre-Reinforced Polymer (FRP) Composites for Structural Applications, J. Bai, Editor, 2013, Woodhead Publishing, 44–68.
[14] Wambua, P., Ivens, J., and Verpoest, I. Natural fibres: can they replace glass in fibre reinforced plastics?, Composites Science and Technology 2003, 63(9), 1259–1264.
[15] Masuelli, M.A., Introduction of fibre-reinforced polymers– polymers and composites: concepts, properties and processes, in Fibre Reinforced Polymers-The Technology Applied for Concrete Repair. 2013, InTech.

[16] Church, D. A revolution in low-cost carbon fibre production, Reinforced Plastics 2018, 62(1), 35–37.
[17] Carbon Fibre Reinforced Plastics – Properties, in Reference Module in Materials Science and Materials Engineering S. Hashmi, Editor, 2016, Oxford, Elsevier, 1–18.
[18] Knoll, J.B. et al. The effect of carbon nanoparticles on the fatigue performance of carbon fibre reinforced epoxy, Composites Part A: Applied Science and Manufacturing 2014, 67, 233–240.
[19] Brunbauer, J., and Pinter, G. Effects of mean stress and fibre volume content on the fatigue-induced damage mechanisms in CFRP, International Journal of Fatigue 2015, 75, 28–38.
[20] Gamstedt, E., and Talreja, R. Fatigue damage mechanisms in unidirectional carbon-fibre-reinforced plastics, Journal of materials science 1999, 34(11), 2535–2546.
[21] Kawai, M., and Saito, S. Off-axis strength differential effects in unidirectional carbon/epoxy laminates at different strain rates and predictions of associated failure envelopes, Composites Part A: Applied Science and Manufacturing 2009, 40(10), 1632–1649.
[22] Hong, B., Xian, G., and Wang, Z. Durability study of pultruded carbon fibre reinforced polymer plates subjected to water immersion, Advances in Structural Engineering 2018, 21(4), 571–579.
[23] Chiao, C., and Chiao, T. Aramid fibres and composites, Handbook of composites, 1982, Springer, 272–317.
[24] Phillips, L.N. Design with advanced composite materials, 1989.
[25] Pıhtılı, H., and Tosun, N. Effect of load and speed on the wear behaviour of woven glass fabrics and aramid fibre-reinforced composites, Wear 2002, 252(11), 979–984.
[26] Yue, C.Y., Sui, G.X., and Looi, H.C. Effects of heat treatment on the mechanical properties of Kevlar-29 fibre, Composites Science and Technology 2000, 60(3), 421–427.
[27] Lewin, M. Handbook of fibre chemistry, 2006, CRC press.
[28] Lewin, M. Handbook of Fibre Science and Technology Volume 2: Chemical Processing of Fibres and Fabrics–Functional Finishes, Vol. 2, 1984, CRC Press.
[29] Li, H. et al. Composite reinforcement: recent development of continuous glass fibres, International Journal of Applied Glass Science 2017, 8(1), 23–36.
[30] Li, H., Richards, C., and Watson, J. High-performance glass fibre development for composite applications, International Journal of Applied Glass Science 2014, 5(1), 65–81.
[31] Yashas Gowda, T. et al. Polymer matrix-natural fibre composites: an overview, Cogent Engineering 2018, 5(1), 1446667.
[32] Benmokrane, B., and Masmoudi, R. Flexural response of concrete beams reinforced with FRP reinforcing bars, Structural Journal 1996, 93(1), 46–55.
[33] Ahmed, E.A., El-Salakawy, E.F., and Benmokrane, B. Performance evaluation of glass fibre-reinforced polymer shear reinforcement for concrete beams, ACI structural Journal 2010, 107 (1).
[34] De Luca, A., Matta, F., and Nanni, A. Behavior of full-scale glass fibre-reinforced polymer reinforced concrete columns under axial load, ACI Structural Journal 2010, 107(5), 589.
[35] Afifi, M.Z., Mohamed, H.M., and Benmokrane, B. Axial capacity of circular concrete columns reinforced with GFRP bars and spirals, Journal of Composites for Construction 2013, 18(1), 04013017.
[36] Tobbi, H., Farghaly, A.S., and Benmokrane, B. Concrete columns reinforced longitudinally and transversally with glass fibre-reinforced polymer bars, ACI Structural Journal 2012, 109(4).
[37] Bouguerra, K. et al. Testing of full-scale concrete bridge deck slabs reinforced with fibre-reinforced polymer (FRP) bars, Construction and building materials 2011, 25(10), 3956–3965.
[38] Hassan, M., Ahmed, E., and Benmokrane, B. Punching-shear strength of normal and high-strength two-way concrete slabs reinforced with GFRP bars, Journal of composites for construction 2013, 17(6), 04013003.

[39] Hota, G., and Liang, R. Advanced fibre reinforced polymer composites for sustainable civil infrastructures. in Proceedings of the International Symposium on Innovation & Sustainability of Structures in Civil Engineering. 2011. Xiamen University.
[40] Cercone, L., and Lockwood, J.D., Review of FRP composite materials for pipeline repair, in Pipelines 2005: Optimizing Pipeline Design, Operations, and Maintenance in Today's Economy. 2005. p. 1001–1013.
[41] Geraghty, M., Pridmore, A., and Sanchez, J., Transitioning from leak detection to leak prevention: proactive repair of steel pipelines using fibre reinforced polymer (FRP) composites, in Pipelines 2011: A Sound Conduit for Sharing Solutions. 2011. p. 100–107.
[42] Sen, R., and Mullins, G. Application of FRP composites for underwater piles repair, Composites Part B: Engineering 2007, 38(5), 751–758.
[43] Duell, J.M., Wilson, J.M., and Kessler, M.R. Analysis of a carbon composite overwrap pipeline repair system, International Journal of Pressure Vessels and Piping 2008, 85(11), 782–788.
[44] Koenig, W. et al. Machining of fibre reinforced plastics, CIRP Annals-Manufacturing Technology 1985, 34(2), 537–548.
[45] Hocheng, H., and Tsao, C. Comprehensive analysis of delamination in drilling of composite materials with various drill bits, Journal of Materials Processing Technology 2003, 140(1–3), 335–339.
[46] Tsao, C.C., and Hocheng, H. The effect of chisel length and associated pilot hole on delamination when drilling composite materials, International Journal of Machine Tools and Manufacture 2003, 43(11), 1087–1092.
[47] Tsao, C. The effect of pilot hole on delamination when core drill drilling composite materials, International Journal of Machine Tools and Manufacture 2006, 46(12–13), 1653–1661.
[48] Tsao, C., and Hocheng, H. Effects of exit back-up on delamination in drilling composite materials using a saw drill and a core drill, International Journal of Machine Tools and Manufacture 2005, 45(11), 1261–1270.
[49] Tsao, C., Hocheng, H., and Chen, Y. Delamination reduction in drilling composite materials by active backup force, CIRP Annals-Manufacturing Technology 2012, 61(1), 91–94.
[50] Mehbudi, P. et al. Applying ultrasonic vibration to decrease drilling-induced delamination in GFRP laminates, Procedia CIRP 2013, 6, 577–582.
[51] Rubio, J.C. et al. Effects of high speed in the drilling of glass fibre reinforced plastic: Evaluation of the delamination factor, International Journal of Machine Tools and Manufacture 2008, 48(6), 715–720.
[52] Babu, J. et al. Machinability of Fibre-Reinforced Plastics, Vol. 4, 2015, Walter de Gruyter GmbH & Co KG.
[53] Liu, D., Tang, Y., and Cong, W. A review of mechanical drilling for composite laminates, Composite Structures 2012, 94(4), 1265–1279.
[54] Babu, J. et al. Examination and modification of equivalent delamination factor for assessment of high speed drilling, Journal of Mechanical Science and Technology 2016, 30(11), 5159–5165.
[55] Babu, J. et al. Assessment of delamination in composite materials: a review. Proceedings of the Institution of Mechanical Engineers, Part B: Journal of Engineering Manufacture 2015, 0954405415619343.
[56] Chen, W.-C. Some experimental investigations in the drilling of carbon fibre-reinforced plastic (CFRP) composite laminates, International Journal of Machine Tools and Manufacture 1997, 37(8), 1097–1108.
[57] Davim, J.P., and Reis, P. Study of delamination in drilling carbon fibre reinforced plastics (CFRP) using design experiments, Composite Structures 2003, 59(4), 481–487.

[58] Tsao, C., Kuo, K., and Hsu, I. Evaluation of a novel approach to a delamination factor after drilling composite laminates using a core–Saw drill, The International Journal of Advanced Manufacturing Technology 2012, 59(5–8), 617–622.
[59] Cai, X.J. et al. Experimental analysis on delamination damage by acoustic emission in high speed drilling of carbon fibre reinforced plastics. in Key Engineering Materials, 2014, Trans Tech Publ.
[60] Seif, M.A., Khashaba, U.A., and Rojas-Oviedo, R. Measuring delamination in carbon/epoxy composites using a shadow moiré laser based imaging technique, Composite Structures 2007, 79(1), 113–118.
[61] Khashaba, U. Delamination in drilling GFR-thermoset composites, Composite Structures 2004, 63(3–4), 313–327.
[62] Faraz, A., Biermann, D., and Weinert, K. Cutting edge rounding: An innovative tool wear criterion in drilling CFRP composite laminates, International Journal of Machine Tools and Manufacture 2009, 49(15), 1185–1196.
[63] Phadnis, V.A. et al. Drilling in carbon/epoxy composites: experimental investigations and finite element implementation, Composites Part A: Applied Science and Manufacturing 2013, 47, 41–51.
[64] Davim, J.P., Rubio, J.C., and Abrao, A. A novel approach based on digital image analysis to evaluate the delamination factor after drilling composite laminates, Composites Science and Technology 2007, 67(9), 1939–1945.
[65] Silva, D.N.R.d. Image processing methodology for assessment of drilling-induced damage in CFRP, 2013, Faculdade de Ciências e Tecnologia.
[66] Nagarajan, V., and Rajadurai, J.S. A digital image analysis to evaluate delamination factor for wind turbine composite laminate blade, Composites Part B: Engineering 2012, 43(8), 3153–3159.
[67] Ho-Cheng, H., and Dharan, C. Delamination during drilling in composite laminates, Journal of Engineering for Industry 1990, 112(3), 236–239.
[68] Piquet, R. et al. Etude analytique et expérimentale du perçage de plaques minces en carbone/époxy, Mécanique & Industries 2000, 1(1), 105–111.
[69] Durão, L., De Moura, M., and Marques, A. Numerical prediction of delamination onset in carbon/epoxy composites drilling, Engineering Fracture Mechanics 2008, 75(9), 2767–2778.
[70] Isbilir, O., and Ghassemieh, E. Numerical investigation of the effects of drill geometry on drilling-induced delamination of carbon fibre reinforced composites, Composite Structures 2013, 105, 126–133.

K. Jessy, Vishal John Mathai, and Jalumedi Babu

4 Drilling of glass fibre-reinforced composites

Abstract: Composite materials have extensive applications in creating products that we use in day-to-day life. However, due to the inhomogeneities present in the material in terms of reinforcement, the machining or processing of the same is extremely difficult. The underlying mechanisms involved in cutting such materials result in the generation of unbalanced cutting forces, rise in cutting temperature and excessive wear of the cutting tool. Such situations directly contributed to the inaccuracies in the machined feature. This chapter discusses the effects of two critical issues that occur during drilling of glass fibre-reinforced polymer composites, namely, heat generation and tool instability. Further different techniques that can be employed for quantifying heat generation, tool vibration and delamination are also discussed in brief.

Keywords: drilling, composites, tool wear, vibration

4.1 Introduction

Fibre-reinforced polymer (FRP) composites have been identified as a potential material for many engineering applications in different functional aspects. High stiffness, strength-to-weight ratio and lower reactivity to the environmental conditions make them a good candidate for using them in creating load bearing structures. Application of these materials has also been increased in automobile domains, owing to their good specific stiffness and strength, high damping and low level of density and thermal expansion [1]. Furthermore, the low thermal and radar signatures and inertness to external chemical and nuclear-based reactions for lightweight fibre-reinforced composites make them appropriate for aerospace applications as well [2]. Apart from all these advantages, the relative ease in manufacture of composite-based products has made these categories of materials a preferable choice in manufacturing various products.

Composite materials consist of a continuous phase called “matrix” and a dispersed phase called “reinforcement.” The matrix phase takes up the load and evenly distributes it to the reinforcement phase, thereby improving the mechanical properties.

K. Jessy, Vishal John Mathai, Department of Mechanical Engineering, Amal Jyothi College of Engineering, Kottayam, Kerala, India
Jalumedi Babu, Department of Mechanical Engineering, St. Joseph College of Engineering, Kottayam, Kerala, India

https://doi.org/10.1515/9783110610147-004

Different types of matrix materials are reported to be used; however, owing to its good balance of mechanical and chemical properties, epoxy resins are widely used for composite development [3]. Apart from properties and characteristics of the matrix and reinforcement, concentration, geometry of the reinforcements and its orientation also contribute to the mechanical and thermal properties of the composites developed [4]. Among a wide range of reinforcing materials proposed, glass fibres, owing to their specific mechanical properties, are the most commonly used as reinforcement in composites used in construction fields.

4.2 Drilling of GFRP: technical challenges

While fabricating products out of polymer composite, it is difficult to form holes using drilling operation, without affecting the reinforcement. This inhomogeneity in a material structure results in a pronounced difference in mechanism of machining, when compared with conventional materials [5]. Analysis of composite machining is hence difficult. Apart from these factors, the complexity that gets added to the geometrical variation in the cutting tool used in a process like drilling also makes the analysis more cumbersome.

During drilling of glass fibre-reinforced polymers (GFRPs), different types of defects come up, either on the reinforcement or in the matrix phase. The commonly observed defects are delamination, which can be inter-laminar or intra-laminar or both, exposure of reinforcing fibre, cracking of fibre, matrix flow and so on [6]. Apart from these defects, unevenness in the features drilled like waviness and roughness, aberrations in roundness and straightness of the holes are prone to occur. Each type of these defects affects the mechanical properties and hence the effective life of the composites [7]. Such defects will induce stress concentration at joints leading to its failure [8, 9].

4.3 Heat generation during drilling of GFRP

4.3.1 Effect of cutting temperature during drilling of GFRP

One of the beneficial features of GFRPs is that they provide good insulation, which makes them suitable for use in components operating at high temperature conditions. However, this property also makes them difficult to machine [10, 11]. Most of the power used in drill bits during drilling gets converted into heat [12, 13]. This occurs because as the drill bits penetrate the composite, friction between the two generates heat. This heat is then dissipated through the drilling machine, through the component being drilled, chips being formed whilst drilling and by the cutting fluid if used. Some of the critical factors that influence in the cutting temperature are

drilling parameters, namely, cutting speed, feed rate, depth of cut, tool geometry and thermal, physical and chemical properties of the workpiece and tool materials [14].

Heat build-up at the drilling site is not high enough in them to significantly impact the machining/drilling process. The problems occur because the sole conducting agent of this heat, whilst machining GFRPs, is the drilling tool. Since heat build-up occurs primarily in the drilling tools, they get damaged during the drilling process. A damaged tool will compromise the efficiency of the holes being drilled, which in turn affects the surface integrity of those components containing the composite [15, 16].

The inhomogeneity in the material, as stated in the previous section, also affects the life of the cutting tool as the heat generated during machining of composites can be fluctuating. The cycloidal change in heat generation due to the active and inactive periods that the tool encounter during drilling may induce thermal fatigue and this will lead to premature failure of the tool compared to that obtained during conventional machining [17, 18]. In line with this, the drilling tools used in this context must be able to resist alternate thermal cycles and mechanical shocks, and have to be able to support high drilling speeds at high temperatures as well [14].

Apart from acting as a source for tool failure, the heat also causes cracks and melting of surface layer of composite and moisture saturation [19]. The bond between the reinforcement fibres and the surrounding matrix gets loosened resulting in delamination. Since the layers of material within the composite have differential conductivity, their rates of expansion under condition of heat also change causing internal stresses and strains within the composite resulting in further delamination.

4.3.2 Different temperature measuring methods

Temperature measurement in the cutting area is a challenging task in machining studies due to the speed at which the operation takes place and difficulty in incorporating the measuring elements near the machining zone or cutting tool. The different techniques proposed for temperature measurement can be classified into analytical techniques, experimental techniques or a hybridized combination of both methods.

In analytical techniques, mathematical models and finite element analysis are used. With these techniques, measurement of temperature distribution as well as transient and steady-state drill temperatures were computed under different conditions like tool geometry and cutting parameters [20–23]. However, as in most of the cases, the values found out to be error prone due to the inclusion of unrealistic assumptions.

Among experimental techniques, temperature measurements can be carried out in two different ways: direct or contact-based measurements and indirect or noncontact-based measurements. In the case of direct measurements, the temperature is measured from the area of interest directly with the help of a physical system.

One of the most commonly used methods to quantify cutting temperature and map thermal gradients during drilling operation is the incorporation of thermocouples

in the machining system. The thermocouples are mounted or embedded on the drilling tools in premachined grooves and fixed using adhesive having high thermal conductivity. However, the limitation of the use to thermocouples is that the same cannot be mounted at the cutting edges, where the heat is more prone to develop. Apart from this, even though the thermocouples can be embedded, the data collection and transmission becomes more complex as the thermocouples are mounted on a rotating part [24, 25].

To counter this issue, studies were carried out in such a way that the tool and workpiece motions involved in a drilling operation are swapped; the drilling tool is made stationary and workpiece is rotated [26, 27]. The technique has been found to be less feasible to obtain sound experimental results as the steady temperature, which is often reached after drilling a number of holes continuously, cannot be measured accurately.

Wireless systems alongside thermocouples are also reported to be used to collect information from the machining spindle during machining of composite materials with the help of a high-frequency transmitter and a technically compatible antenna [28, 29]. Such a system is reported to provide relatively accurate results; however, the cost pertaining to individual preparation of the drilling tool and the cost of the wireless tool holder system make it a costly affair.

In line with this, the concept of dynamic thermocouple was also proposed for measuring temperature. In this technique, a dynamic thermocouple is created between drill bit and the workpiece. The technique requires prior characterization. Prior to use, a calibration of the system is done to develop a relation between the temperature developed in the tool and the electromotive force. The most highlighting advantage of this technique is that it can be used for detection of temperature at the cutting edges [30, 31]. However, the calibration of the dynamic thermocouple is difficult due to the inferior values of thermal conductivity of the polymer composites.

4.3.3 Use of cutting fluids in GFRP drilling for reducing temperature effects

Use of cutting fluids in the drilling zone can improve the process in multiple facets. Providing coolant to the machining zone will reduce the temperature accumulation on the cutting edges and this aids the use of high levels of drilling parameters. Further, such a system will help in flushing out the chip from the machining zone, thereby contributing to better surface quality of drilled features.

In addition to the tool wear in terms of adhesion of chips on the rake face of the tool can be reduced due to the presence of a liquid film between the rake surface and the flowing chip [32]. The presence of such a lubrication film will reduce the friction between the chip and the tool, resulting in lower heat accumulation on the tool surface and hence lower tool wear [33, 34]. Further, it has also been inferred

from the literatures that the effects of cutting temperature are distinctively lower than that in the case of dry machining when a cutting fluid is used during drilling of FRPs [35]. Further, it has also been reported that the use of cutting fluids will reduce cutting forces and thermal distortion of the drilled holes compared to the case of dry drilling [36]. As discussed in the previous sections, the inhomogeneity in the material results in mechanical cycle as well as thermal loading on the drilling tool during machining of composites. Under such conditions, the drilling tools are prone to axial as well as radial distortion. Under cutting condition, the drill bit tends to have a reduction in its length and corresponding increase in drilling tool diameter. This aberration on the drilling tool results in change in the geometry of the drilling tool, leading to generation of holes with poor accuracy.

Owing to the high cutting resistance, drilling of GFRP requires mechanically sound tool materials like polycrystalline diamond and carbide tools. Since drill bit cost is relatively high compared to conventional drill bits, it is economical to implement a proper coolant system on the machine tool, so that precise amount of coolant can be distributed at the interface between cutting edge and workpiece externally and internally. The coolant is supplied to the machining zone externally in most cases. However, since the heat accumulation tends to be on the higher side, internal cooling through the tool is also a mode of coolant supply method used during drilling of GFRPs. It has been reported that the cutting temperature observed in a system with internal cooling is lower than that observed in the case of external cooling [37].

Figure 4.1 shows the average cutting temperature under different cooling conditions employed during drilling of GFRP composites. It can be inferred from the graph

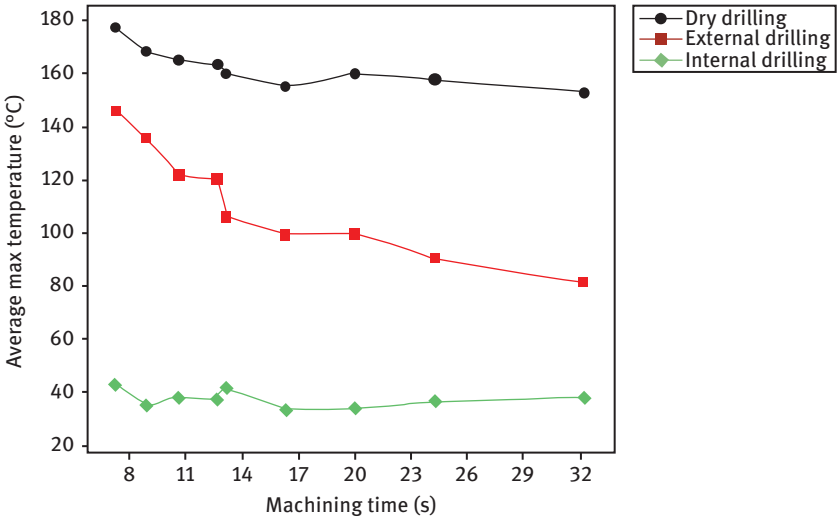

Figure 4.1: Comparison of cutting temperature observed under different cooling techniques (drilling parameters: V = 750 rpm, f = 0.05 mm/rev, tool diameter = 10 mm).

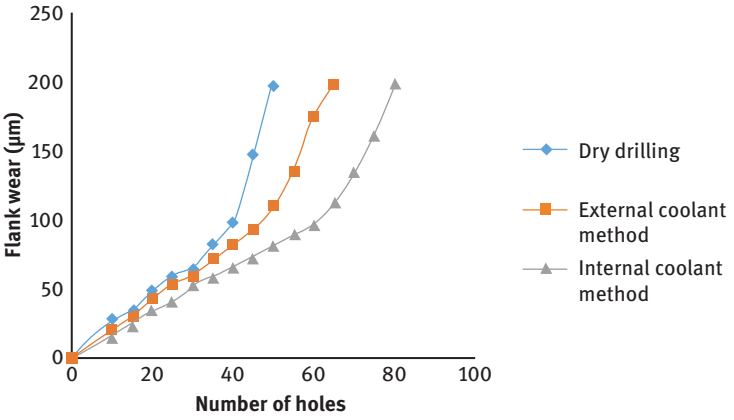

Figure 4.2: Effect of cooling methods on flank wear during drilling of GFRP (cutting conditions: V = 750 rpm, f = 0.05 mm/rev, tool diameter = 10 mm).

that throughout the duration of machining the cutting temperature can be significantly reduced with the help of internal cooling method. Furthermore, Figure 4.2 shows an increase in the number of holes that can be drilled on a 5-mm-thick GFRP composite using TiN/TiAlN-coated carbide drill with internal/external cooling methods and dry drilling. For 200 µm flank wear on coated carbide drills, the internal coolant method facilitated in drilling of a maximum of 80 holes, whereas in case of dry drilling, only 45 and 60 holes have been successfully drilled under dry drilling and external coolant technique. Hence, it can be understood that the use of internal cooling technique can simultaneously reduce heat accumulation and wear on the tool.

4.4 Tool vibration effects and tool wear during drilling of GFRP

Machine tool chatter is a case of dynamic instability that occurs in a cutting process and such an aberration can result in inferior surface quality, tool breakage and ill effect to ear drums because of the exposure to intense noise [38, 39].

The fluctuating mechanical and thermal stresses imposed due to the physical contact between the cutting tool and the workpiece and the pressure imposed by the chip on the tool, the shape of the drilling tool tends to change. At the same time, the drilling tool tends to fail either gradually as wear on the tool or abruptly when the tool breaks or fractures [40]. The aim of tool condition monitoring is to

use appropriate sensor as well as pattern recognition systems to identify and predict the drilling tool condition, so that losses due to tool failures can be minimized.

4.4.1 Tool vibration measurement and prediction techniques

Chatter detection during machining can be done using two different methods: frequency domain method and time domain method. Frequency domain method is based on fast Fourier transformation techniques [41, 42]. At the occurrence of chatter, the variation in the signal pertaining to cutting force and other related parameters is analyzed and the standout signal is identified. However, analyzing the spectrum and identifying the threshold signal are complex when the cutting conditions are not the same throughout the process [43]. Hence, for more easier and faster approach, time domain-based techniques like forecasting time series are used [44, 45].

Tool condition can be monitored in two different methods: direct monitoring and indirect monitoring. Direct monitoring methods include techniques like usage of optical and vision systems to measure the geometric deviations of the drilling tool [46–48]. In the case of indirect monitoring methods, the condition of the tool is not directly assessed, but with the help of analyzing a measurable signal [49]. The signal is extracted through various stages of signal processing for accurate assessment of the tool condition. The commonly assessed parameters for indirect monitoring are cutting forces [50, 51], cutting tool vibration [16–20], acoustic or sound emission [52, 53] and feed current [54, 55].

Even though direct monitoring techniques have the advantage of capturing and assessing live geometrical changes that arise from the tool wear or tool breakage, the same is difficult to implement due to the nature of the contact between the tool and the workpiece, and the presence of cutting fluids makes the assessment more cumbersome. Such facts can be sorted out in the case of indirect monitoring techniques in which the setup is less complex.

In line with the indirect method of monitoring, the use of neural networks is gaining more attention for solving difficult tasks in machining and detection of chatter instability [56, 57]. The advantage of using neural networks is that only a small amount of data is required to estimate the chatter frequency. However, as in the case of direct monitoring techniques, identification of threshold chatter frequency is an issue. Such issues can be sorted out to an extent by hybridizing neural network systems with the concepts like adaptive resonance. It has been reported that such systems are capable of identifying the threshold value from a thrust force spectrum. Such systems when used in conjunction in a spindle speed regulation method can very well be employed for detection of chatter and modification of spindle speed accordingly [58].

4.4.2 Effects of machining conditions on tool wear

Excess tool wear is considered to be undesirable in any metal cutting process. Tool wear increases the friction between tool and workpiece and also increases the power consumption. Owing to the non-homogenous nature of the composite material, the mechanical properties of the same will be different at different points in the same material, leading to inconsistent responses during machining, which results in the occurrence of a pulsating load on the drilling tool. Further, the intense interaction of the tool flank face with the fibres present in the material during drilling will result in extensive wear as well [58].

It has been identified that the cutting conditions such as cutting speed, feed rate, depth of cut and fibre orientation angle in workpiece have greater influences on tool wear [59–61]. Feed rate is reported to have a dominant effect on tool wear, as a higher feed rate results in increased heat generation and chatter [62]. However, wear on the tool may also depend on the spindle speed employed and the problem will be magnified when the same is too high. This may be attributed to the increase in thrust and tangential forces, which may impair the quality of the machined component [63]. Figure 4.3(a, b) shows the end of the drilling tool used for drilling GFRP composites under different conditions of cutting speed and feed rate. It can be clearly inferred that the wear is more pronounced on the tool used under high feed rate and cutting speed.

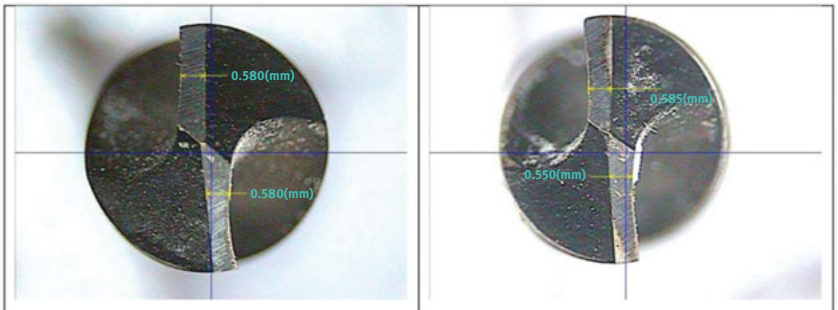

V	750 rpm	1,250
f	0.05 mm/rev	0.15
	(a)	(b)

Figure 4.3: (a) and (b) Flank wear observed on drilling tools during machining of GFRP.

Properties of the cutting tool material is important as it should be capable of withstanding unstable machining conditions. The tool used for machining FRP composites should have high hot hardness and superior mechanical properties. It is

reported that tool materials like carbides, which have higher hot hardness, outperform conventional tool materials like high speed steel (HSS) during drilling of FRPs [64, 65]. Further, performance of the tool can be improved by providing tool coating [66]. However, it has also been reported that after a threshold level of machining time, the coated tools have a tendency to wear out at a faster rate. Such an observation could be mainly due to the weakening of adhesive forces between the coating and the tool material, leading to its removal from the tool surface in terms of peeling and chipping [67].

4.4.3 Effects of machining conditions on feature quality

Quality of holes drilled can get affected by different factors such as influence of cutting temperature, change in cutting conditions and any errors that get induced in the machining system during the time of cutting [68–72]. Rise in cutting temperature in the machining zone results in thermal expansion of the drilling tool or that of the workpiece. The change in cutting conditions, that too when the material is non homogeneous, results in development of unbalanced forces and this can result in deflection of the drilling tool. Similarly, the errors can come into the feature if there is some issue in the alignment of the drilling tool or run out in drilling spindle, resulting in whirling of the tool.

The lack of quality can be quantified by either measuring the diameter of the drilled hole or by assessing the level of defects in the machined composites like fibre pullout, fibre fragmentation, burring and fuzzing and, most importantly, delamination that occurred after drilling. The main reason for such aberrations is reported to be the difference in hardness of reinforcement and matrix [73].

Delamination may be defined as the process of debonding of layers in a composite [74]. It occurs due to the stacked nature of GFRP composites, which split when subject to tensile or compressive forces and occur slowly and progressively through a succession of cracks. Amongst all the negative side effects of a machining process, possibly delamination is the most pernicious as it affects the fastening efficiency of composite materials, which then results in structural weaknesses and the tensile strength of a structure based on the region of delamination. Further, the durability of the composite material, its look and finish as well as its load bearing capacities are all negatively impacted by this mode of defect.

Delamination can be of two types: peel-up delamination and push-out delamination. As the drill enters the FRP due to the cutting force at the drill corners, there exists a peel-up delamination, which is schematically shown in Figure 4.4(a). Similarly, as the drill approaches the end of the lamination, wall thickness of the material is smaller so that its resistance to deformation due to thrust force reduces. This leads to push-out delamination as shown in Figure 4.4(b).

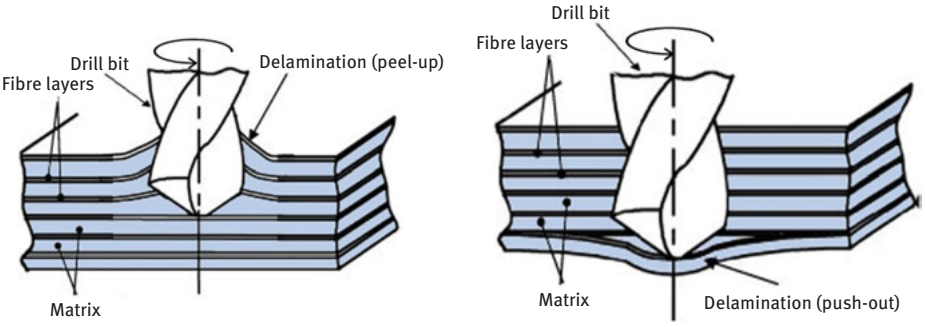

Figure 4.4: Delamination types: (a) peel-up and (b) push-out.

Delamination can be mathematically computed as the ratio of maximum diameter of the zone around the drilled hole to the actual diameter. Different mathematical expressions that are used for quantifying delamination are listed in Table 4.1. Parameters required for calculating delamination can be measured by using visual

Table 4.1: Methods to evaluate delamination.

Factor name	Expression	Proposed by
Delamination factor	$F_d = \frac{D_{max}}{D}$	Chen [77]
	D_{max} = maximum diameter of delamination D = nominal diameter of drilled hole	
Two-dimensional delamination factor	$F_a = \left(\frac{A_d}{A_{nom}}\right)\%$	Faraz et al. [78]
	A_d = delamination area A_{nom} = nominal area	
Damage ratio	$D_{RAT} = \frac{D_{MAR}}{A_{AVG}}$	Mehta et al. [79]
	D_{MAR} = damaged area at hole periphery A_{AVG} = nominal area of drilled hole	
Adjusted delamination factor	$F_{da} = \alpha\frac{D_{max}}{D_0} + \beta\frac{A_{max}}{A_0}$	Davim et al. [80]
	α, β = weights A_{max} = area corresponding to D_{max} A_0 = area corresponding to D_0	

Table 4.1 (continued)

Factor name	Expression	Proposed by
Equivalent delamination factor	$F_{ed} = \frac{D_e}{D_0}$	Tsao et al. [81]
	D_e = equivalent diameter	
Refined delamination factor	$F_{DR} = \frac{D_{max}}{D_o} + 1.783\left(\frac{A_H}{A_o}\right) + 0.7156\left(\frac{A_M}{A_o}\right)^2 + 0.03692\left(\frac{A_L}{A_o}\right)^3$	Nagarajan et al. [82]
	A_H = heavy damage area A_M = medium damage area A_L = low damage area	
Shape's circularity	$f = 4\pi\frac{A}{P^2}$	Durao et al. [83]
	A = area of damage P = perimeter length of damage area	
Minimum delamination factor	$F_{d_{min}} = \frac{D_{min}}{D_0}$	Silva [84]
	D_{min} = minimum enclosing area D_0 = pretended drill area	
Refined equivalent delamination factor	$F_{red} = \frac{D_e}{D_0}$	Babu et al [85].
Effective equivalent delamination factor	$\text{FEED} = \frac{D_{ea} + D_{ep}}{2D_0}$	Babu et al. [86]
	D_{ea} = equivalent diameter of a circle whose area is the same as the area enclosed by the envelope of the damaged zone D_{ep} = equivalent diameter of a circle whose perimeter is the same as the area enclosed by the envelope of the damaged zone	

techniques such as optical microscope, ultrasonic and acoustic-based methods and conventional photography.

Some of the major machining influences of delamination include high thrust forces, feed rate, drilling speeds and the use of blunt tools. It was reported that low feed rates are preferable for reducing delamination effects. However, increase in feed rate tends to change the effective rake angle at times, making the material pushed sideways instead of shearing, leading to delamination [75].

Even though proper selection of cutting as well as tooling parameters are important, the level of delamination may be influenced by other factors as well. It has

been reported that in the case of continuous winding composites, the possibility of push-out delamination is relatively high. However, it was also reported that by providing a back-up plate, the cutting mechanism can be changed and the level of delamination can be controlled to a certain extent [76].

Surface finish of the drilled features should also be considered as it is an important factor in defining fit as well as different types of loads involved in an assembly during static as well as running condition. Selection of appropriate drilling process parameters is very much important in machining accurate feature and high-quality features, as all these parameters are highly influential on surface roughness of the features machined.

Even though it can be inferred that keeping parameters at a low level will help in drilling composites with lower surface, simultaneous reduction of thrust forces, surface roughness and delamination is a difficult task. In such cases, one may need to approach multiobjective optimization techniques for more acceptable results.

4.5 Conclusions

An overall review on different issues that arise during drilling of GFRP composites has been discussed. Since the cutting mechanism is complex compared to drilling of more homogeneous materials, analysis of different aspects is a tedious work. The nonhomogeneity of the composite contributes to a tendency in occurrence of fluctuating load on the drilling tool and the accumulation of heat in the same. Both these factors will contribute to distortion of the drilling tool and to some extent the working material as well. In line with, the commonly used temperature measurement and tool chatter assessment tools are briefly discussed. It has been understood from the literatures that use of internal cooling can reduce the rise in temperature as well as tool wear to a great extent. It has also been inferred that it is preferable to use a noncontact system to measure the heat generation in the machining zone due to the difficulties in including such a system in a rotating tool. Effects of tool chatter can be monitored and reduced by incorporating live systems with the machine tool interface. Artificial Intelligence-based systems have a good potential in that regard. Further, different methods to analyse one of the most commonly observed postmachined defects in composites, namely, delamination, have also been discussed. Entities like roughness of the drilled hole have been reported to be affected mostly by the cutting parameter combinations.

Acknowledgments: The authors hereby acknowledge the services rendered by Prof. Sreerag V., Asst. Professor, and Mr. Alen Issac, UG student in Department of Mechanical Engineering, Amal Jyothi College of Engineering, Kanjirapally, Kerala, India, for the preparation of this chapter.

References

[1] El-Sonbaty, Khashaba U.A., and Machaly, T. Factors affecting the machinability of GFR/epoxy composites, Composite Structures 2004, 63, 329–338.

[2] Velayudham, A., Krishnamurthy, R., and Soundarapandian, T. Evaluation of drilling characteristics of high volume fraction fibre glass reinforced polymeric composite, International Journal of Machine Tools and Manufacture 2005, 45, 399–406.

[3] Callister, W.D. Materials Science and Engineering: An Introduction, 2002, Sixth ed, Wiley, Canada.

[4] Nassar, M.M.A., Arunachalam, R., and Alzebdeh, K.I. Machinability of natural fibre reinforced composites: A review, International Journal of Advanced Manufacturing Technology 2016, 88, 2985–3005.

[5] Hejjaji, A., Singh, D., Kubher, S. et al. Machining damage in FRPs: Laser versus conventional drilling, Composites A: Applied Science and Manufacturing 2016, 82, 42–52.

[6] Lopresto, V., Caggiano, A., Teti, R. et al (2016) High performance cutting of fibre reinforced plastic composite materials. In: Procedia CIRP. 7th HPC – CIRP conference on high performance cutting, Chemnitz

[7] Lazar, MB., and Xirouchakis, P. Experimental analysis of drilling fibre reinforced composites, International Journal of Machine Tools and Manufacture 2011, 51, 937–946.

[8] Park, K Y., Choi, J H., and Lee, D G. Delamination-free and high efficiency drilling of carbon fibre reinforced plastics, Journal of Composite Material 1988–2002, 29, 15.

[9] Tagliaferri, V., Caprino, G., and Diterlizzi, A. Effect of drilling parameters on the finish and mechanical properties of GFRP composites, Journal of Machine Tools and Manufacture 1990, 30(1), 77–84.

[10] Abrao, A.M., Faria, P.E., Campos Rubio, J.C., Reis, P., and Davim, J.P. Drilling of fibre reinforced plastics: A review, Journal of Materials Processing Technology 2007, 186, 1–7.

[11] Liu, D.F., Tang, Y. J., and Cong, W. L. A review of mechanical drilling for composite laminates, Composite Structures 2012, 94, 1265–1279.

[12] Bever, M.B., Marshall, E.R., and Ticknor, L.B. The energy stored in metal chips during orthogonal cutting, Journal of Applied Physics 1953, 24, 1176–1179.

[13] Shaw, M.C. Metal Cutting Principles, 1984, Oxford University Press, London, ISBN 0-19-859002-4, 594.

[14] da Silva, Marcio Bacci., and Bank, J. W. Cutting temperature: Prediction and measurement methods-a review, Journal of Material Processing Technology. 1999, 88(1-3), 195–202.

[15] Nakayama, K., Shaw, M.C., and Brewer, R.C. Relationship between cutting forces, temperature, built-up edge and surface finish, Annals of CIRP 1966, 14, 211–223.

[16] Shouckry, A.C. The effect of cutting conditions on dimensional accuracy, Wear 1982, 80, 197–205.

[17] Bathia, S.M., Pandey, P.C., and Shaw, H.S. The Thermal condition of the tool cutting edge in intermittent cutting, Wear 1986, 61, 21–30.

[18] Chakraverti, G., Pandey, P.C., and Mehta, N.K. Analysis of tool temperature fluctuation in interrupted cutting, Precision Engineering 1984, 6(2), 99–105.

[19] Zehnder, A.T., and Czabaj, Michael W., (2009) Blistering and Delamination in high temperature polymer matrix composites, Proceedings of the SEM Annual Conference, Albuquerque New Mexico USA.

[20] Agapiou, J.S., and De Vries, M.F. On the determination of thermal phenomena during a drilling process, International Journal of Machine Tools Manufacturing 1990, 30, 203–215.

[21] Agapiou, J.S., and Stephenson, D.A. Analytical and experimental studies of drill temperatures, Journal of Engineering 1994, 116(1), 54–60.

[22] Bagci, E., and Ozcelik, B. Finite Element and Experimental investigation of temperature changes on a twist drill in a sequential dry drilling, International Journal of Advanced Manufacturing Technology 2006, 28(7–8), 680–687.
[23] Fuh, K., and Liang, W.C. Temperature rise in twist drills with a finite element approach, International Communication on Heat Mass Transfer 1984, 21(3), 345–358.
[24] Da Silva, MB., and Wallbank, J. Cutting temperature: Prediction and measurement methods – A review, Journal of Materials Processing Technology 1999, 88(1), 195–202.
[25] Davies, MA., Ueda, T., M'Saoubi, R., Mullany, B., and Cooke, AL. On the measurement of temperature in material removal processes, CIRP Annals – Manufacturing Technology 2007, 56(2), 581–604.
[26] Ozcelik, B., and Bagci, E. Experimental and numerical studies on the determination of twist drill temperature in dry drilling: A new approach, Materials Design 2006, 27(10), 920–927.
[27] Weinert, K., and Kempmann, C. Cutting temperatures and their effects on the machining behaviour in drilling reinforced plastic composites, Advanced Engineering Materials 2004, 6(8), 612.
[28] Le Coz, G., Marinescu, M., Devillez, A., Dudzinski, D., and Velnom, L. Measuring temperature of rotating cutting tools: Application to MQL drilling and dry milling of aerospace alloys, Applied Thermal Engineering 2012, 36(1), 434–441.
[29] Kerrigan, K., Thil, J., Hewison, R., and O'Donnell, GE. An Integrated Telemetric Thermocouple Sensor for Process Monitoring of CFRP Milling Operations, Procedia CIRP 2012, 1, 449–454.
[30] Bono, M., and Ni, J. A method for measuring the temperature distribution along the cutting edges of a drill. Journal of Manufacturing Science and Engineering, Transactions of ASME 2002, 124(4), 921–923.
[31] Yashiro, T., Ogawa, T., and Sasahara, H. Temperature measurement of cutting tool and machined surface layer in milling of CFRP, International Journal of Machine Tools and Manufacture 2013, 70, 63–69.
[32] Rivero, A., Aramendi, G., and Herranz, S. An experimental investigation of the effect of coatings in cutting parameters on the dry drilling performance of Aluminium alloys, International Journal of International Manufacturing Technology 2006, 28(1), 1–11.
[33] Motta, M.F., Machado, A.R., and de Corte, Fluidos. Tipos, Funco es, Selecao, Me´todos de Aplicacao e Manutencao, Maquinas e Metais, 44–56.
[34] Lenz, E., Katz, Z., and Ber, A. Investigations on the flank wear of cemented carbide tools, Journal of Engineering for Industry 1976, 98(1), 246–250.
[35] Weinert, K., and Kempmann, C. Cutting temperatures, and their effects on the machining behaviour in drilling reinforced plastic composite, Journal of Advanced Engineering Materials. 2004, 6–8, 684–689.
[36] Hann, D.M., Batzer, S.A., Olson, WW., and Sutherland, JW. An experimental study of cutting fluids effect in drilling, Journal of Materials Processing Technology 1997, l71, 305–313.
[37] Jessy, K., Kumar, S. S., Dinakaran, D., and Rao, V. S. Influence of different cooling methods on drill temperature in drilling GFRP, The International Journal of Advanced Manufacturing Technology 2015, 76(1–4), 609–621.
[38] Tobias, S. A. Machine Tool Vibration, 1965, Blackie and Son, London.
[39] Koenigsberger, F., and Tlusty, J. Structure of Machine Tools, 1971, Pergamon Press, Oxford.
[40] Shaw, M. C. Metal Cutting Principles, second ed, 2005, Oxford University Press, New York.
[41] Altintas, Y., and Chan, P. In-process detection and suppression of chatter in milling, International Journal of Machine Tools and Manufacture 1992, 32, 329–347.
[42] Delio, T., Tlusty, J., and Smith, S. Use of audio signals for chatter detection and control, Journal for Engineering in Industry 1992, 114, 146–157.

[43] Braun, S. Signal processing for the determination of chatter threshold, Annals of CIRP 1975, 24, 315–320.
[44] Subramaniam, T., Devries, M., and Wu, S. M. An investigation of computer control of machining chatter, Journal for Engineering in Industry 1976, 98, 1209–1214.
[45] Eman, K. F., and Wu, S. M. A feasibility study of on-line identification of chatter in turning operations, Journal for Engineering in Industry 1980, 102, 315–321.
[46] Oguamanam, D.C.D., Raafat, H., and Taboun, S.M. A machine vision system for wear monitoring and breakage detection of single-point cutting tools, Computers in Industrial Engineering 1994, 26(3), 575–598.
[47] Kurada, S., and Bradley, C. A review of machine vision sensors for tool condition monitoring, Computers in Industry 1997, 34(1), 55–72.
[48] Wang, W.H., Hong, G.S., Wong, Y.S., and Zhu, K.P. Sensor fusion for on-line tool condition monitoring in milling, International Journal of Production Research 2007, 45(21), 5059–5116.
[49] Childs, T.H.C., Maekawa, K., Obikawa, T., and Yamane, Y. Metal Machining: Theory and Applications, 2000, Elsevier, Amsterdam.
[50] Altintas, Y. In-process detection of tool breakages using time series monitoring of cutting forces, International Journal of Machine Tools and Manufacture 1988, 28(2), 157–172.
[51] Altintas, Y., and Yellowley, I. In process detection of tool failure in milling using cutting force models, Journal of Engineering for Industry 1989, 111, 149–157.
[52] Berger, B.S., Minis, I., Harley, J., Rokni, M., and Papadopoulos, M. Wavelet based cutting state, identification, Journal of Sound and Vibration 1998, 213(5), 813–827.
[53] Dimla, Sr. D.E., and Lister, P.M. On-line metal cutting tool condition monitoring I: Force and vibration analyses, International Journal of Machine Tools and Manufacture 2000, 40, 739–768.
[54] Altintas, Y. Prediction of cutting forces and tool breakage in milling from feed drive current measurement, Journal of Engineering for Industry 1992, 114, 386–392.
[55] Li, X. On-line detection of the breakage of small diameter drills using current signature wavelet transform, International Journal of Machine Tools and Manufacture 1999, 39, 157–164.
[56] Tansee, I. N., Wagiman, A., and Tziranis, A. Recognition of chatter with neural networks, International Journal of Machine Tools and Manufacture 1992, 31, 539–552.
[57] Tarng, Y., and Hwang, S. A neural network controller for constant turning force, International Journal of Machine Tools and Manufacture 1993, 34(4), 453–460.
[58] Santhanakrishnan, G., and Krishnamurthy, R., (1993) Mechanics of tool wear during machining of advanced fibrous composites. International conference on machining of advanced material, New York.
[59] Sakuma, K., and Seto, M. Tool wear in cutting glass-fibre reinforced plastics (the relation between fibre orientation and tool wear), Bulletin of JSME 1983, 26(218), 1420–1427.
[60] Takeyama, H., and Lijima, N. Machinability of glass fibre reinforced plastics and application of ultrasonic machining, CIRP Annals 1988, 37, 93–96.
[61] Bhatnagar, N., and Ramakrishnan, N. On the machining of fibre reinforced plastic (RP) composite laminates, International Journal of Machine Tools and Manufacture. 1995, 35(5), 701–716.
[62] Palanikumar, K., (2004) Studies on machining characteristics of glass fibre reinforced polymer composites. Doctoral Thesis submitted to Anna University, Chennai.
[63] Lin, S.C., and Chen, I.K. Drilling of carbon fibre-reinforced composite material at high speed, Wear 1996, 194(1–2), 156–162.
[64] Kim, D., and Ramulu, M. Drilling process optimization for graphite titanium alloy stacks, Composite Structures 2004, 63, 101–114.
[65] Kalidas, S., DeVor, R. E., and Kapoor, S. G. Experimental investigation of the effect of drill coatings on hole quality under dry and wet drilling conditions, Surface and Coatings Technology, 2001, 148(2–3), 117–128.

[66] Lee, S.J., Eman, K.F., and Wu, S.M. An analysis of the drill wandering motion, Journal for Engineering in Industry 1987, 109, 297–302.
[67] Ramkumar, J., Malhotra, S.K., and Krishnamurthy, R. Studies on drilling of glass/epoxy laminates using coated high speed steel drills, Journal of Materials and Manufacturing Process 2002, 15(2), 213–222.
[68] Fuhi, H., Marui, E., Ema, S., Fuji, H., Marui, E., and Ema, S. Whirling vibration in drilling. Part 3: Vibration analysis in drilling workpiece with a pilot hole, Journal of Engineering for Industry 1986, 110(4), 315–321.
[69] Surendran, V. (1998) A study of hole quality in drilling. Master's thesis, University of Illinois at Urbana-Champaign
[70] Jalisi, M.N., Lin, C., and Ehmann, K.F. In: Manufacturing Processes and Materials Challenges in Microelectronic Packaging, 1991, ASME, 25–33.
[71] Watanabe, K., Yokoyuma, K., and Ichimaya, R. Thermal Analyses of the Drilling Process, Bulletin of Japanese Society for Precision Energy 1977, 11, 71–74.
[72] Mohan, N.S., Ramachandra, S.M., and Kulkarni, S. Machining of fibre reinforced thermoplastics: Influence of feed and drill size on thrust force and torque during drilling, Journal of Reinforced Plastic Composites. 2005, 24(12), 1247–1257.
[73] Zhang, L.B., Wang, L.J., Liu, X.Y., Zhao, H.W., Wang, X., and Lou, H.Y. Mechanical model for predicting thrust and torque in vibration drilling fibre-reinforced composite materials, International Journal of Machine Tools & Manufacture 2001, 41(5), 641–657.
[74] Birhan, I., and Ergun, E. Experimental investigations of damage analysis in drilling of woven glass fibre-reinforced plastic composites, International Journal of Advanced Manufacturing Technology 2010, 49, 861–869.
[75] Caprino, V., and Tagliaferri, S. Damage development in drilling glass fibre reinforced plastics, International Journal of Machine Tools Manufacturing 1995, 35(6), 817–829.
[76] Capello, E. Work Piece damping and its effects on delamination damage in drilling thin composite laminates, Journal of Material Processing Technology 2004, 148(2), 186–195.
[77] Chen, W. C. Some experimental investigations in the drilling of carbon fibre-reinforced plastic CFRP composite laminates, International Journal of Machine Tools and Manufacture 1997, 378, 1097–1108.
[78] Faraz, A., Biermann, D., and Weinert, K. Cutting edge rounding: An innovative tool wear criterion in drilling CFRP composite laminates, International Journal of Machine Tools and Manufacture 2009, 49, 1185–1196.
[79] Mehta, M., Reinhart, T. J., and Soni, A. H. (1992) Effect of fastener hole drilling anomalies on structural integrity of PMR-15/Gr composite laminates. In: Proceedings of the machining composite materials symposium, ASM materials week, Chicago, IL, 1–5 November. ASM International.
[80] Davim, J. P., Clemente, V. C., and Silva, S. Evaluation of delamination in drilling medium density fibre board, Proceedings of Institution of Mechanical Engineers: Part B: Engineering Manufacture 2007, 221(4), 655–658.
[81] Tsao, C. C., Kuo, K. L., and Hsu, I. C. Evaluation of a novel approach to a delamination factor after drilling composite laminates using a core–Saw drill, International Journal of Advanced Manufacturing Technology 2012, 59, 617–622.
[82] Nagarajan, V. A., Selwin Rajadurai, J., and Annil Kumar, T. A digital image analysis to evaluate delamination factor for wind turbine composite laminate blade, Composites: Part B: Engineering 2012, 43, 3153–3159.
[83] Durao, L. M. P., Tavares, M. R. S., and de Albuquerque, V. H. C. Damage evaluation of drilled carbon/epoxy laminates based on area assessment methods, Journal of Composite Structures 2013, 96, 576–583.

[84] Silva, D. N. R. (2013) Image processing methodology for assessment of drilling induced damage in CFRP. Thesis, Faculdade de Ciencias e Tecnologia, Universidade Nova de Lisboa.
[85] Babu, J., Sunny, T., Paul, N. A. et al. Assessment of delamination in composite materials: A review, Institution of Mechanical Engineers: Part B: Journal of Engineering Manufacture 2016, 230(11), 1990–2003.
[86] Babu, J., Alex, N. P., Abraham, S. P., Philip, J., Anoop, B.N., and Davim, J. P. Development of a comprehensive delamination assessment factor and its evaluation with high speed drilling of composite laminates using a twist drill, Institution of Mechanical Engineers: Part B – Engineering Manufacture 2017. DOI: 10.1177/0954405417690552.

Vinod Kumar Sharma, Sunil Pathak, I.S.N.V.R. Prasanth,
D. V. Ravishankar, M. Manzoor Hussain, Chandra Mouli Badiganti,
and Nagaraju Bejgam

5 Influence of milling process parameters on the surface quality of GFRP composites

Abstract: The intensified stiffness and lightweight structural designed components such as glass fibre-reinforced plastic (GFRP) composites are becoming an alternative to metallic materials to improve the performance of aircraft, shipbuilding and automobiles. Machining damages on the machined texture or subsurface due to the catastrophic nature of composites result in rejection of components at the last stage of production cycle, and necessitate the minimization of such damages by improving the manufacturing quality in secondary manufacturing process. In this chapter, various fibre orientation (FO) angled GFRP workpieces were milled with different tool rake angles (RA) of end milling cutters. Random experiments were done to test the effects of important milling parameters, such as spindle speed, depth of cut (DOC), FO angle and tool's RA. The machined wall surface and subsurface were thoroughly analyzed by scanning electron microscope. A reasonable reduction in subsurface damages was observed when using the DOC is low (1 mm) and FO angle of workpiece is less than 90°. At this instance, the machining force and the surface roughness are increased proportionally to a DOC, FO angle of the workpiece and tool RAs, where the surface damages were found to be more. It has also been observed that the damage mechanisms of GFRP composite laminates were dominated by their FO angle.

Keywords: end milling tools, GFRP composites, surface integrity, scanning electron microscope (SEM)

Vinod Kumar Sharma, School of Mechanical Engineering, VIT University, Vellore, India
Sunil Pathak, Faculty of Engineering Technology, University Malaysia, Pahang, Malaysia
I.S.N.V.R. Prasanth, Department of Mechanical Engineering, Guru Nanak Institute of Engineering and Technology, Hyderabad, India
D. V. Ravishankar, Department of Mechanical Engineering, T.K.R. College of Engineering and Technology, Hyderabad, India
M. Manzoor Hussain, Department of Mechanical Engineering, Jawaharlal Nehru Technological University (JNTUH), Hyderabad, India
Chandra Mouli Badiganti, Department of Mechanical Engineering, RISE Krishna Sai Prakasam Group of Institutions, Ongole, India
Nagaraju Bejgam, Department of Mechanical Engineering, RISE Krishna Sai Prakasam Group of Institutions, Ongole, India

https://doi.org/10.1515/9783110610147-005

5.1 Introduction

Fibre-reinforced plastic (FRP) composites have been widely used in aircraft, automobile and structural applications. The components need a high-quality machined surface, better dimensional accuracy and surface consistency. It is difficult to understand the machining mechanism of composite materials because of their inhomogeneous and anisotropic behavior. Machining can cause damages, such as fibre cracks, delamination, fibre pull-out and fibre burning. There is a dearth of studies on milling of glass fibre-reinforced plastic (GFRP) composites compared with those on metals. Researchers have mainly studied the influence of tool nomenclature and material characterization on machined surface of FRP composites [1, 2]. A study discussed the mechanism of chip formation in machining of carbon FRP (CFRP) composites, and its findings suggested that the defects were due to inhomogeneous nature of the material [3]. Vaziri and Shakerikia [4] studied the chip formation mechanism by considering the reference angle and found it was one of the most effective parameters to understand the complexity of milling and drilling operations. They successfully studied the chip formation mechanisms in milling of GFRP composites using high-speed photography footages. They concluded that delamination failures occur at lowest machining speeds [5]. Studies on milling process have mostly focused on different fibre orientation (FO) angles of workpiece and varieties of helix angled tools. Taguchi's design for experiments was considered for the study. The results showed that higher helix angled (35°) tools provide better surface quality [6]. Experimental studies were also conducted on orthogonal cutting of FRP composites. The results showed the effect of input process parameters, and subsurface damage mechanisms of machined laminates were significantly varied by FO of the workpiece [7]. Earlier, the same researcher conducted experiments on edge trimming of graphite-epoxy laminates using polycrystalline diamond tools. The material removal rate was analyzed by examining chip forming mechanisms and topography of machined surfaces. It was found that the FO angle was responsible for chip deformation [8]. In order to understand the tool–material interaction and chip formation mechanisms, the researcher conducted experiments on unidirectional CFRP (UD-CFRP) composites. It was found that parasitic effects were responsible for chip deformation [9]. Due to lack of machinability studies in GFRP, chip deformation mechanisms have not been clearly understood. A researcher had conducted an experiment on side milling of CFRP composites using different helix angled end milling tools. He studied the machining force and tool wear based on different FO angles. Better-machined surface quality is achieved with high helix angled end milling tools [10]. Another researcher conducted experiments on different UD-CFRP composites with different rake and clearance angled lathe tools to study measurable outcomes and machined surface morphology related to chip roots [11]. Considering the input process parameters, namely cutting speed, FO angle and workpiece temperature, experiments were conducted on random designs to understand the integrity of milled surfaces and analyze the surface topography using

scanning electron microscope (SEM) micrographs. The results showed at higher cutting speeds, there were greater fibre damages in tandem with increased thermomechanical loads [12, 13]. None of these studies have clearly investigated the consistency of machining mechanisms. Therefore, this chapter was aimed at assessing the machinability indices of unidirectional glass fibres reinforced by polyester matrix material. All experiments were performed with different helix angled customized brazed carbide tipped end milling tools on different GFRP composites. The machined surface quality of GFRP composites was evaluated using SEM analysis.

5.2 Experimentation

Identifying milling conditions, experimental procedures were based on relevant literature findings [12] (see Table 5.1 for more details). The experimental setup (10 HP capacity and maximum spindle speed 2,500 rpm milling machine) is shown in Figure 5.1 and Table 5.1. It lists the machining conditions for the experiments. Here, considers resultant force F as the machining force: $F = \sqrt{F_X^2 + F_Y^2 + F_Z^2}$. The surface roughness (SR, R_a) of machined texture was measured using a Mitutoyo profile meter (centerline average method, cut-off length is 0.5 mm). Postmachined surface quality was analyzed using SEM.

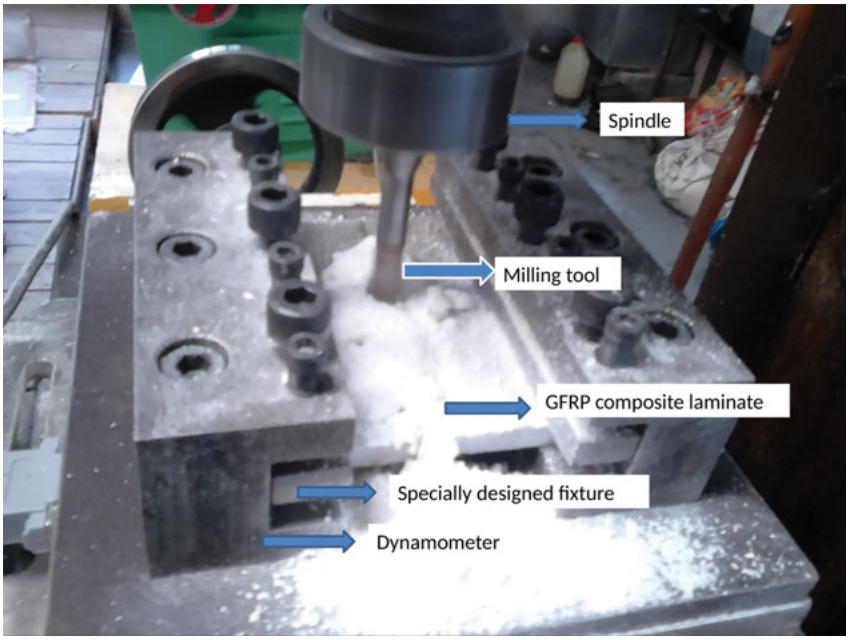

Figure 5.1: Arrangement developed for the experiments on milling machine.

Table 5.1: Milling conditions for GFRP laminates.

Machining conditions	Values
Fibre orientation (degrees)	0, 30, 60, 90, 120 and 150
Rake angle (degrees)	−15, 0, 15 and 30
Depth of cut (mm)	1, 2

A three-dimensional strain gauge-type dynamometer was used for measuring cutting forces. Additionally, a specially designed fixture was placed on it to avoid machining vibrations during machining.

The workpieces of GFRP composites were fabricated by using hand lay-up compression molding technique. Ten layers of mat size of 1 mm E-glass fibre mats (300 mm × 300 mm) were laid up according to the arrangement of varied FO angles (θ) (0°, 30°, 60°, 90°, 120° and 150°) on a flat 10-mm-thick mold panel, and GFRP composite sheet was cured after 5 h. Each sheet was cut into 100 mm × 100 mm × 10 mm for the purpose of experiment. The input process parameters were specially designed (customized) brazed carbide tipped end milling tools with 10° clearance angle and −15°, 0°, 15° and 30° RAs, and the FOs of the workpiece were 0°, 30°, 60°, 90°, 120° and 150°, depth of cut (DOC) of the tool were 1 and 2 mm under the invariable spindle speed 2,500 rpm and the feed rate was 1.4 mm/s.

5.3 Results and discussions

In order to understand the effect of machining conditions, experiments were conducted with all variable machining conditions under the invariable spindle speed of 2,500°rpm and 1.4 mm/s of feed rate on measurable outputs (SR and the machining force). This is discussed in the following sections.

5.3.1 Surface roughness

This refers to the machine texture. A total of 72 workpieces were tested to examine the influence of input parameters on their SR.

The SR R_a values of machined UD-GFRP laminates are shown in Figure 5.2(a), while Figure 5.2(b) shows the effect of FO (θ) of each laminate, when milled by varied rake angled (RA) tools (−15°, 0°, 15° and 30°).

Experimental arrangement (trial number 1–36) and results are shown in Figure 5.2(a). When (0°, 30°, 60°, 90°) fibre-oriented workpieces were milled with all varieties of RA tools at a DOC of 1 mm, the obtained SR was in the range of 2.5 μm.

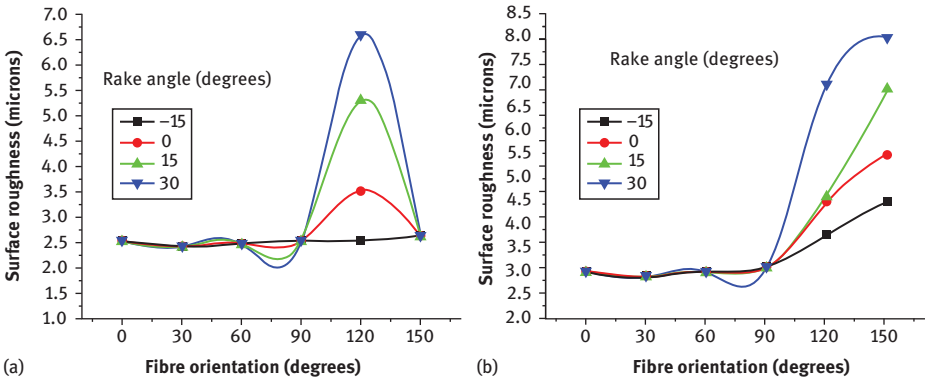

Figure 5.2: Influence of FO on SR of GFRP laminates when (a) DOC = 1 mm and (b) DOC = 2 mm.

When 120° fibre-oriented workpiece was milled with 30° RA, value of tool SR changed from 2.5 to 6.5 µm. Lower SR value of 2.5 µm was obtained when milling with –15° RA tool.

Experimental arrangement (trial number 1–36) and results are shown in Figure 5.2(b). SR was 3 µm when (0°, 30°, 60°, 90°) fibre-oriented workpiece was milled with all varieties of RA tools at a DOC of 2 mm. Beyond 90° fibre orientation (i.e. 120°, 150°), workpiece was milled with all varieties of RA tools obtained with SR drastically changing from 3 to 8 µm.

A higher range of SR ranging from 6.5 to 8 µm was obtained when 120° and 150° fibre-oriented workpieces were milled with 30° RA tool. Lower SR value ranging from 3 to 4 µm was obtained when milling with –15° RA tool.

In sum, we can say that when FO of workpiece is $\theta \leq 90°$, the effect of varied RAs on the tools is insignificant.

5.3.2 Machining forces (*F*)

Machining force or cutting force can help one understand the impact of input process parameters on measurable outcomes. This study examined 72 workpieces to understand the influence of machining force effect on milled surface quality of workpiece under the specified input process parameters.

Figures 5.3(a, b) and 5.4(a, b) show that the results of the machining forces were obtained when machined with different tools on different fibre angled workpieces and under the different machining conditions during experiment number 1–36 (see Table 5.2).

Compared with FO angle and DOC, the effect of tool RA is not significant. From Figure 5.3(a), milling at a DOC was 1 mm and the machining force variation was less

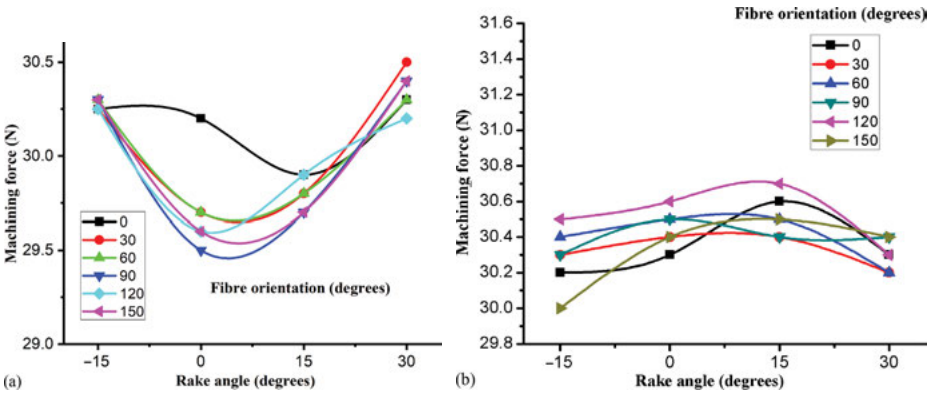

Figure 5.3: Influence of RA on machining force of GFRP laminates when (a) DOC = 1 mm and (b) DOC = 2 mm.

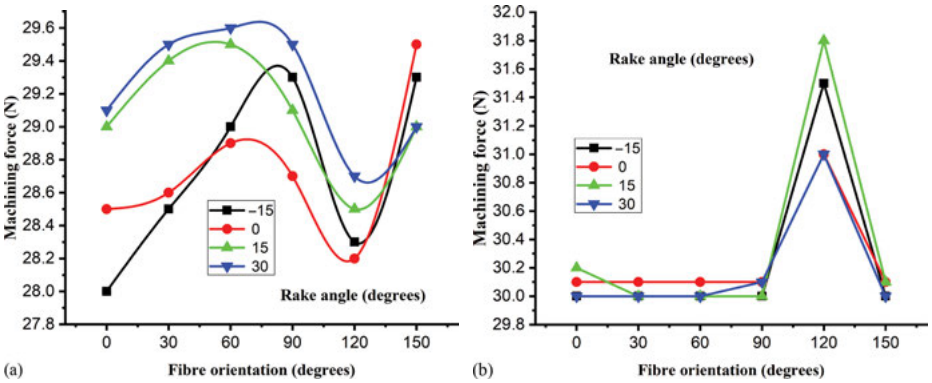

Figure 5.4: Fibre orientation effect on machining force of GFRP laminates when (a) DOC = 1 mm and (b) DOC = 2 mm.

from 29.5 to 30 N, when 12 numbers of workpieces were milled with RA tools of 0° and 15°. The machining force was slightly increased to 30.5 N, when six numbers of workpieces were milled with 30° RA tool.

When milling at a higher DOC of 2 mm, the machining force was slightly increased from 30 to 30.6 N, when 18 numbers of the workpieces were milled with tools having RAs of –15°, 0° and 30°. The machining force was slightly decreased to 30.2 N and six workpieces were milled with 30° RA tool. This is shown in Figure 5.3(b).

The machining force was strongly affected by different FO angled workpieces when milled with varied RA tools (Figure 5.4(a, b)).

From Figure 5.4(a), milling with a DOC was 1 mm and the machining force F was increased from 28 to 29.6 N for the workpiece with FO angle (θ) from 0° to 60°,

Table 5.2: Test planning for milling operations.

Trial number	Fibre orientation angle (degrees)	Tool type [rake angle (γ, degrees)]	Depth of cut (mm)
1–6	0°	−15°/0°/15°/30°	½
7–12	30°	−15°/0°/15°/30°	½
13–18	60°	−15°/0°/15°/30°	½
19–24	90°	−15°/0°/15°/30°	½
25–30	120°	−15°/0°/15°/30°	½
31–36	150°	−15°/0°/15°/30°	½

Experiment number	Trial number	Fibre orientation angle θ (degrees)	Tool type [rake angle (γ, degrees)]	Depth of cut (mm)
1	1	0°	−15°	1/2
1	2	0°	−15°	1/2
1	3	0°	−15°	1/2
1	4	0°	−15°	1/2
1	5	0°	−15°	1/2
1	6	0°	−15°	1/2

Note: Five other experiments were separately conducted with DOC of 1 and 2°mm for the workpiece having FOs of 0°, 30°, 60°, 90°, 120° and 150°. Total experimental runs were 36 × 2 = 72.

while F was decreased to 28 N with "θ" at 90°. Beyond the limit of FO at 90°, the machining forces were increased up to 29.8 N.

Figure 5.4(b) shows the results of all workpieces milled with a DOC at 2 mm. The machining force was 30 N, with milled workpiece with angles ranging from 0° to 90°. At 120°, workpieces were milled by all of the RA tools and the machining forces were increased to 31.8 N. This led to increased SR. F was decreased to 30 N, when 150° angled workpieces were milled by all varieties of the RA tools.

From the above, it is evident that the measurable outcomes (SR and machining force) were maximum with an increase in process parameters (FO angle of workpiece, RA of the tool and DOC). The cutting forces were higher on the tool, which led to dragging of fibre from the surroundings of the milled surface. By pulling the fibres from the milled texture, there were greater surface irregularities. These adverse effects are explained in the section on SEM analysis (see also Figures 5.7(a–d), 5.8 (a, b) and 5.9 (a, b)). The above phenomenon can also be understood from the machining surface deformation mechanisms studied [4] (Figure 5.5 (a–e)).

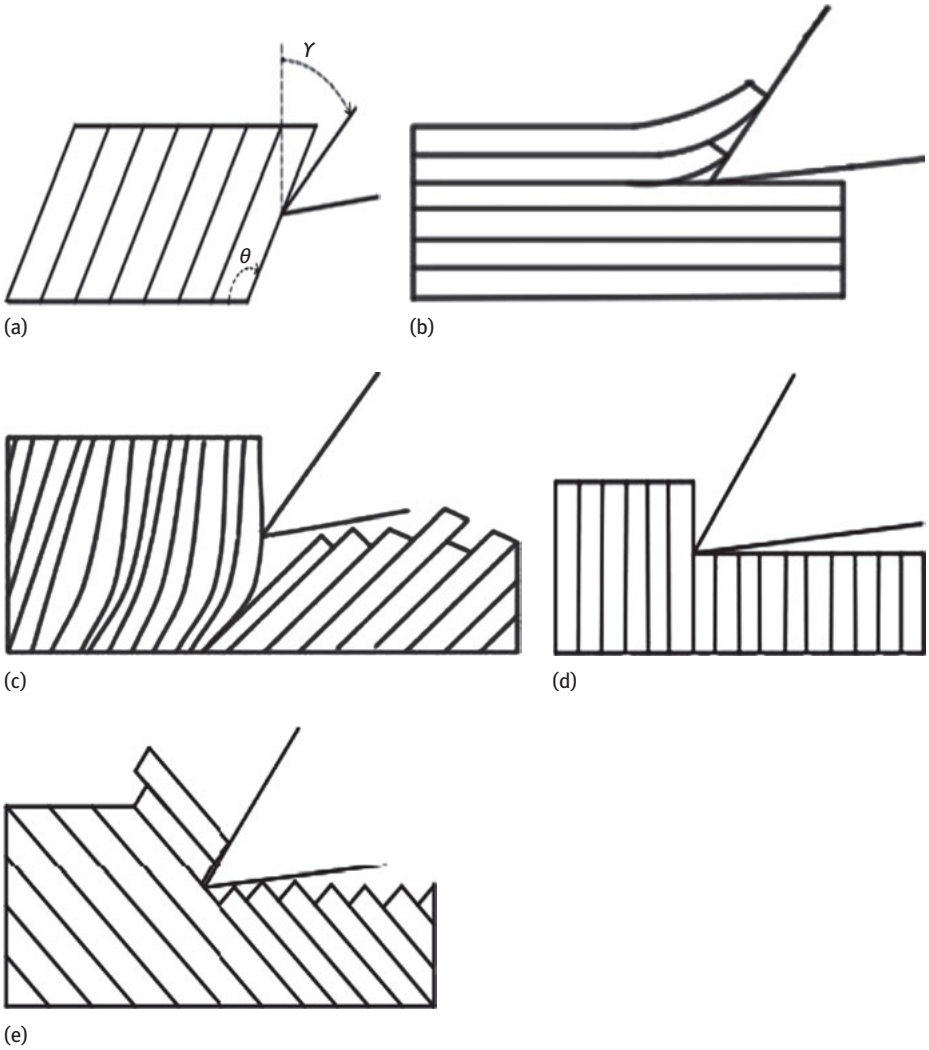

Figure 5.5: (a) Machining deformation mechanisms [4], where θ = fibre direction angle, γ = RA of the tool, (b) when $\theta = 0$ and $\gamma > 0$, (c) $0 < \theta < 90$ and $\gamma > 0$, (d) $\theta = 90$ and $\gamma > 0$ and (e) $90 < \theta < 150$ and $\gamma > 0$.

Usually, when "θ" is less than 90°, the fibre is strongly supported and it results in less bending. However, with variation in DOC and when "θ" is greater than 90°, the fibre is subjected to normal compression force and the surrounding matrix material becomes brittle and cracked. This leads to greater surface irregularities. Hence, SR is varied with FO angle of the workpiece.

These effects were seen from the above two cases. The topography of milled surfaces will be discussed in the following section.

5.3.3 The surface quality evaluation with SEM

The machined surface of GFRP laminates is resolute as shown in the following SEM images. This provides qualitative information on topology of the milled surface.

Under definite milling conditions, the better surface quality of machined texture is revealed in Figure 5.6(a, b). Although by varying the milling conditions, surface damages (fibre pull-out, distorted failure and fibre bending) happen at 120° and 150° milled composites with DOC of 2 mm, and the RA of tools are 0°, 15° and 30° as shown in Figure 5.7(a–d). At this stage, machining forces were increased up to 31.8 N and the SR was higher around 6.5–7 μm. All of these surface damages were assessed with respect to variable parametric conditions.

Figure 5.6(a, b) shows that when machining at lower DOC (1 mm) with the RA of the tool at –15°, it has fewer surface damages at 90° and 150° fibre-oriented laminates. At this stage, the machining forces were low around 30 N and the SR was 2.5 μm.

However, higher DOC at 2 mm and FO beyond 120°, the machined laminate texture becomes rougher, and more machining force at 31.8 N is generated, specially milled with RA of the tool at 30° as shown in Figure 5.8(a, b). The FO plays a significant role on machinability outcomes (SR and machining force).

Moreover, when $\theta \leq 90°$, the milled surface is not affected by the influenced process parameters such as FO, RA of the tool and DOC.

Figure 5.9(a) shows the machined surface texture with the FO of workpiece is 0°, the DOC is 2 mm and RA of the tool is 15°. At this stage, few fibres have experienced surface failures, such as crack growth formation, fibre shear failure and fibre bending. Figure 5.9(b) represents the surface damage when "θ" is 90°, the DOC is 2 mm and the tool RA is 15°.

From the foregoing, it is clear that when $\theta > 90°$, the machined surface texture becomes affected by all machining conditions.

SEM images are consistent with the above results of SR and machining forces.

5.4 Conclusion

- This study found that FO (θ) influences surface integrity of milled GFRP laminates. $\theta \leq 90°$ is a significant angle, and beyond this, the SR is increased, which results in greater surface damages (when milled with positive RA tools, i.e. 0°, 15° and 30°).
- The RA of the tool (y) has a greater impact on SR (R_a) and machining force "F." From the above, it is clear that better surface finish is obtained with lower RA (–15°).
- It is clearly observed under the milling conditions at a higher FO angled (120°) workpiece, larger RA tool (30°) and maximum DOC at 2 mm, machining forces

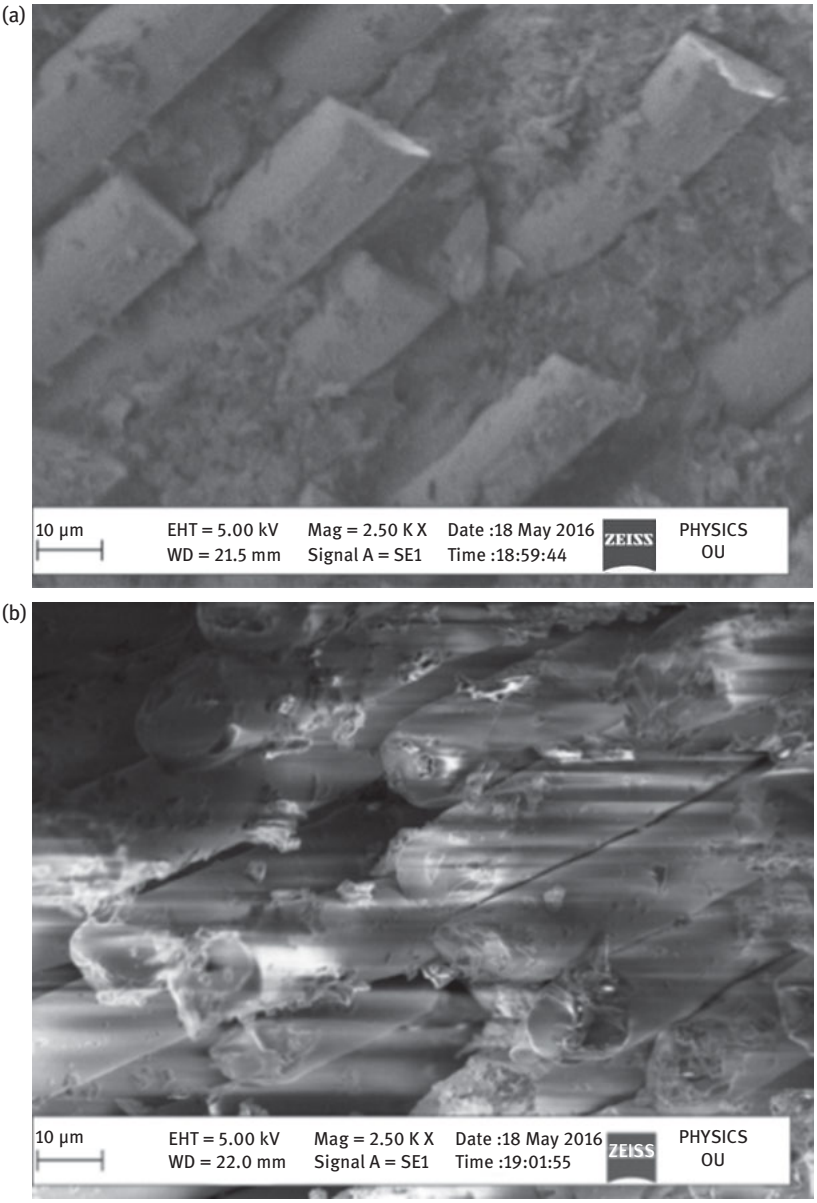

Figure 5.6: Better surface quality on machined UD-GFRP laminates when (a) RA = –15°, DOC = 2 mm and FO = 90° and (b) RA = –15°, DOC = 1 mm and FO = 150°.

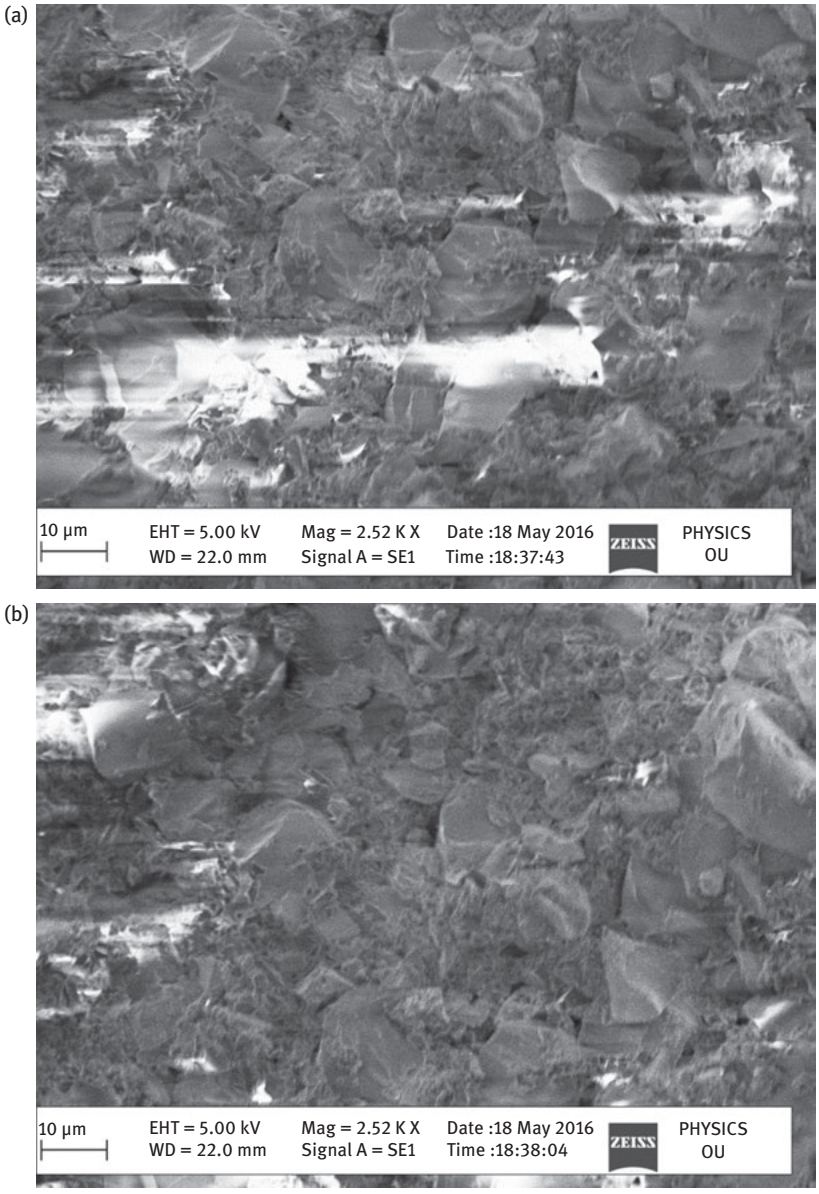

Figure 5.7: Surface damages of machined UD-GFRP laminates: (a) FO = 120°, DOC = 2 mm and RA = 0°; (b) FO = 150°, DOC = 2 mm and tool RA = 0°; (c) FO = 120°, DOC = 2 mm and tool RA = 15°; and (d) FO = 120°, DOC = 2 mm and tool RA = 30°.

(c)

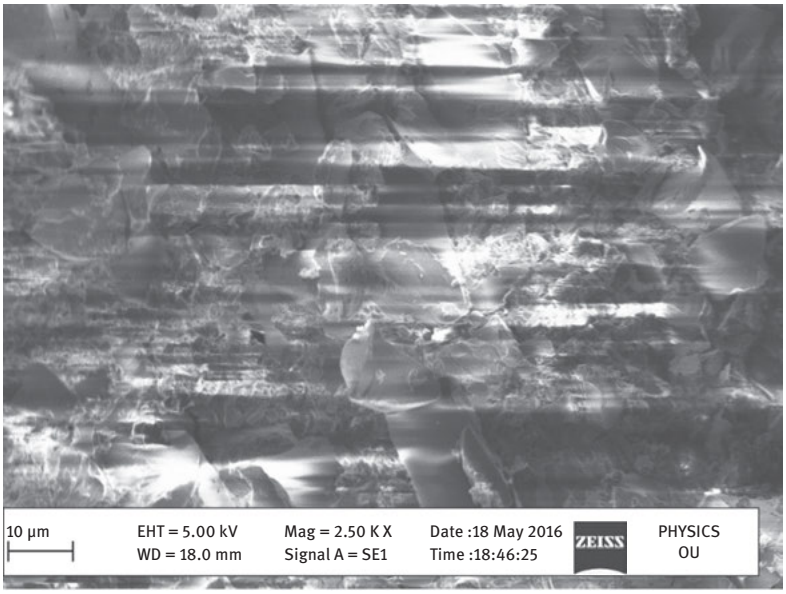

(d)

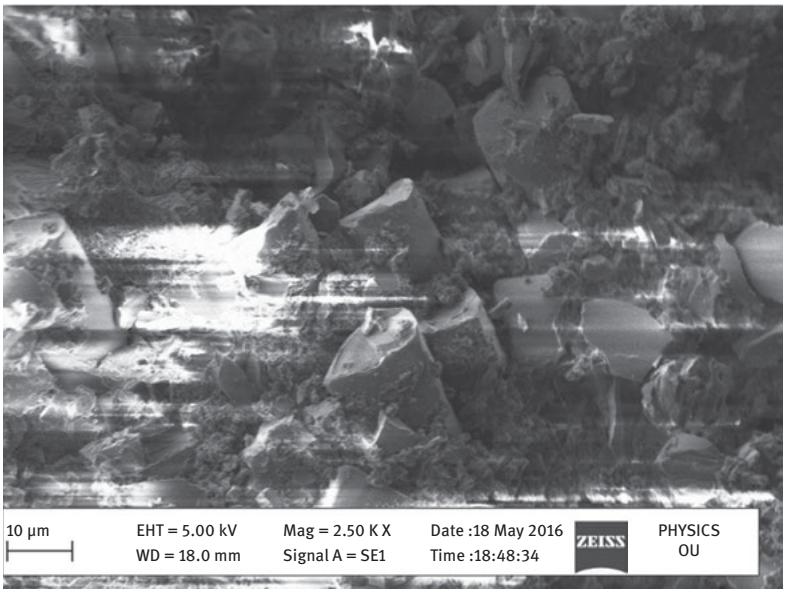

Figure 5.7 (continued)

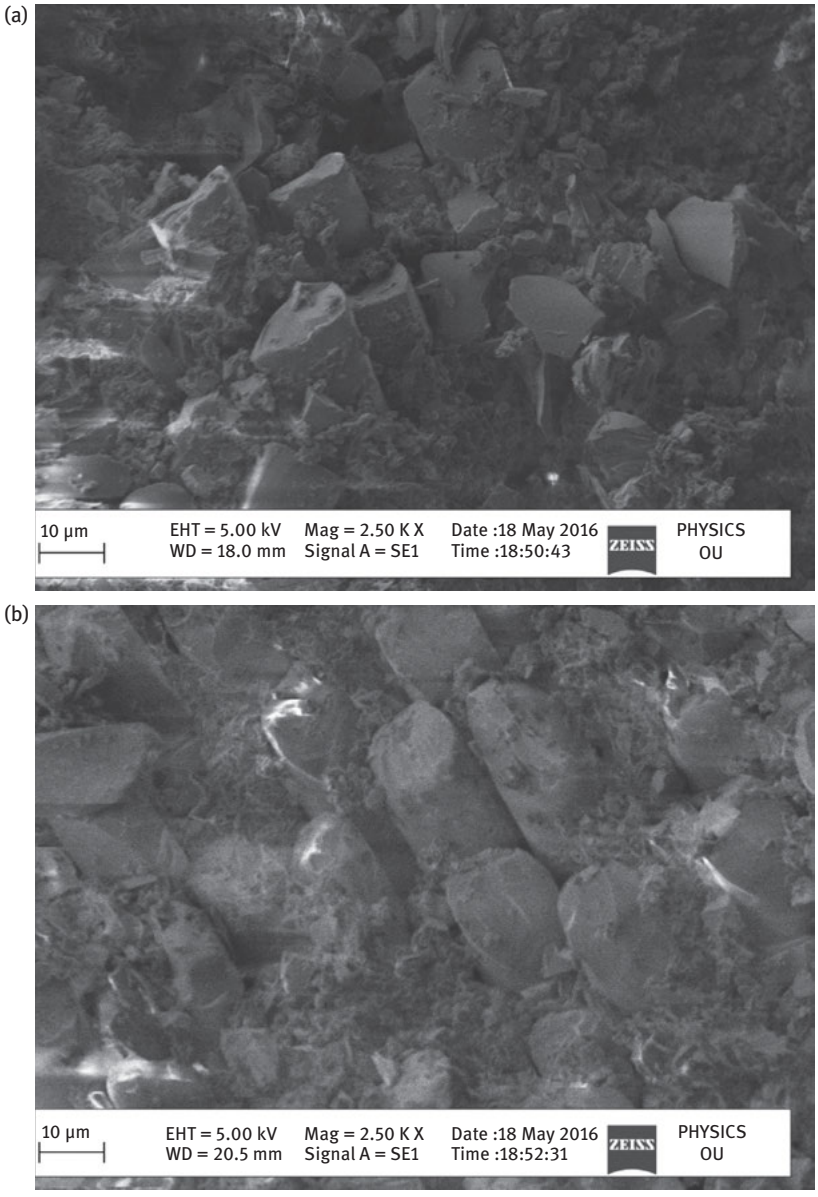

Figure 5.8: Surface damages of machined UD-GFRP laminates: (a) FO = 150°, RA = 30° and depth of cut (DOC) = 1 mm and (b) FO = 150°, RA = 30° and DOC = 2 mm.

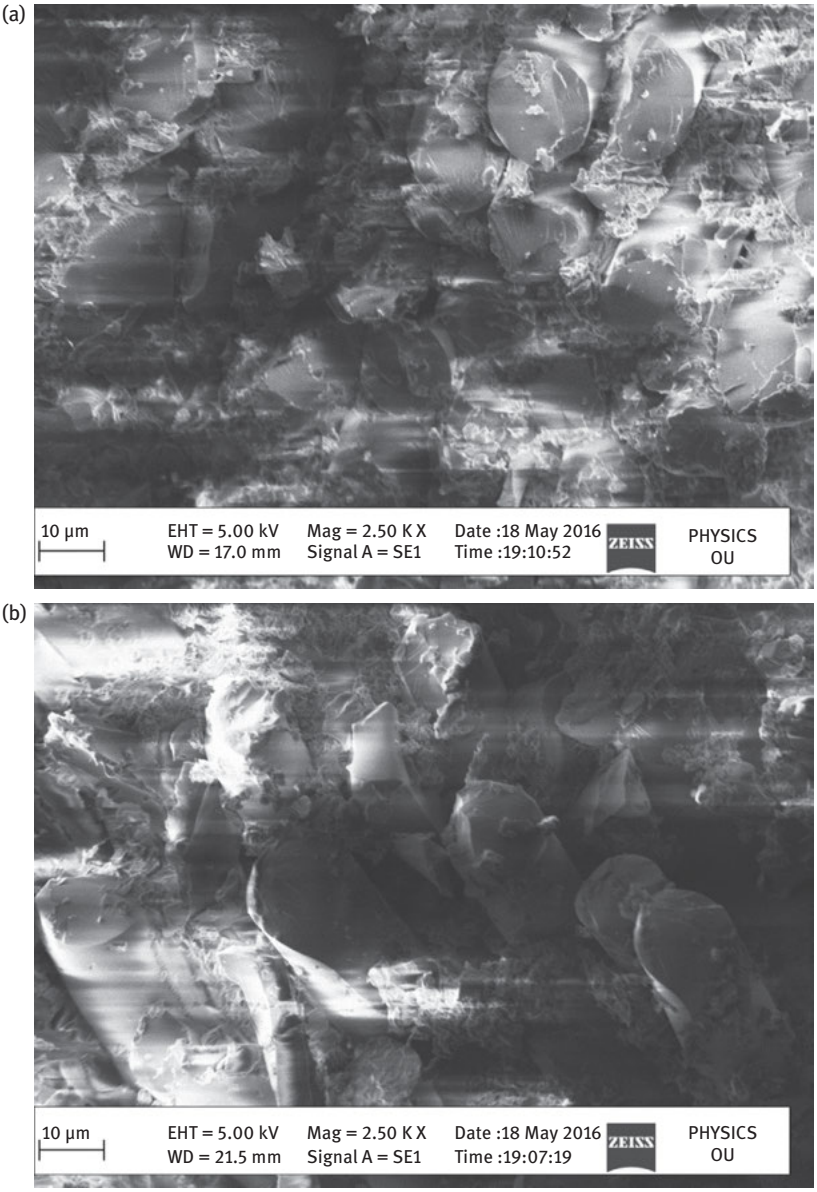

Figure 5.9: Surface damages of machined UD-GFRP laminates: (a) DOC = 2 mm, tool RA = 15° and FO = 0° and (b) DOC = 2 mm, RA = 15° and FO = 90°.

and the SR are elevated. At this stage, the machined surface quality is poor, which is described in Section 5.3.3.

– Cutting mechanism in milling is not only influenced by the process parameters, but its mechanical characterization of workpiece also plays a major role.

References

[1] An, S O., Lee, E.S., and Noh, S.L. A study on the cutting characteristics of glass fibre reinforced plastics with respect to tool materials and geometries, Journal of Materials Processing Technology 1997, 68, 60–70.

[2] Lee, J.H., Kim, D.E., and Lee, S. Statistical analysis of cutting force ratios for flank-wear monitoring, Journal of Materials Processing Technology 1998, 74, 104–114.

[3] Pwu, H.Y., and Hocheng, H. Chip formation model of cutting fibre- reinforced plastics perpendicular to fibre axis, Journal of Manufacturing Science and Engineering 1998, 120(1), 192–196.

[4] Vaziri Sereshk, M.R., and Shakerikia, A. Investigation of the effect of fracture modes involved in chip separation and corresponding effect on quality of machining of fibre reinforced polymer composites, Journal of Current Research in Science 2016, 4(3), 74–84.

[5] Azmi, A.I. Chip formation studies in machining fibre reinforced polymer composites, International Journal of Materials and Product Technology 2013, 46(1), 32–46.

[6] Jenarthanan, M.P., and Jeyapaul, R. Evaluation of machinability index on milling of GFRP composites with different fibre orientations using solid carbide end mill with modified helix angles, International Journal of Engineering Science Technology 2014, 6(4), 1–10.

[7] Wang, X.M., and Zhang, L.C. An experimental investigation into the orthogonal cutting of unidirectional fibre reinforced plastics, International Journal of Machine Tools and Manufacture 2003, 43, 1015–1022.

[8] Wang, D.H., Ramulu, M., and Arola, D. Orthogonal cutting mechanisms of graphite/epoxy composite. Part 1: Unidirectional laminate, International Journal of Machine Tools and Manufacture 1995, 35(12), 1623–1638.

[9] Caprino, G., Santo, L., and Nele, L. Interpretation of size effect in orthogonal machining of composite materials, Part I: Unidirectional glass fibre reinforced plastics, Composites Part A 1998, 29A, 887–892.

[10] Hosakawa, H., Hirose, N., Ueda, T., and Furumoto, T. High-quality machining of CFRP with high helix end mill, CIRP Annals – Manufacturing Technology 2014, 63, 89–92.

[11] Voba, Robert., Henerichsa, Marcel., Kustera, Friedrich., and Wegenera, Konrad., Chip root analysis after machining carbon fibre reinforced plastics (CFRP) at different fibre orientations. 6th CIRP International Conference on High Performance Cutting, HPC Procedia CIRP 14(2014) 217–222.

[12] Pecata, Oliver., Rentscha, Rudiger., and Ekkard, Brinksmeiera., Influence of milling process parameters on the surface integrity of CFRP, 5th CIRP Conference on High Performance Cutting Procedia CIRP 1, (2012) 466–470.

[13] Prasanth, I.S.N.V.R., Ravishankar, D.V., Manzoor Hussain, M., Badiganti, CM., Sharma, VK., and Pathak, Sunil. "Investigations on performance characteristics of GFRP composites in milling", The International Journal of Advanced Manufacturing Technology 2018, 99(5–8), 1351–1360. (DOI: 10.1007/s00170-018-2544-2).

Index

https://doi.org/10.1515/9783110610147-006